

PONTE SULLO STRETTO DI MESSINA



PROGETTO DEFINITIVO

EUROLINK S.C.p.A.

IMPREGILO S.p.A. (MANDATARIA)
 SOCIETÀ ITALIANA PER CONDOTTE D'ACQUA S.p.A. (MANDANTE)
 COOPERATIVA MURATORI E CEMENTISTI - C.M.C. DI RAVENNA SOC. COOP. A.R.L. (MANDANTE)
 SACYR S.A.U. (MANDANTE)
 ISHIKAWAJIMA - HARIMA HEAVY INDUSTRIES CO. LTD (MANDANTE)
 A.C.I. S.C.P.A. - CONSORZIO STABILE (MANDANTE)

<p>IL PROGETTISTA</p>  <p>Ing. E.M. Veje Dott. Ing. E. Pagani Ordine Ingegneri Milano n° 15408</p> 	<p>IL CONTRAENTE GENERALE</p> <p>Project Manager (Ing. P.P. Marcheselli)</p>	<p>STRETTO DI MESSINA</p> <p>Direttore Generale e RUP Validazione (Ing. G. Fiammenghi)</p>	<p>STRETTO DI MESSINA</p> <p>Amministratore Delegato (Dott. P. Ciucci)</p>
--	---	--	---

<p><i>Unità Funzionale</i></p> <p><i>Tipo di sistema</i></p> <p><i>Raggruppamento di opere/attività</i></p> <p><i>Opera - tratto d'opera - parte d'opera</i></p> <p><i>Titolo del documento</i></p>	<p>OPERA DI ATTRAVERSAMENTO</p> <p>CONCEZIONE / DIMENSIONAMENTO GENERALE E DISEGNI D'ASSIEME</p> <p>ANALISI GLOBALI</p> <p>Generale</p> <p>Seismic analyses for soil-foundation systems, Annex</p>	<p>PB0032_F0</p>
---	--	------------------

CODICE	C G 1 0 0 0	P	C L	D	P	S B	A 2	0 0	0 0	0 0	0 0	0 1	F0
--------	-------------	---	-----	---	---	-----	-----	-----	-----	-----	-----	-----	----

REV	DATA	DESCRIZIONE	REDATTO	VERIFICATO	APPROVATO
F0	20/06/2011	EMISSIONE FINALE	RC	GV	LC/ABI

		Ponte sullo Stretto di Messina PROGETTO DEFINITIVO		
Seismic analyses for soil-foundation systems, Annex	<i>Codice documento</i> PB0032_F0_ANX	<i>Rev</i> F0	<i>Data</i> 20/06/2011	

INDICE

1	Executive summary	3
2	Scope of the work and methodology	4
3	Soil Profile and Geotechnical Characterisation	6
3.1	Sicilia shore	6
3.1.1	Sicilia Anchor Block	7
3.1.2	Sicilia Tower and of the Terminal Structure	8
3.2	Calabria shore	10
3.2.1	Calabria Tower and Terminal Structure	12
3.2.2	Calabria Anchor Block	15
4	2D Numerical Dynamic Analyses	18
4.1	Soil model	18
4.1.1	Geometrical soil model	18
4.1.2	Soil constitutive model	19
4.1.3	Soil parameters	21
4.2	Structural elements	23
4.2.1	Equivalent dimensions	23
4.2.2	Towers	26
4.2.3	Anchor blocks	28
4.2.4	Terminal structures	29
4.3	Procedure of analysis	29
4.4	Seismic input	31
4.5	Results of the analyses	33
5	REFERENCES	40
6	FIGURES	42

		Ponte sullo Stretto di Messina PROGETTO DEFINITIVO		
Seismic analyses for soil-foundation systems, Annex	<i>Codice documento</i> PB0032_F0_ANX	<i>Rev</i> F0	<i>Data</i> 20/06/2011	

1 Executive summary



The present report illustrates the methodology and the results of the seismic soil-structure interaction analyses carried out at the verification stage of the design process. The aim of these analyses is two-folded: on the one hand, they serve to evaluate the seismic performance of the bridge foundation (namely, the foundations of the tower and of the terminal structures, and the anchor blocks); on the other hand, these analyses provide full time histories of displacements and rotations at the soil-structure contact points, that may be employed in time-domain structural analyses of the bridge superstructure.

The soil-structure interaction analyses were carried out in the time-domain using a non linear hysteretic soil model implemented in the finite difference code FLAC. The seismic input is made by two particular seismic recordings, selected by prof. Braga to be sufficiently representative of the maximum credible earthquake in the Messina strait. Each seismic record includes three time histories of mutually orthogonal acceleration components.

The analyses were carried out under two dimensional plane strain conditions, and studied separately the seismic response on the Sicily and on the Calabria shores. This implied the use of eight different calculation grids, that is, two longitudinal grids (Sicily and Calabria), and six transversal grids, one for each soil-structure contact point (blocks, terminal structures, and foundations).

The input seismic record were deconvoluted at the base of the calculation grids and were applied as time histories of horizontal and vertical acceleration. It was necessary to consider four different combination for each seismic record, each considering a different sign of the horizontal acceleration and a different orientation of the bridge with respect to the two reference horizontal directions of the record.

All the seismic analyses were preceded by a static stage, which simulated the pre-earthquake stress state. As the soil stiffness and strength is dependent on the effective stresses, the static stages were needed to describe the distributions of the pore pressure and of the geostatic stresses, and included a construction stage in which the foundation elements were loaded with the static actions transmitted by the bridge superstructure. A check was made that the computed displacement produced by the static loads were in good agreement with those evaluated with static three-dimensional finite-element analyses.

		Ponte sullo Stretto di Messina PROGETTO DEFINITIVO		
Seismic analyses for soil-foundation systems, Annex	<i>Codice documento</i> PB0032_F0_ANX	<i>Rev</i> F0	<i>Data</i> 20/06/2011	

For the foundations of the bridge tower, it was felt that the dynamic response of the superstructure could influence significantly the soil-structure interaction phenomena. Therefore, simplified structural models of the bridge towers were explicitly included in the longitudinal and transversal calculation grids. The properties of these simplified models were chosen to reproduce the first vibration modes of the tower structures. This was checked by performing additional independent dynamic analyses of the isolated simplified structural elements, using the same computer code and the same methodology adopted in the complete soil-structure interaction analyses.

The results were analysed in terms of permanent displacements and rotations of the foundation elements, and in terms of the amplification of seismic waves. As a general result, the permanent displacements of the main foundation structures do not exceed 20-30 mm and the maximum rotation, occurring for the Calabria tower, is smaller than 0.015 deg.

Full time histories of displacements and rotations were extracted from the analysis results; these time histories will be applied to the base of a structural model of the bridge, in order to perform corresponding time-domain seismic structural analyses.



2 Scope of the work and methodology

This report describes a number of soil-structure interaction analyses carried out to simulate the seismic behaviour of the Messina Bridge under severe earthquake loading.

In principle, it would be desirable to analyse the soil-structure interaction using a complete, three-dimensional fully coupled numerical simulation of the entire bridge and of the soil volume that influences the propagation of the seismic waves. However, the solution of any engineering problem benefits from some level of decoupling, that not only makes the computations shorter and easier to control, but also allows the analyst to gain some insight into the physical behaviour of the system under study and hence to analyse critically the results obtained.

For the present analyses, a decoupling strategy was conceived, that consists essentially of the following methodology:

- the effect of seismic waves that propagate through the soil is analysed separately from the effects on the bridge structure;

		Ponte sullo Stretto di Messina PROGETTO DEFINITIVO		
Seismic analyses for soil-foundation systems, Annex	<i>Codice documento</i> PB0032_F0_ANX	<i>Rev</i> F0	<i>Data</i> 20/06/2011	

- the stress increments induced in the soil by the static loads transmitted by the bridge structure to the foundations produce changes in the soil strength and stiffness, and therefore are always taken into account;
- where it is expected that the stiffness of the structural components of the bridge affects the dynamic response of the soil-foundation system (e.g. for the towers' structure), this stiffness is included explicitly in the analysis, using simplified structural schemes that reproduce the most important dynamic features of the actual structure;
- the behaviour of the bridge foundations of the Sicilia and Calabria shores is analysed separately;
- each soil-structure interaction analysis is carried out under two-dimensional, plane strain conditions; this implies a strategy to convert the actual three-dimensional geometry into an equivalent two-dimensional, plane strain scheme;
- the seismic input is applied to the bottom boundary of each calculation model in the form of two acceleration time histories (in the horizontal and vertical directions), that are derived from the original seismic input through a suitable de-convolution technique;
- liquefaction was analysed separately, using two-dimensional free-field analyses for the Calabria shore and one-dimensional free-field analyses for the Sicilia shore; these numerical analyses describe the behaviour of the soil using a constitutive model based on hardening plasticity, particularly suitable for liquefaction analysis (see report CG1000-P-CL-D-P-ST-F3-TO-00-00-00-01_A_Towers_Liq_pot_ANX);
- the results of the analyses are expressed at each soil-structure contact point in terms of time histories of displacements and rotations; in turn, these time histories constitute the seismic input of a set of separate time-domain structural analyses. The time histories of displacements and rotations computed in the present soil-structure interaction analyses take into account implicitly the soil stiffness and its damping properties. Therefore, the corresponding structural analyses do not need to model the soil behaviour through equivalent springs and dampers: these structural analyses must be carried out simply applying the computed time histories at the soil-structure contact points.

		Ponte sullo Stretto di Messina PROGETTO DEFINITIVO		
Seismic analyses for soil-foundation systems, Annex		<i>Codice documento</i> PB0032_F0_ANX	<i>Rev</i> F0	<i>Data</i> 20/06/2011

3 Soil Profile and Geotechnical Characterisation

3.1 Sicilia shore

The geotechnical site investigations carried out between 1988 and 1992 together with the geological and geophysical investigations performed for the preliminary design study make it possible to define the general soil profile in the area of the Messina Strait.



Figure 1 shows the soil profile on the Sicilia shore. Starting from ground level and moving downwards the following units are encountered:

1. *Depositi Costieri* (Coastal Deposits). Sand and gravel with very little or no fine content; occasionally, silty peaty layers appear in the lower part of the formation. The thickness of this formation is difficult to evaluate as it rests on the very similar formation of the *Ghiaie di Messina*.
2. *Ghiaie di Messina* (Messina Gravel)/*Sedimenti dei terrazzi* (Terrace Deposits). Gravel and sand, with very occasional silty layers. The thickness of this formation can reach more than 170 m.
3. *Depositi Continentali* (Continental Deposits)/*Calcarenite di Vinco* (Vinco Calcarenite). Clayey-sandy deposit, consisting of layers of silt or silt and sand, with significant gravel content/Bio-calcarenite and fossiliferous calcarenite, with thin silty layers.
4. *Conglomerato di Pezzo* (Pezzo Conglomerate). Soft rock, consisting of clasts of different dimensions in a silty-sandy matrix and sandstone. The thickness of this formation is larger than 200 m.
5. *Cristallino* (Crystalline bedrock). Tectonised granite.

The present level of the ground at the location of the Sicilia Anchor Block is between +22 m a.s.l. and +59 a.s.l.; the sea shore is at a distance of about 1000 m from the anchor block.

The level of the ground at the location of the Sicilia Terminal Structure and at the location of the Sicilia Tower is about 4 m a.s.l.; the sea shore is at a distance of about 270 m from the centre of the terminal structure and of about 70 m from the centre of the tower foundation.

The groundwater level coincides with the sea level, at 0 m a.s.l..

		Ponte sullo Stretto di Messina PROGETTO DEFINITIVO		
Seismic analyses for soil-foundation systems, Annex	<i>Codice documento</i> PB0032_F0_ANX	<i>Rev</i> F0	<i>Data</i> 20/06/2011	

The soil layers sequence encountered at the location of the Sicilia Tower and of the Terminal Structure, and that encountered at the location of the Sicilia Anchor Block are partially different, as the two locations are more than 900 m distant.

In the following, a short geotechnical characterization of the sites is reported in two different sections. A detailed characterization of the soil profile on the Sicilia shore is contained in the report *Updated geotechnical characterisation based on the 2010 site and laboratory investigations (CG1003-P-RG-D-P-SB-G3-00-00-00-00_01_A_Upd_Geot_Char_ANX)*.

Figure 2 shows a global geotechnical section of the Sicilia shore. Three enlarged and more detailed views of the longitudinal section, respectively referred to the Sicilia Anchor Block site, Tower site and Terminal Structure site, are reported from Figure 3 to Figure 5.

3.1.1 Sicilia Anchor Block

Figure 6 shows a plan view at the location of the Sicily Anchor Block, together with the available site investigation. The longitudinal section indicated in Figure 6 is plotted in Figure 3.

The Messina Gravel/Terrace Deposits unit extends from the ground level over a thickness of about 200m, but at about -70 m a.s.l. an increase in stiffness is observed for about 15 m.



Since no *in-situ* evaluation of permeability was carried out at the location of the Sicily Anchor Block, reference can be made to the data obtained from the *in-situ* test carried out at the location of Sicily Tower: the horizontal permeability of the deposits evaluated by pumping tests is $k_h = 5 \times 10^{-3}$ m/s. The values of the vertical permeability k_v obtained from Lefranc permeability tests, assuming $k_h/k_v = 10$, range from 2×10^{-3} to 5×10^{-2} (m/s); for $k_h/k_v = 1$, k_v is not substantially different from that obtained by the well pumping test, being in the range of 2.6×10^{-4} to 5.8×10^{-3} (m/s).

In the area of the Sicilia Anchor Block erosion phenomena of the Messina Gravel are less important than on the site of Sicilia Tower, so that deviation of K_0 from its normally consolidated value is mainly due to ageing effects. The maximum estimated increase of K_0 due to ageing effects is of the order of 42%. It follows:

$$K_0 = 1.42 \times K_0(\text{NC}) = 1.42 \times (1 - \sin \phi'_p) = 0.47 \quad (1)$$

in which $\phi'_p = 42^\circ$ as described below.

The relative density of the Messina Gravel was estimated from the SPT and LPT results using the

		Ponte sullo Stretto di Messina PROGETTO DEFINITIVO		
Seismic analyses for soil-foundation systems, Annex	<i>Codice documento</i> PB0032_F0_ANX	<i>Rev</i> F0	<i>Data</i> 20/06/2011	

procedure proposed by Cubrinovski and Ishihara (1999): values of $D_R = 40\%$ to 60% were obtained as shown in Figure 7. The angle of shearing resistance at peak $\phi'_p = 41^\circ - 44^\circ$ (Figure 8) was then evaluated through the relationship proposed by Schmertmann (1975).

The stiffness profile of Messina gravel was obtained from three cross-hole tests carried out in the vicinity of the Sicily Anchor Block, down to a depth of 100 m b.g.l. The results of the cross-hole tests in terms of shear wave velocity, V_s , versus depth are given in Figure 9 (a). The same results are shown in Figure 9 (b) as profiles of small strain shear modulus, G_0 .

G_0 increases from about 100 MPa at the ground level to about 550 MPa at a depth of 80 m b.g.l.; below this depth the data are more dispersed with an average value of 800 MPa.

Table 1 summarizes the main mechanical parameters obtained from the geotechnical characterisation above.

Table 1. Sicilia Anchor Block - summary of main mechanical parameters

Geological formation	depth (m b.g.l.)	D_r (%)	K_0	ϕ'_p ($^\circ$)	K_h (m/s)	G_0 (MPa)
Messina Gravel	0÷20	40÷60	0.43	44	5×10^{-3}	50÷150
Messina Gravel	20÷80	40÷60	0.47	42	5×10^{-3}	150÷550
Messina Gravel	77÷93	40÷60*	0.47*	42*	5×10^{-3}	800

* These values could not be calculated as no in situ test at failure (SPT, LPT, CPT) reached the depth of this formation, and were estimated based on the information retrieved from the other locations on the Sicilian side.



3.1.2 Sicilia Tower and of the Terminal Structure

Figure 10 shows a plan view at the location of the Sicily Tower and of the Terminal Structure, together with the available site investigations. The longitudinal section indicated in Figure 10 are shown in Figure 4 and in Figure 5.

The Coastal Deposits unit extends from the ground level over a thickness of about 80 m below the tower foundations and of about 50 m below the terminal structures.

Below this layer the Messina Gravel unit is encountered; at about -70 m a.s.l. an increase in stiffness is observed for about 15 m.

The permeability of the deposits was evaluated by pumping tests carried out from a well located in the area of the Sicily Tower and extending 40 m b.g.l., and by Lefranc permeability tests carried out in a borehole at depths of 10 m b.g.l. to 38 m b.g.l..

		Ponte sullo Stretto di Messina PROGETTO DEFINITIVO		
Seismic analyses for soil-foundation systems, Annex	<i>Codice documento</i> PB0032_F0_ANX	<i>Rev</i> F0	<i>Data</i> 20/06/2011	

Due to the small distance of the source line (sea) from the well, the high permeability and the small compressibility of the deposits, the pumping tests were interpreted assuming steady state conditions (Mansur and Kauffman, 1962). The resulting value of the horizontal permeability is $k_h = 5 \times 10^{-3}$ m/s.

Lefranc permeability tests have a more local character than well pumping tests and are affected by the disturbance created during borehole formation; in addition, their interpretation depends on the assumed ratio k_h/k_v . Their results must therefore be considered reliable within one order of magnitude. The values of k_v assuming $k_h/k_v = 10$ range from 2×10^{-3} to 5×10^{-2} (m/s); for $k_h/k_v = 1$, k_v is not substantially different from that obtained by the well pumping test, being in the range of 2.6×10^{-4} to 5.8×10^{-3} (m/s).

The relative density was estimated from the SPT and LPT results using the procedure proposed by Cubrinovski and Ishihara (1999): values ranging from 40% to 70% in the upper part of the deposit (down to 25÷30 m b.g.l.), and from about 30%÷50% in the lower part were obtained as shown in Figure 11 and in Figure 12.

For the Coastal Deposits, which from a geological point of view can be considered normally consolidated, values of K_0 can be estimated from the values of relative density D_R (SPT and LPT results) using the relationship proposed by Bellotti *et al.* (1985):

$$z < 25 \div 30 \quad 40\% < D_R < 70\% \quad 0.49 > K_0 > 0.43$$

$$z > 25 \div 30 \quad 30\% < D_R < 50\% \quad 0.54 > K_0 > 0.46$$

The Messina Gravel is geologically over-consolidated by erosion of an estimated thickness of at least 100 m, and, in the area of the Sicilian Tower foundation, presently overlain by about 80 m of Coastal Deposits. At a depth of 100 m, geological over-consolidation can account for an increase of the values of K_0 of about 9%; the effect of geological over-consolidation decreases with depth.

The order of magnitude of ageing effects can be estimated using the relationship of Mesri, 1993: the maximum estimated increase of K_0 due to ageing effects is of the order of 30%.

It follows:

$$K_0 = 1.09 \times 1.3 \times K_0(\text{NC}) = 1.42 \times (1 - \sin \phi'_p) = 0.47 \quad (2)$$

in which $\phi'_p = 42^\circ$ as described below.

The angle of shearing resistance at peak $\phi'_p = 42 \div 44^\circ$ (Figure 13 and Figure 14) was evaluated through the relationship proposed by Schmertmann (1975):

		Ponte sullo Stretto di Messina PROGETTO DEFINITIVO		
Seismic analyses for soil-foundation systems, Annex	<i>Codice documento</i> PB0032_F0_ANX	<i>Rev</i> F0	<i>Data</i> 20/06/2011	

for $z < 25\div 30$ m $D_R = 0.70$ $\phi'_p = 44^\circ$
 for $z > 25\div 30$ m $D_R = 0.50$ $\phi'_p = 42^\circ$

The stiffness profile of the deposits was obtained from three cross-hole tests carried out in the vicinity of the Sicilia Tower foundation and one test carried out in the vicinity of the Sicilia Terminal Structures, down to a depth of 100 m b.g.l. The results of the cross-hole tests in terms of shear wave velocity, V_s , versus elevation are given in Figure 15 (a) and in Figure 16 (a). The same results are shown in Figure 15 (b) and in Figure 16 (b) as profiles of small strain shear modulus, G_0 :

$$G_0 = \rho V_s^2 \quad (3)$$

In the Coastal Deposits the variation of G_0 does not vary much with depth oscillating around the value of 100 MPa, but local and sharp increases of G_0 are observed between -20 and -50 m a.s.l.. Below -70 m a.s.l. an increase in stiffness is observed that identifies the Messina Gravel deposits. Table 2 summarizes the main mechanical parameters obtained from the geotechnical characterisation above.

Table 2. Sicilia Tower and Terminal Structure - summary of main mechanical parameters

Geological formation	elevation (m a.s.l.)	D_r (%)	K_0	ϕ'_p (°)	K_h (m/s)	G_0 (MPa)
Coastal Deposits	+5÷-30	70	0.43÷0.49	44	5×10^{-3}	100
Coastal Deposits	<-30	50	0.46÷0.54	42	5×10^{-3}	100
Messina Gravel	-70÷-85	50*	0.46÷0.54*	42*	5×10^{-3}	450÷600

* These values could not be calculated as no in situ test at failure (SPT, LPT, CPT) reached the depth of this formation, and were estimated based on the information retrieved from the other locations on the Calabrian side.

3.2 Calabria shore

The geotechnical site investigations carried out between 1988 and 1992 together with the more recent geological and geophysical investigations performed in the 2010 campaign make it possible to define the general soil profile in the area of the Messina Strait.

Figure 17 shows the soil global profile on the Calabria shore. Starting from ground level and moving downwards the following units are encountered:

1. Depositi Costieri (Coastal Deposits). Sand and gravel with very little or no fine content, with a thickness varying between a minimum of 5 m towards inner land and a maximum of 45 m

		Ponte sullo Stretto di Messina PROGETTO DEFINITIVO		
Seismic analyses for soil-foundation systems, Annex	<i>Codice documento</i> PB0032_F0_ANX	<i>Rev</i> F0	<i>Data</i> 20/06/2011	

towards the sea shore. At this location, these deposits are generally coarser in the first 15 to 20 m b.g.l. and become sandier with depth; towards inner land these deposits are generally sandier. Occasionally, silty peaty layers appear in the lower part of the formation.

2. Ghiaie di Messina (Messina Gravel). Gravel and sand, with very occasional silty layers; difficult to distinguish from the Coastal Deposits and of small thickness, at times totally absent, so that the Coastal Deposits rest directly above the underlying Continental Deposits/Vinco Calcarenite.
3. Depositi Continentali (Continental Deposits)/Calcarenite di Vinco (Vinco Calcarenite). Clayey-sandy deposit, consisting of layers of silt or silt and sand, with significant gravel content/Bio-calcarenite and fossiliferous calcarenite, with thin silty layers. The thickness of this layer varies along the footprint of the tower foundation between a minimum of 2 m towards inner land and a maximum of about 7 m towards the sea shore.
4. Conglomerato di Pezzo (Pezzo Conglomerate). Soft rock, consisting of clasts of different dimensions in a silty-sandy matrix and sandstone. The thickness of this formation is larger than 200 m.
5. Cristallino (Crystalline bedrock). Tectonised granite.

The present level of the ground at the location of the Calabria Tower is about 2.5 m a.s.l.; the sea shore is located at a distance of 50 to 60 m from the centre of the tower foundation. The inclination of the sea bottom in this area is about 26°. The Calabria Terminal Structure is about 200 m far from the Calabria Tower and the ground level is at 40 m a.s.l.

The geotechnical profile in the area of the Calabria Tower is characterised by significant variations of the level of the layers in the direction orthogonal to the coastline and to a lesser extent in the direction parallel to the coastline.

The Calabria Anchor Block is at a distance of about 850 m from the Calabria Tower, that is, at a distance of about 900 m from the seashore. The present level of the ground at the location of the Calabria Anchor Block is between +114 m and +127 m a.s.l. The soil profile in the area of the Calabria Anchor Block is characterised by significant variations of the level of the soil layers in the direction parallel to the coastline and to a lesser extent in the direction orthogonal to the coastline. The groundwater level varies between +95 m a.s.l in the north-west corner of the anchor block and +107 m a.s.l. in the opposite corner, in the south-east position.

		Ponte sullo Stretto di Messina PROGETTO DEFINITIVO		
Seismic analyses for soil-foundation systems, Annex	<i>Codice documento</i> PB0032_F0_ANX	<i>Rev</i> F0	<i>Data</i> 20/06/2011	

The groundwater level results from a steady state seepage between a hydraulic head of about 100 m a.s.l at the anchor block and the surrounding area, to a head of 0 m a.s.l. at the sea, at the location of the tower foundation.

The thicknesses and the mechanical properties of the soil layers encountered at the location of the Calabria Tower and of the Terminal Structure, and that encountered at the location of the Calabria Anchor Block are partially different, as the two locations are more than 800 m distant. In the following, a short geotechnical characterization of the sites is reported in two different sections. A detailed characterization of the soil profile on the Calabria shore is contained in the report *Updated geotechnical characterisation based on the 2010 site and laboratory investigations (CG1003-P-RG-D-P-SB-G3-00-00-00-00_01_A_Upd_Geot_Char_ANX)*.



Figure 18 shows a global geotechnical section of the Calabria shore. Two enlarged and more detailed views of the longitudinal section, respectively referred to the Calabria Tower and Terminal Structure site and to the Calabria Anchor Block site, are reported in Figure 19 and Figure 20.

3.2.1 Calabria Tower and Terminal Structure

The geotechnical profile in the area of the Calabria Tower and of the Calabria Terminal Structure is characterised by significant variations of the level of the layers in the direction orthogonal to the coastline and to a lesser extent in the direction parallel to the coastline. Figure 19 shows an enlarged view of the longitudinal cross section at this site. A plan view of the Calabria Tower site and of the Calabria Terminal Structure site is shown in Figure 21 and Figure 22, respectively, together with the location of the site investigations.

The present level of the ground at the location of the Calabria Tower is at about 2.5 m a.s.l.; the sea shore is located at a distance of 50 to 60 m from the centre of the tower foundation. The inclination of the sea bottom in this area is about 26°. The Calabria Terminal Structure is about 200 m far from the Calabria Tower and the ground level is at 40 m a.s.l. The groundwater level results from steady state seepage between a head of about 32 m a.s.l at a distance of 320 m from the centre of the tower, to a head of 0 m a.s.l. at the sea and at the location of the tower foundation.

Starting from ground level and moving downwards the following units are encountered: a) Coastal Deposits, followed by Messina Gravel; the single thickness of these formations is difficult to evaluate as they are very similar; the global thickness of the cohesionless upper soils is about 60-

		Ponte sullo Stretto di Messina PROGETTO DEFINITIVO		
Seismic analyses for soil-foundation systems, Annex		<i>Codice documento</i> PB0032_F0_ANX	<i>Rev</i> F0	<i>Data</i> 20/06/2011

70 m at the Tower Foundation site, with a progressive reduction toward the inland; b) the thin layer of the Continental Deposits (Vincio Calcarenite) is encountered at the Tower Foundation site, with a maximum thickness of 7 m; it disappears towards the inland; c) the formation of the Pezzo Conglomerate, weathered in its upper 20 - 25 m, overlays the bedrock.

The permeability of the Coastal Deposits was evaluated by pumping tests carried out from a well located in the area of the Calabria Tower and extending 33 m b.g.l., and by Lefranc permeability tests carried out in two boreholes at depths between about 5 m b.g.l. and 45 m b.g.l. The value of the horizontal permeability resulting from the more reliable well pumping tests is $k_h = 2.6 \cdot 10^{-3}$ m/s; the measured value of the ratio between vertical and horizontal permeability ranges between $k_v/k_h = 0.10$ and $k_v/k_h = 0.17$. The permeability of the Pezzo Conglomerate was evaluated by Lugeon tests carried out in one of the boreholes used for Lefranc tests, at pressures of 1, 2, and 3 atm, between depths of 48 to 58 m b.g.l. The results show values of permeability possibly decreasing with depth, with an average value of $2.3 \cdot 10^{-2}$ m/s.

The relative density of the Coastal Deposits and Messina Gravel was estimated from the SPT and LPT results using the procedure proposed by Cubrinovski and Ishihara (1999). At the location of the Calabria Tower and Terminal Structure, the thickness of the upper formation of Coastal Deposits increases moving towards the coast (Figure 19). For this formation, at this site there is a difference in N_{SPT} clearly linked to in situ tests location. In the Northern side (Figure 23), closer to the sea shore, a unique trend can be identified: relative density is higher at shallow depths and decreases to a depth of 20 m, maintaining a rather constant value below this depth. Moving inland (Southern side, Figure 24), the denser shallower deposit tends to disappear, and a larger scatter with no clear trend of test results is observed. The following ranges can be identified: $D_R = 40 - 80\%$ for $z < 20$ m and $D_R = 20 - 60\%$ for $20 \text{ m} < z < 60 \text{ m}$ at the Northern site, and $D_R = 10 - 60\%$ at the southern site.

The Pezzo conglomerate is a mostly cemented material, and therefore SPT results were not used for the evaluation of relative density.

Values of K_0 for the Coastal Deposits can be estimated from the relative density D_R using the relationship proposed by Bellotti *et al.* (1985) for normally consolidated silica sands. This yields values of $K_0 = 0.42 - 0.49$ for the upper 20 m and $K_0 = 0.44 - 0.65$ for higher depths in the Northern side; $K_0 = 0.44 - 0.87$ in the Southern side.

		Ponte sullo Stretto di Messina PROGETTO DEFINITIVO		
Seismic analyses for soil-foundation systems, Annex	<i>Codice documento</i> PB0032_F0_ANX	<i>Rev</i> F0	<i>Data</i> 20/06/2011	

The Pezzo Conglomerate is mostly cemented and geologically relatively old (Miocene); it is likely that the geological history of the formation includes mechanical overconsolidation. An estimate of the values of the coefficient of earth pressure at rest is $K_0 = 0.6-0.9$.

The peak friction angle has been estimated on the bases of SPT results, Schmertmann (1975). The values of φ'_p are shown in Figure 25 (Northern side) and Figure 26 (Southern side). At the Northern side, from ground level to a depth of 20 m, the peak friction angle decreases with depth with values included in the range $38^\circ < \varphi'_p < 44^\circ$, while below 20 m it is $36^\circ < \varphi'_p < 40^\circ$; at the Southern side, the values do not show a clear trend and are dispersed in the range $36^\circ < \varphi'_p < 40^\circ$. The results of triaxial tests carried out on reconstituted specimens taken from four different samples are consistent with the results of the in situ tests.

For the Pezzo Conglomerate, the shear strength parameters were obtained from the results of large diameter (865 mm) plate loading tests carried out in the area of the Calabria Anchor Block (see § 3.2.2 and Figure 33). Values of the cohesion intercept c' were obtained at depths between 5 and 16 m b.g.l. assuming that the friction angle is in the range $\varphi' = 38^\circ-42^\circ$; these values of c' increase with depth up to a value of 70 kPa attained at the depth of 16 m; at larger depths it is conservative to assume that c' does not increase any more. This profile of c' is consistent with the presence at the top of the Pezzo conglomerate unit of a layer of altered conglomerate. The interpretation of some triaxial tests carried out on specimens retrieved from a borehole at the location of Calabria Anchor Block (see § 3.2.2 and Figure 34) confirms that the interpretation of the plate loading test is conservative.

At the Terminal Structure location, a rock dilatometer test was carried out (Figure 27). The friction angle has values between 36° and 40° , while the cohesion has values around 400 kPa, larger than those obtained from the back analysis of the plate loading test previously described. Values of $K_0 = 0.7$ were obtained.

The stiffness characteristics of the deposits were obtained from three cross-hole tests: two of them carried out in the area of the Calabria Tower, the third in the area of the Terminal Structure. The results of cross-hole tests in terms of shear wave velocity V_s versus depth are given in Figure 28, while the small strain shear stiffness $G_0 (= \rho V_s^2)$ profile is shown in Figure 29. The results confirm the presence of a weathered layer in the upper part of the Pezzo Conglomerate geological formation.

		Ponte sullo Stretto di Messina PROGETTO DEFINITIVO		
Seismic analyses for soil-foundation systems, Annex		<i>Codice documento</i> PB0032_F0_ANX	<i>Rev</i> F0	<i>Data</i> 20/06/2011

In the Coastal Deposits G_0 varies from about 50 MPa to about 150 MPa. In the weathered Pezzo Conglomerate, regardless of the absolute depth, G_0 varies from 200 MPa to a maximum of about 800 MPa. For the lower formation of the Pezzo Conglomerate, data from FC FD1 and OTC CH1 505 show a sharper increase of G_0 than those from FC CH1 508, whose location is closer to the sea; for the Pezzo Conglomerate a range of $G_0 = 800 - 2000$ MPa can be considered, the lower values pertaining to the location closer to the footprint of the Tower Foundation.

Table 3 summarises the main mechanical parameters obtained from the geotechnical characterization above.

Table 3: Calabria Tower and Terminal Structure - summary of main mechanical parameters

layer	depth* (m b.g.l.)	D_r (%)	K_0	ϕ'_p (°)	c' (kPa)	K_h (m/s)	G_0 (MPa)
Coastal Deposits (northern site)	0÷20	40÷80	0.42÷0.49	38÷44	---	2.6×10^{-3}	50÷200
Coastal Deposits (northern site)	20÷60	20÷60	0.44÷0.65	36÷40	---	2.6×10^{-3}	50÷200
Coastal Deposits (southern site)	0÷30	10÷60	0.44÷0.87	36÷40	---	2.6×10^{-3}	50÷250
Weathered Conglomerate	30÷80	---	0.6÷0.9	38÷42	0÷70	2.3×10^{-2}	200÷800
Pezzo Conglomerate	>50	---	0.6÷0.9	38÷42	≥ 70	2.3×10^{-2}	800÷2000



*depths are indicative as soil layers are not horizontal

3.2.2 Calabria Anchor Block

The soil profile in the area of the Calabria Anchor Block is characterised by significant variations of the level of the soil layers in the direction parallel to the coastline and to a lesser extent in the direction orthogonal to the coastline. Figure 20 shows an enlarged view of the longitudinal cross section at this site. A plan view of the Calabria Anchor Block site is shown in Figure 30, together with the location of the site investigations.

The ground level at the location of the Calabria Anchor Block is between +114 m and +127 m a.s.l.; the sea shore is at a distance of about 900 m from the anchor block. The groundwater level varies between about +95 m a.s.l. in the north-west corner of the anchor block to about +107 m a.s.l. in the south-east corner.

At the location of the Anchor Block, the Coastal Deposits and Messina Gravel, difficult to distinguish from one another and in the following considered as one layer, have a thickness that varies between a minimum of 7 m towards the north-east corner and a maximum of 18 m towards the south-east corner of the anchor block area. They overly the Pezzo Conglomerate, weathered in

		Ponte sullo Stretto di Messina PROGETTO DEFINITIVO		
Seismic analyses for soil-foundation systems, Annex	<i>Codice documento</i> PB0032_F0_ANX	<i>Rev</i> F0	<i>Data</i> 20/06/2011	

its upper 20 m. Pezzo Conglomerate extends over a thickness of about 130 m. It follows that for the Calabria Anchor Block the relevant geological unit is the Pezzo Conglomerate, with a weathered shallow layer ($20 \text{ m} < z < 40 \text{ m}$), overlain by the Terrace Deposits of small thickness.

The permeability of the Coastal Deposits and of the Pezzo Conglomerate was evaluated by well pumping tests and Lugeon tests carried out in the area of the Calabria Tower (§ 2.2.1). The value of the horizontal permeability resulting from the well pumping tests in the Coastal Deposits is $k_h = 2.6 \cdot 10^{-3} \text{ m/s}$, with a measured value of the ratio between vertical and horizontal permeability ranging between $k_v/k_h = 0.10$ and $k_v/k_h = 0.17$. The permeability of the Pezzo Conglomerate evaluated by Lugeon tests is possibly decreasing with depth, with an average value of $2.3 \cdot 10^{-2} \text{ m/s}$.

Standard and large penetration tests provided high values of N_{SPT} and N_{LPT} in the Coastal Deposits, although a large scatter was observed (Figure 31); an estimate of the coefficient of earth pressure at rest is $K_0 = 0.43 - 0.47$. The Pezzo Conglomerate is cemented and geologically relatively old (Miocene); it is likely that the geological history of the formation includes mechanical overconsolidation. An estimate of the values of the coefficient of earth pressure at rest is $K_0 = 0.6 \div 0.9$.

The relative density of the Coastal Deposits and the Messina Gravel was estimated from the SPT and LPT results using the procedure proposed by Cubrinovski and Ishihara (1999): values of $D_R = 40\%$ to 70% were obtained as shown in Figure 32. The angle of shearing resistance $\varphi' = 41^\circ - 44^\circ$ was then evaluated through the relationship proposed by Schmertmann (1975, Figure 32).

The shear strength parameters of the Pezzo Conglomerate were obtained from the results of large diameter (865 mm) plate loading tests carried out in the area of the Calabria Anchor Block. These were carried out at three different depths of 5, 11.85, and 16 m b.g.l. within a 2.5 m diameter shaft. The results were interpreted adopting the available solutions for the limiting pressure, q_u , of a circular shallow foundations (Berezantzev, 1964):

$$q_u = C_k c' + B_k \gamma D + A_k \gamma \frac{B}{2} \quad (4)$$

in which $\gamma = 20 \text{ kN/m}^3$ is the unit weight of the soil, c' is the cohesion of the soil, $B = 0.865 \text{ m}$ is the diameter of the plate, $D = 0$ is the depth of the plate and A_k , B_k and C_k are capacity factors depending on the friction angle φ' . The values of q_u were obtained directly for the test carried out at 5 m b.g.l. which was taken to failure, and extrapolated with a hyperbolic law for the other two tests. In this manner, for any given value of φ' it is possible to calculate the corresponding value of c' .

		Ponte sullo Stretto di Messina PROGETTO DEFINITIVO		
Seismic analyses for soil-foundation systems, Annex	<i>Codice documento</i> PB0032_F0_ANX	<i>Rev</i> F0	<i>Data</i> 20/06/2011	

Figure 33 shows the values of c' obtained at depths between 5 and 16 m b.g.l. assuming that the friction angle is in the range $\varphi' = 38^\circ \div 42^\circ$. For depths larger than 16 m b.g.l. it is conservative to assume that c' is constant and equal to its value at 16 m b.g.l.; this assumption is consistent with the existence at the top of the Pezzo conglomerate unit of a layer of weathered conglomerate, also shown by the shear wave velocity profiles of the following section. In this type of materials, an increase of cohesion with depth does not affect the friction angle (Jamiolkowski *et al.*, 1991). The interpretation of some TX tests carried out on specimens retrieved from a borehole at the location of Calabria Anchor Block (Figure 34) confirm that the interpretation of the plate loading test is conservative.

The stiffness characteristics of the deposits were obtained from one cross-hole test carried out in the vicinity of the Calabria Anchor Block (AC-BH1), using three boreholes reaching a maximum depth of 100 m b.g.l., at a distance of 5 m from one another. The results of the cross-hole test in terms of shear wave velocity v_s versus depth are given in Figure 35. In Figure 36 the same results are shown as profiles of small strain shear modulus G_0 . This has been obtained from the shear wave velocity as $G_0 = \rho v_s^2$.

The three data sets refer to the values obtained in each of the three boreholes, while the continuous line is the average of the three data at each depth.

The G_0 profile with depth shows three different trends: for $0 \text{ m} < z < 20 \text{ m}$ G_0 increases rapidly from 190 MPa to 1200 MPa; for $20 \text{ m} < z < 40 \text{ m}$ G_0 varies from about 1200 MPa to about 1400 MPa; below $z = 40 \text{ m}$ the data are more dispersed with an average value of 2000 MPa.

Table 4 summarises the main mechanical parameters obtained from the geotechnical characterisation discussed above.

Table 4: Calabria Anchor Block: summary of main mechanical parameters

layer	depth* (m b.g.l.)	D_r (%)	K_0	φ'_p (°)	c' (kPa)	K_h (m/s)	G_0 (MPa)
Coastal Deposits.	0÷20	40÷70	0.43÷0.47	41÷44	---	2.6×10^{-3}	190÷1200
Weathered Conglomerate	20÷40	---	0.6÷0.9	38÷42	0÷70	2.3×10^{-2}	1200÷1400
Pezzo Conglomerate	>40	---	0.6÷0.9	38÷42	≥ 70	2.3×10^{-2}	2000

*depths are indicative as soil layers are not horizontal

		Ponte sullo Stretto di Messina PROGETTO DEFINITIVO		
Seismic analyses for soil-foundation systems, Annex		<i>Codice documento</i> PB0032_F0_ANX	<i>Rev</i> F0	<i>Data</i> 20/06/2011

4 2D Numerical Dynamic Analyses

4.1 Soil model

4.1.1 Geometrical soil model



Figures 37 to 44 show the 2D finite difference mesh used in the analyses. Four different sections were considered for each shore: one longitudinal section, parallel to the bridge, including the tower, the terminal structures, and the anchor block, and three transversal sections, orthogonal to the bridge, one for each main structure (tower, terminal structures, and anchor block). The meshes extend vertically down to the top of the Continental deposits layer in the Sicilia shore, and down to the top of the Crystalline layer in the Calabria shore. The widths of the meshes of the longitudinal sections are 1680 m and 1530 m for the Sicilia and the Calabria shore respectively, while the width of all the meshes of the transversal sections is about 700 m.

In the longitudinal section of the Sicilia shore (Figure 37), the ground level is located at +4 m a.s.l. at the location of the tower foundation and of the terminal structures, and at +56 m a.s.l. at the location of the anchor block; the ground slopes down towards the sea with an angle of 13°. The layer of Messina gravel was further sub-divided into three different regions depending on the values of the shear stiffness of the deposit, as detailed below. The initial distribution of pore water pressures is hydrostatic, with a total head of 0.0 m a.s.l..

The soil layers included in the three transversal sections of the Sicilia shore (Figure 38, Figure 39 and Figure 40) are the same as those used in the 2D longitudinal sections at the locations of the tower, of the terminal structure and of the anchor block. The layers are horizontal and therefore the meshes are symmetric in the horizontal direction.

In the longitudinal section of the Calabria shore (Figure 41), the ground level is located at +4.5 m a.s.l. at the location of the tower foundation, at +40 m a.s.l. at the location of the terminal structures, and at +118 m a.s.l. at the location of the anchor block. The ground slopes down towards the sea with an angle of 25°. The initial distribution of pore water pressures is hydrostatic at the location of both the tower foundation, with a total head of 0.0 m a.s.l., and the anchor block, with a total head of 100 m a.s.l., while the groundwater level in the region between the two structures results from a steady state seepage analysis.

The soil layers included in the three transversal sections of the Calabria shore (Figure 42, Figure

		Ponte sullo Stretto di Messina PROGETTO DEFINITIVO		
Seismic analyses for soil-foundation systems, Annex		<i>Codice documento</i> PB0032_F0_ANX	<i>Rev</i> F0	<i>Data</i> 20/06/2011

43 and Figure 44) are the same as those used in the 2D longitudinal analyses at the locations of the tower, of the terminal structure and of the anchor block. These layers are horizontal in the transversal sections of the tower and of the terminal structures, while they are inclined on the horizontal in the transversal section of the anchor block. The initial distribution of pore water pressures is hydrostatic and the groundwater level is at 18 m b.g.l. in the transversal sections of the terminal structures.

The dimension of the zones in the finite difference mesh is defined in order to have compatibility with the wavelength of the earthquakes applied in the dynamic stage.

4.1.2 Soil constitutive model

In the dynamic analyses, cyclic soil behaviour was described through a hysteretic constitutive model available in the library of the Finite Difference code FLAC. Basically, the model consists in an extension to general strain conditions of the one-dimensional non-linear models that make use of the Masing (1926) rules to produce hysteresis loops. Under plane strain conditions, the relationship between shear stress τ and the corresponding shear strain γ may be expressed as:

$$\frac{\tau}{G_0} = \frac{G_s(\gamma)}{G_0} \cdot \gamma = M_s(\gamma) \cdot \gamma \quad (5)$$

where $G_s(\gamma)$ is the secant shear modulus, function of γ , G_0 is the small-strain modulus and M_s is the normalized secant shear modulus. If the relationship between M_s and γ is known from an appropriate modulus decay curve, then the tangent shear modulus M_t can be evaluated by differentiating the previous equation with respect to γ .

Strain reversal is detected by changes in sign of the scalar product of the current strain increment and the direction of the strain path at the previous time instant. At each strain reversal, the Masing rule is applied by scaling stress and strain differences by one half; this produces hysteresis loops in the stress-strain curves that allow for an appropriate energy dissipation. Figure 45 shows a typical response of the present soil model, as a relationship between the tangential stress τ and the corresponding shear strain γ .

The calibration of the hysteretic model requires the small-strain shear modulus G_0 and a modulus decay curve that describes the reduction of the secant shear modulus with shear strain amplitude. For the present analyses, the small strain shear modulus was calibrated on the basis of the results

		Ponte sullo Stretto di Messina PROGETTO DEFINITIVO		
Seismic analyses for soil-foundation systems, Annex	<i>Codice documento</i> PB0032_F0_ANX	<i>Rev</i> F0	<i>Data</i> 20/06/2011	

of the cross-hole tests and was described as a function of the mean effective stress. The modulus decay for the Messina gravels and the coastal deposits was described using the experimental results obtained by Tanaka *et al.* (1987) on undisturbed gravelly soils (curve 1), while the modulus decay curves for the Pezzo Conglomerate were taken from those included in the EERA code by Bardet *et al.* (2000) for a soft rock (curve 2).

These modulus decay curves can be approximated using the following expression for the function $M_s(\gamma)$:



$$M_s = y_0 + \frac{a}{1 + \exp[-(\log_{10} \gamma - x_0)/b]} \quad (6)$$

using the values for the soil parameters a , b , x_0 and y_0 reported in Table 5 for the two different modulus decay curves.

Table 5. Constitutive parameters used for the hysteretic soil model

curve	a	b	x_0	y_0
1	0.9762	-0.4393	-1.285	0.03154
2	0.9900	-1.1000	-0.100	0.05000

Figure 46 shows a satisfactory comparison between the modulus decay curve predicted using the parameters of Table 5 and the target curve. The same figure also reports for comparison a very similar modulus decay curve provided by Seed & Idriss (1970) for coarse-grained soils and the corresponding variation of the equivalent damping ratio D with the shear strain amplitude. In the present soil model the equivalent damping ratio is merely a response of the constitutive model and cannot be further calibrated. Although for $\gamma > 0.01\%$ this equivalent damping ratio is somewhat higher than that found by Seed & Idriss (1970), it should be remarked that the present numerical analyses use a truly non-linear soil model, and are carried out in the time domain. Therefore, the values of D predicted by the hysteretic model have a different physical meaning than those normally used in a visco-elastic analysis: in an equivalent linear analysis (Schnabel *et al.* 1972), once convergence has been achieved, the secant values of the damping ratio used to compute the dynamic soil response do not vary in time; in the present model the larger equivalent values of D are only activated in the time instants when the strains are largest. Preliminary one-dimensional free-field comparisons between the predictions of the hysteretic soil and those of an equivalent linear calculations with a visco-elastic model (Schnabel *et al.* 1972) yielded a reasonable

		Ponte sullo Stretto di Messina PROGETTO DEFINITIVO		
Seismic analyses for soil-foundation systems, Annex	<i>Codice documento</i> PB0032_F0_ANX	<i>Rev</i> F0	<i>Data</i> 20/06/2011	

agreement, and showed that, under the seismic input used in the present simulations, values of the shear strain larger than 0.01 % are only locally and instantaneously attained.

In the numerical computations, the hysteretic model was used to update at each calculation step the (tangent) shear modulus of an elastic-perfectly plastic soil model with a Mohr-Coulomb failure criterion. For the present analysis, a non-associated flow rule was used, with a constant dilatancy set to zero.

Coupling the hysteretic behavior with a perfectly plastic model has the consequence that plastic strains associated to full strength mobilization can provide additional energy dissipation.

The hysteretic model provides no damping at very small strains. A small viscous damping ($D = 4\%$) was used in the computations, in order to provide some energy dissipation also at small strains. Preliminary parametric studies showed that this small viscous damping does not alter significantly the results, but helps in smoothing out some minor high-frequency response that is an inevitable consequence of the fully explicit time integration scheme used by the FLAC program (Joyner & Chen 1975).

4.1.3 Soil parameters

The mechanical properties of the soil layers in the elasto-plastic soil model of the Sicilia shore are summarized in Table 6 and Table 7.

For all the soil layers, a small non zero value of cohesion has been introduced, which does not influence significantly the results of the analyses. For Coastal deposits and Messina gravels (1) soil layers, the shear modulus at small strain is given by the expression:

$$\frac{G_0}{p_{ref}} = K_G \left(\frac{p' + B}{p_{ref}} \right)^m \quad (7)$$

where p' is the mean effective stress, $p_{ref} = 100$ kPa is a reference pressure, and K_G , B and m were obtained by best fitting of the cross-hole test results. The modulus decay curve 1 was used for the Messina gravels (1) and the Coastal deposits, while the curve 2 was used for the Messina gravels (2) and (3) and for the Continental deposits. The porosity and the permeability of the soil layers are always $n = 0.5$ and $k_h = 10^{-3}$ m/s respectively.

		Ponte sullo Stretto di Messina PROGETTO DEFINITIVO		
Seismic analyses for soil-foundation systems, Annex	<i>Codice documento</i> PB0032_F0_ANX	<i>Rev</i> F0	<i>Data</i> 20/06/2011	

Table 6. Sicilia shore. Numerical simulation: physical and mechanical properties of soil layers

layer	Model	hysteretic curve	γ (kN/m ³)	c' (kPa)	ϕ' (°)
Coastal deposits (z<30 m b.g.l.)	MC	1	20	2	44
Coastal deposits (z>30 m b.g.l.)	MC	1	20	2	42
Messina Gravel (1) (z<30 m b.g.l.)	MC	1	20	2	44
Messina Gravel (1) (z>30 m b.g.l.)	MC	1	20	2	42
Messina Gravel (2)	MC	2	20	2	42
Messina Gravel (3)	MC	2	20	2	42
Continental deposits	MC	2	20	2	42

Table 7. Sicilia shore. Numerical simulation: stiffness parameters of soil layers

layer	ν	K_G	B (kPa)	m	G_0 (Mpa)	K_0 (Mpa)
Coastal deposits (z<30 m b.g.l.)	0.2	800	15	0.5	-	-
Coastal deposits (z>30 m b.g.l.)	0.2	800	15	0.5	-	-
Messina Gravel (1) (z<30 m b.g.l.)	0.2	892	60	0.86	-	-
Messina Gravel (1) (z>30 m b.g.l.)	0.2	892	60	0.86	-	-
Messina Gravel (2)	0.2	-	-	-	2420	3227
Messina Gravel (3)	0.2	-	-	-	3645	4860
Continental deposits	0.2	-	-	-	3645	4860

The mechanical properties of the soil layers in the elasto-plastic soil model of the Calabria shore are summarized in Table 8 and Table 9.

For the Coastal deposits, the Messina gravels and the Terrace deposits a small non zero value of cohesion was introduced for numerical stability, that cannot influence the results of the analyses. For the layer of weathered Pezzo Conglomerate a reduced value of cohesion, $c' = 35$ kPa, was assumed consistently with the indications of the plate loading tests.

For Coastal deposits and Terrace deposits layers, the shear modulus at small strain is defined as a function of the mean effective stress, through eq (7) above, where K_G , B and m were obtained by best fitting of the cross-hole test results. Modulus decay curve 1 was used for the Coastal and Terrace deposits and for the Weathered Conglomerate, while curve 2 was used for the other

		Ponte sullo Stretto di Messina PROGETTO DEFINITIVO		
Seismic analyses for soil-foundation systems, Annex	<i>Codice documento</i> PB0032_F0_ANX	<i>Rev</i> F0	<i>Data</i> 20/06/2011	

layers. The porosity and the permeability of the soil layers are always $n = 0.5$ and $k_h = 10^{-3}$ m/s respectively.

Table 8. Calabria shore. Numerical simulation: physical and mechanical properties of soil layers

layer	Model	hysteretic curve	γ (kN/m ³)	c' (kPa)	ϕ' (°)
Coastal deposits	MC	1	20	2	44
Messina Gravel	MC	2	20	2	42
Weathered Conglomerate	MC	1	20	35	40
Pezzo Conglomerate	MC	2	20	70	40
Terrace deposits	MC	1	20	2	40
Crystalline	elastic	2	20	-	-



Table 9. Calabria shore. Numerical simulation: stiffness parameters of soil layers

layer	ν	K_c	B (kPa)	m	G_0 (Mpa)	K_0 (Mpa)
Coastal deposits	0.2	800	15	0.5	-	-
Messina Gravel	0.2	-	-	-	3645	4860
Weathered Conglomerate	0.2	-	-	-	563	750
Pezzo Conglomerate	0.2	-	-	-	750	1000
Terrace deposits	0.2	5000	15	1	-	-
Crystalline	0.2	-	-	-	5780	7705

4.2 Structural elements

4.2.1 Equivalent dimensions

Dynamic analyses were carried out under 2D conditions both in the longitudinal and transversal directions. In the plane strain analyses, the real foundations of the different structures (towers, terminal structures, and anchor blocks) had to be replaced by equivalent strip footings, as detailed below.

		Ponte sullo Stretto di Messina PROGETTO DEFINITIVO		
Seismic analyses for soil-foundation systems, Annex		<i>Codice documento</i> PB0032_F0_ANX	<i>Rev</i> F0	<i>Data</i> 20/06/2011

Towers

In the longitudinal 2D analyses, the real foundation of each tower, consisting of two circular footings of diameter $D = 55$ m or $D = 50$ m for Sicilia and Calabria, respectively, at a centre-to-centre distance $i = 77.15$ m, was replaced by one equivalent strip footing of width B_{eq} . The equivalent unit loads to be applied to the equivalent strip foundation were obtained by dividing the loads applied to the real foundation by an equivalent length, L_{eq} .

The equivalent dimensions, B_{eq} and L_{eq} , were obtained from the condition that the settlement and the rotation of the equivalent strip under the equivalent loads should be equal to the settlement and the rotation of the actual 3D foundation under the corresponding applied loads. Linear elastic analyses were used to establish the equivalence: to this purpose, the solutions for the settlement and the rotation of a rigid circular footing and a rigid strip on an isotropic linear elastic half space published by Gerrard & Harrison (1970) were used, accounting for the interaction between the two adjacent circular footings.

Stress increments produced by the loads applied at the bottom of the footings (-15 m a.s.l.) were evaluated, and the resulting strains were integrated over the thickness of the deformable layer. In linear elasticity the equivalent dimensions do not depend on the elastic modulus, E , nor on the value of the applied loads, while they depend on the thickness of the deformable layer, H . The thickness of the deformable layer below the level of foundation of the Sicilia and of the Calabria Towers are $H = 70$ m and $H = 18$ m, respectively. The equivalent dimensions were then found as those minimising the magnitude of the difference of the solutions obtained for the equivalent strip foundation and the 3D foundation. The obtained minimising values of the equivalent dimensions are $B_{eq} = 41.25$ m and $L_{eq} = 146.75$ m and $B_{eq} = 40.4$ m and $L_{eq} = 129.4$ m for the Sicilia Tower and the Calabria Tower, respectively.

In the transversal 2D analyses, the foundation of each tower was replaced by two equivalent strip footings of width $B_{eq} = D$. The equivalent unit loads to be applied to each equivalent strip foundation were obtained by dividing the loads applied to the real foundation by an equivalent length, L_{eq} . As the two footings interact with one another, the equivalent length, L_{eq} , was obtained from the condition that the settlement of each equivalent strip under the equivalent loads should be equal to the settlement of a rectangular foundation with dimensions $B = l + D$ and $L = D$, under the total load applied to the two footings. In this case, the settlements of the rectangular enveloping foundation and of the strip footings were calculated using the elastic solutions by Gazetas (1991).

		Ponte sullo Stretto di Messina PROGETTO DEFINITIVO		
Seismic analyses for soil-foundation systems, Annex	<i>Codice documento</i> PB0032_F0_ANX	<i>Rev</i> F0	<i>Data</i> 20/06/2011	

Terminal structures

The foundation of each terminal structure consists of two rectangular footings of dimensions $B = 21.2$ m, in the longitudinal direction, and $L = 70.0$ m, in the transversal direction, at an axis-to-axis distance $i = 55.0$ m, in the longitudinal direction, or $B = 20.0$ m, $L = 75.0$ m, and $i = 32.0$ m, for the Sicilia and Calabria shores, respectively. As no loads were applied to the terminal structures the real dimensions of the foundations were kept both in the longitudinal and transversal sections.



Anchor Blocks

Figure 47 shows a plan view and a longitudinal section of the Sicilia anchor block as defined in the tender design; it consists of a reinforced concrete block with a trapezoidal shape in plane. It is 100 m long in the longitudinal direction while in the transversal direction the smaller side is about 80 m in length, whereas the larger one is about 120 m long, with an average width of 100 m. The top and the bottom of the block consist of different planes, respectively: the front of the anchor block has an inclination of about 15° at the top and of about 25° at the bottom; the rear end of the anchor block has an inclination of about 7° at the top and of about 8° at the bottom.

Figure 48 shows a plan view and a longitudinal section of the Calabria anchor block as defined in the tender design; it consists of a reinforced concrete block, with the shape of a trapezoid-based prism. The dimensions in plan of the upper rectangle are 98 m in the transversal direction and 87.5 m in the longitudinal direction; the lower rectangle at the base has dimensions of 98 m in the transversal direction and 25 m in the longitudinal direction.

In the longitudinal sections the blocks were substituted by strip footings with the same shape and dimensions of the real anchor blocks. The equivalent unit loads to be applied to the equivalent strip foundations were obtained by dividing the loads applied to the real blocks by an equivalent length, $L_{eq} = 184$ m, for both the Sicilia and Calabria anchor blocks. This equivalent length was obtained from the condition that the vertical and horizontal displacements of the equivalent strips under the equivalent loads should be equal to the vertical and horizontal displacements of the actual blocks under the applied loads.

In the transversal direction, the blocks were substituted by rectangular strip footings of $B = 118$ m, and $B = 100$ m, for the Sicilia and Calabria anchor blocks respectively. As for the longitudinal

		Ponte sullo Stretto di Messina PROGETTO DEFINITIVO		
Seismic analyses for soil-foundation systems, Annex	<i>Codice documento</i> PB0032_F0_ANX	<i>Rev</i> F0	<i>Data</i> 20/06/2011	

sections, the equivalent unit loads to be applied to the equivalent strip footings were obtained by dividing the loads applied to the real block by an equivalent length, $L_{eq} = 119$ m and $L_{eq} = 139$ m, for the Sicilia and the Calabria blocks respectively, obtained from the condition that the vertical and horizontal displacements of the equivalent strip under the equivalent loads should be equal to the vertical and horizontal displacements of the actual blocks under the applied loads.

In all cases, the displacements of the actual foundations and of the strip footings were calculated using the elastic solutions by Gazetas (1991).

4.2.2 Towers

The structural model of the tower included in analyses was derived starting from simplified 2D finite element models prepared by E.d.in. S.r.l.. These model consist of concentrated masses and one-dimensional beams as shown in Figure 49. The top of the tower is connected to springs representing the stiffness of the suspension system. For use within the present soil-structure interaction analyses, the base contact between the tower and its foundation was modelled through weightless beam elements of high stiffness ($E = 3 \times 10^7$ kN/m², $A = 1 \times 10^2$ m²/m, $I = 1 \times 10^4$ m⁴/m), in order to make rotations equal with those of the foundation plinths.

Before carrying out the interaction dynamic numerical analyses, the dynamic response of the simplified structural models of the towers was tested through specific time-domain dynamic analyses. Specifically, the first natural vibration frequency of the model and the first normalised modal shape were defined with the procedure outlined below.

A wavelet pulse was applied to the base of the tower and the natural frequencies of vibration were evaluated from the Fourier spectra of the free vibrations of selected nodes of the tower. Alternatively, a sinusoidal displacement time history with a duration of 100s and a linear continuous sweep of frequency between 0.2 Hz and 2 Hz was applied to the base of the models and the natural frequencies of vibration were evaluated from Fourier spectra of the displacement time histories of selected nodes of the model, while the first modal shape was recovered at the time instants in which the displacements of the tower were maximum.

The results of these preliminary analyses in terms of natural frequencies of vibration are summarised in Figure 50 and Figure 51 for the longitudinal models of the Sicilia and Calabria towers, respectively, and in Figure 52 and Figure 53 for the transversal models of the Sicilia and

		Ponte sullo Stretto di Messina PROGETTO DEFINITIVO		
Seismic analyses for soil-foundation systems, Annex	<i>Codice documento</i> PB0032_F0_ANX	<i>Rev</i> F0	<i>Data</i> 20/06/2011	

Calabria towers, respectively. The first natural frequency of the structure of the Sicilia tower is $f_n = 0.39$ Hz in the longitudinal direction and $f_n = 0.34$ Hz in the transversal direction; for the Calabria tower the first natural frequency of the structure is $f_n = 0.39$ Hz in the longitudinal direction and $f_n = 0.30$ Hz in the transversal direction.

The first modal shapes obtained in both the longitudinal and transversal direction for the simplified 2D model of the tower structures are shown in Figure 54 and Figure 55, for the Sicilia tower and the Calabria tower, respectively. The comparison with the first modal shape obtained in the longitudinal direction from the full 3D model of the same structures is indeed very good.

Foundations

The foundations of the towers were assumed to behave as an elastic material with the properties listed in Table 10. The equivalent unit weight of the foundations in the longitudinal and transversal sections was obtained from the condition that the self-weight of the real 3D foundation should be equal to the self-weight of the equivalent 2D foundation. Two portions of the foundations were considered, one above and one below the ground level, of unit weight γ_1 and γ_2 respectively. Table 10 reports the values of γ_1 and γ_2 computed for the 2D analyses in the longitudinal and transversal sections.

Table 10. Properties of the tower foundations

shore	section	γ_1 (kN/m ³)	γ_2 (kN/m ³)	ν	E (MPa)
sicilia	longitudinal	10.03	23.83	0.15	4.0E+04
sicilia	transversal	12.07	23.45	0.15	4.0E+04
calabria	longitudinal	10.99	22.91	0.15	4.0E+04
calabria	transversal	10.16	22.17	0.15	4.0E+04

Jet grouting

The soil below the tower foundations will be treated with secant jet grouting columns, of a nominal diameter of 0.6 m, extending down to a depth of 37 m b.g.l. on the Sicilia shore and down to the Pezzo Conglomerate on the Calabria shore. Moreover, jet-grouting will be used to treat the soil adjacent to the tower foundations, extending about 30-40 m from the external perimeter of the foundations, and down to a depth of about 30 m b.g.l. on the Sicilia shore and to the Pezzo Conglomerate on the Calabria shore. The ratio of the treated area to the total area of soil is $A_{tr}/A_{tot} = 100\%$ below the tower foundations and to 42% in the area around the tower foundations. The mechanical properties of the jet-grouted columns were obtained using the values of the design unconfined strength $\sigma_c = 6$ MPa and of the ratio $E/\sigma_c = 500$, proposed by Rocksoil, and published

		Ponte sullo Stretto di Messina PROGETTO DEFINITIVO		
Seismic analyses for soil-foundation systems, Annex	<i>Codice documento</i> PB0032_F0_ANX	<i>Rev</i> F0	<i>Data</i> 20/06/2011	

results (Croce *et al.*, 2004). The mechanical properties of the jet-grouted areas reported in Table 11 were then computed using a homogenisation procedure based on the percentages of treated area of soil. Modulus decay curve 1 was used for the jet-grouted soil below the tower foundations, while curve 2 was assumed for the lateral jet grouted soil.

Table 11. Model parameters for the jet-grouted soil

	Model	hyst. curve	γ (kN/m ³)	c' (kPa)	ϕ' (°)	ν	G_0 (Mpa)
jet grouting	MC	2	22	1560	35	0.2	1250
lateral jet grouting	MC	1	22	655	35	0.2	525

Connection beam

In the transversal 2D analyses of the Sicilia and Calabria Towers the connection beam between the foundations of the two columns is modelled with elastic beam elements located at the ground surface. Table 12 shows the mechanical and geometrical properties of the connection beams.

Table 12. Numerical simulation: geometrical and mechanical properties of the connection beam elements

shore	ν	E (MPa)	A (m ² /m)	I (m ⁴ /m)
sicilia & calabria	0.2	3.4E+04	2.79	55.9

Applied loads

In the dynamic analyses, additional vertical loads equal to the difference between the normal load applied to the base of each tower, $N = 2.6 \times 10^5$ t, and the sum of the structural weights due to the lumped masses included in the simplified models of the towers were applied to the foundations of the towers. These were equal to 1.45×10^5 t, in the longitudinal direction and to 2.02×10^5 t in the transversal direction for the Sicilia tower, and to 1.24×10^5 t in the longitudinal direction and 2.02×10^5 t in the transversal direction for the Calabria tower. All normal loads were divided by the equivalent lengths to obtain the unit loads applied to the model foundations.

4.2.3 Anchor blocks

The anchor blocks were assumed to behave as an elastic material with the properties listed in Table 13. The equivalent unit weight of the anchor blocks in the longitudinal and transversal sections was obtained from the condition that the self-weight of the real 3D block should be equal to the self-weight of the equivalent 2D block.

		Ponte sullo Stretto di Messina PROGETTO DEFINITIVO		
Seismic analyses for soil-foundation systems, Annex		<i>Codice documento</i> PB0032_F0_ANX	<i>Rev</i> F0	<i>Data</i> 20/06/2011

Table 13. Properties of the anchor blocks

shore	section	γ (kN/m ³)	ν	E (MPa)
sicilia	longitudinal	24.8	0.15	4.0E+04
sicilia	transversal	25.1	0.15	4.0E+04
calabria	longitudinal	21.8	0.15	4.0E+04
calabria	transversal	21.6	0.15	4.0E+04

Forces transmitted by the suspension cables were applied to the anchor blocks in the longitudinal models, according to the structural analyses carried at the tender design stage for the ULS load combinations. These are equal to $F = 3933$ MN and $F = 3964$ MN for the Sicilia and Calabria blocks, respectively, with an inclination of 15 degrees to the horizontal, upwards, toward the sea. These forces were divided by the equivalent lengths to obtain the unit loads to apply to the equivalent 2D models of the block, and were applied in the convergence node of the cables of the bridge, as indicated in the tender design.

4.2.4 Terminal structures

In all models, the foundations of the terminal structures were assumed to behave as elastic solids with a unit weight $\gamma = 25$ kN/m³, a Poisson's ratio $\nu = 0.15$ and a Young's modulus $E = 4.0 \times 10^4$ MPa. On the Sicilia shore the soil below the foundations of the terminal structures will be treated with secant jet grouting columns, of a nominal diameter of 0.6 m, extending down to a depth of 26 m b.g.l., with a ratio of the treated area to the total area of soil $A_{tr}/A_{tot} = 100\%$. The mechanical properties of the jet-grouted soil below the foundations of the terminal structures are the same as those of the jet-grouted soil below the foundations of the towers (see Table 11 above).

No loads other than self weight were applied to the foundations of the terminal structures.

4.3 Procedure of analysis

The 2D numerical analyses include an initial static stage, in which the correct initial stress state and pore pressures in the soil mass are computed, followed by a dynamic stage, in which the scenario earthquakes are applied to the base of the models.

During the static stage, the base of the mesh was fixed so as to prevent displacements in all directions, and the horizontal displacements of all vertical boundaries were inhibited. Moreover, a

		Ponte sullo Stretto di Messina PROGETTO DEFINITIVO		
Seismic analyses for soil-foundation systems, Annex	<i>Codice documento</i> PB0032_F0_ANX	<i>Rev</i> F0	<i>Data</i> 20/06/2011	

reduced secant shear modulus is introduced for the upper soil layers, to take into account the shear strain level induced into the soil during the construction sequences of the bridge. The computed displacement produced by the static loads were in good agreement with those evaluated with static three-dimensional finite-element analyses.



After the initial stress state at rest is calculated, displacements of all the nodes are reset to zero and the secant shear modulus is updated for the soil layers where this is defined as a function of the mean effective stress. The structural element of the bridge are then activated: the equivalent unit weights of the foundations of the towers and of the terminal structures, and those of the anchor blocks, are activated together with the static loads applied at the tower foundations and at the anchor blocks. At the end of the static stage all displacements are reset to zero, and the shear modulus of the soils is set to its small strain value, G_0 , which is a function of the newly computed effective stress state, that takes into account the stress change induced by the construction of the bridge.

Before applying the seismic input to the base of the model, all lateral restraint are removed from the vertical boundaries of the mesh. On the vertical sides of the mesh, FLAC free-field boundary conditions are applied: the lateral boundaries of the main grid are coupled to free-field columns through viscous dashpots, similar to the quiet boundaries developed by (Lysmer & Kuhlemeyer, 1969). Along these free-field columns a one-dimensional seismic response analysis is carried out in parallel with the main grid calculation. In this way, the dashpots are activated to absorb energy only when the main grid motion differs from that of the free-field columns.

The time increment used in the explicit time integration scheme is $\Delta t = 5 \times 10^{-6}$ s in all analyses but in the dynamic analysis of the transversal section of the Sicilia tower, where the time interval is $\Delta t = 2.5 \times 10^{-6}$ s.

The constitutive model adopted for the soil dissipates energy via hysteresis loops. In addition, a moderate amount of viscous damping (damping ratio $D = 4\%$) was introduced, to provide some energy dissipation at small strains (see section 4.1.2). For the structural elements, a local damping equivalent to a viscous damping ratio $D = 5\%$ was introduced. Local in FLAC damping operates by adding or subtracting mass from structural nodes at a certain time during a cycle of oscillation; there is overall conservation of mass because the amount added is equal to the amount subtracted at any stage of calculation.

The seismic inputs were applied to the base of the numerical models following the procedures described in section 4.4. The analysis was carried out under drained conditions, that is neglecting potential changes in pore water pressure that may be induced by the earthquake.

		Ponte sullo Stretto di Messina PROGETTO DEFINITIVO		
Seismic analyses for soil-foundation systems, Annex		<i>Codice documento</i> PB0032_F0_ANX	<i>Rev</i> F0	<i>Data</i> 20/06/2011

4.4 Seismic input

Two scenario earthquakes were used in the 2D dynamic analyses, namely the acceleration time histories corresponding to records N14 (Kocaeli earthquake 17 Aug 1999, Arcelik station) and NZ (New Zealand Earthquake 03 Sept 2010, Darfield station) selected by prof. Braga.

(see documents CG3600_P_CL_D_P_SB_A2_G0_00_00_00_01_A_Analisi and CG3600_P_RX_D_P_SB_A2_G0_00_00_00_01_A_Seismic.Action).



Figure 56 and Figure 57 show the three recorded components, two horizontal and one vertical, of the two earthquakes, together with their Fourier spectra. Both records were taken to be representative of outcrop motions $a_{outcrop}$.

The seismic inputs to be applied at the base of the models were computed from the outcrop acceleration time histories by one dimensional de-convolution to the depth of the bedrock and upward propagation to the elevation corresponding to the bottom of the mesh, following the procedure outlined schematically in Figure 58 and Figure 59. The bedrock was taken to correspond to the top of the Pezzo Conglomerate on the Sicilia shore and to the top of the Crystalline on the Calabria shore. The shear stiffness of the Pezzo Conglomerate on the Sicilia shore at a depth of 450 m b.g.l., ($G = 5780$ MPa, Faccioli, DT_ISP_S_E_R1_001 03 Apr 2004, DT_ISP_S_E_R2_001 22 OCT 2004) is sufficiently high compared to the stiffness of the superficial deposits of interest for the structures to be considered as the bedrock; anyway, the stiffness of this elastic bedrock is explicitly taken into account in the procedure outlined below. The soil layers included in each one-dimensional column are the same as those used in the 2D analyses at the locations specified in Figure 58 and Figure 59. On the Sicilia shore, while the two-dimensional calculation grid extends to the top of the continental deposits, the one-dimensional column used to obtain the acceleration time histories at the base of the model is deeper, reaching the top of the Pezzo Conglomerate.

To satisfy the zero shear stress condition at the free surface, the amplitudes of the upward and downward propagating accelerations at the soil surface must be equal. Therefore, the upward propagating wave motion in the bedrock $a_{l,bedrock}$ can be computed as one half of the outcrop motion:

$$a_{l,bedrock}(t) = 0.5 \cdot a_{outcrop}(t) \quad (8)$$

The upward propagating acceleration can then be converted to a stress wave (Joyner & Chen 1975):

		Ponte sullo Stretto di Messina PROGETTO DEFINITIVO		
Seismic analyses for soil-foundation systems, Annex	<i>Codice documento</i> PB0032_F0_ANX	<i>Rev</i> F0	<i>Data</i> 20/06/2011	

$$\begin{aligned}
 \tau(t) &= 2\rho V_s v_{x,l}(t) \\
 \sigma(t) &= 2\rho V_p v_{y,l}(t)
 \end{aligned}
 \tag{9}$$

where $\rho = 2 \text{ Mg/m}^3$ is the mass density, V_s and V_p are the shear and compression wave velocities of the bedrock, and $v_{x,l}$ and $v_{y,l}$ are the horizontal and vertical components of the incident particle velocity computed by integrating of the upward propagating acceleration.

In addition to the stress time histories, quiet boundaries are applied at the bottom of the one-dimensional columns, which consist of dashpots attached independently to the boundary in the normal and tangential directions. The dashpots provide viscous normal and shear tractions:

$$\begin{aligned}
 t_s &= -\rho V_s v_x \\
 t_n &= -\rho V_p v_y
 \end{aligned}
 \tag{10}$$

where v_x and v_y are the horizontal and vertical components of the velocity at the bottom boundary. The simultaneous application of the stress time histories and the quiet boundaries at the bottom of the one-dimensional columns permits to take into account the finite stiffness of the bedrock.

On both Sicilia and Calabria shores, deconvolution and upward propagation was carried out twice for each earthquake, combining the vertical component with either the maximum (H_{\max}) or the minimum (H_{\min}) horizontal component of the acceleration (see Table 14). The recorded accelerations were filtered using a Butterworth low-pass filter at 15 Hz, for compatibility with the dimensions of the elements of the mesh, and a quadratic baseline correction was applied before they were converted into stress time histories. To reduce the computational time for earthquake NZ, with a total duration of about 82 s, only the accelerations between 15 s and 70 s of the original recording were considered in the 2D numerical analyses.

The vertical and horizontal accelerations computed in the one-dimensional numerical analyses at a depth corresponding to the base of the numerical model ($z = 220 \text{ m b.g.l.}$ for the Sicilia shore and $z = 370 \text{ m b.g.l.}$ for the Calabria shore) were used as the input motions for the 2D numerical analyses. The vertical accelerations computed at the base of the model combining the vertical acceleration with either H_{\max} or H_{\min} are practically identical. Therefore, the vertical acceleration time histories extracted from analyses 1, 3, 5, and 7 in Table 14 are considered as the vertical input motion for the 2D analyses, both in the longitudinal and transversal direction. Figure 60 and Figure 61 compare the computed input acceleration time histories with the original records of outcrop motions.

		Ponte sullo Stretto di Messina PROGETTO DEFINITIVO		
Seismic analyses for soil-foundation systems, Annex	<i>Codice documento</i> PB0032_F0_ANX	<i>Rev</i> F0	<i>Data</i> 20/06/2011	

Table 14. One-dimensional de-convolution and upward propagation analyses

deconvolution analysis	shore	design earthquake	horizontal acceleration	vertical acceleration
1	sicilia	N14	H _{max}	V
2	sicilia	N14	H _{min}	V
3	sicilia	NZ	H _{max}	V
4	sicilia	NZ	H _{min}	V
5	calabria	N14	H _{max}	V
6	calabria	N14	H _{min}	V
7	calabria	NZ	H _{max}	V
8	calabria	NZ	H _{min}	V

The input seismic records were applied to the base of the 2D models using the four combinations summarised in Table 15. A positive sign for the horizontal acceleration indicates that this is positive toward South and toward East, in the longitudinal and transverse section, respectively.

Table 15. Seismic input combinations used in dynamic stages of 2D numerical analyses

combination	Longitudinal	Transversal	Vertical
1	H _{max}	H _{min}	V
2	-H _{max}	-H _{min}	V
3	H _{min}	H _{max}	V
4	-H _{min}	-H _{max}	V

4.5 Results of the analyses

The results of the soil-structure interaction analysis were expressed in terms of time-histories of displacements and rotations at selected points in the anchor blocks, tower foundations, and terminal structures. These time-histories constitute the input to additional structural dynamic analyses of the bridge.

The main results of the analyses are summarised in Table 16 to Table 19 and in Figure 62 to Figure 67. Table 16 and Table 17 collect the final displacements and rotations of the bridge foundations, for the two seismic records N14 and NZ and for the four different ways in which each

		Ponte sullo Stretto di Messina PROGETTO DEFINITIVO		
Seismic analyses for soil-foundation systems, Annex	<i>Codice documento</i> PB0032_F0_ANX	<i>Rev</i> F0	<i>Data</i> 20/06/2011	

record can be applied at the model boundaries (combinations 1 to 4, see chapter 4.4) The sign of displacements and rotations is consistent with the reference axes of the calculation grids (rotations positive counter-clockwise)

These final displacements and rotations are plotted in the bar charts of Figure 62 to Figure 65. Rotations in the transversal plane are always negligible and were not plotted in the bar charts. The longitudinal permanent displacements and rotations in these figures are always directed towards the sea.

As a general comment, the maximum permanent horizontal displacements in the longitudinal direction occur on the Calabria side, while the maximum horizontal displacements in the transversal direction take place on the Sicily shore. The order of magnitude of the final horizontal displacements induced by the two seismic records is comparable. The towers' foundations move toward the sea of about 20 mm (Sicily) to 30 mm (Calabria), the corresponding rotation in the longitudinal plane being of about 0.005 deg (Sicily) and 0.015 deg (Calabria). The horizontal displacements of the foundations of the Sicily tower in the transversal direction is of about 16 mm, while that of the Calabria tower is smaller than 2 mm.

The anchor blocks undergo permanent displacements that are always smaller than 10 mm (Sicily) and 20 mm (Calabria) in the longitudinal direction. Permanent transversal displacements of the Sicily anchor block is smaller than 4 mm, while that of the Calabria anchor block is negligible. Earthquake-induced settlements are larger for the foundations of the Calabria tower and the Sicily terminal structure, but they do not exceed 10 mm.

In general, the foundations of the terminal structure show permanent displacements that are somewhat intermediate between those of the towers and of the anchor blocks. An exception is represented by the longitudinal rotation of the foundation of the Sicily terminal structure, that is the largest on the Sicily side, attaining about 0.01 deg.

Table 18 and Table 19 report the maximum accelerations computed in the bridge foundations during the earthquakes. These maximum accelerations are plotted in the bar charts of Figure 66 and Figure 67, where the maximum accelerations applied to the base of the calculation grids are also shown for comparison. Note that the deconvolution analyses yielded smaller maximum accelerations at the base of the Sicily calculation grids.

Inspection of Figure 66 and Figure 67 reveals that the most significant amplifications are computed on the Calabria side for both the seismic records. Conversely, the horizontal accelerations on the Sicily side undergo some de-amplification, notably for the NZ seismic record. Therefore, the

		Ponte sullo Stretto di Messina PROGETTO DEFINITIVO		
Seismic analyses for soil-foundation systems, Annex	<i>Codice documento</i> PB0032_F0_ANX	<i>Rev</i> F0	<i>Data</i> 20/06/2011	

maximum horizontal acceleration in the Calabria foundations reaches about 0.4 – 0.45 g for the NZ record, while the horizontal acceleration in the Sicily side is always smaller than 0.3 g.

The N14 seismic record is characterised by peak accelerations significantly smaller than those of the NZ record, and this is reflected in the smaller values of the accelerations computed in the bridge foundations. Remarkably, the N14 seismic record is still able to produce displacements similar to those induced by the NZ record, probably for its frequency content, richer in low frequencies.

The vertical acceleration is significantly amplified for all the foundation elements, and this amplification is similar on the Sicily and the Calabria sides.

Figure 68 to Figure 91 show a selection of the computed time-histories, in terms of both accelerations and displacements. Acceleration time histories are always shown together with their Fourier spectra. Specifically, these figures show acceleration and displacement time histories in the longitudinal direction only; the Calabria time histories are relative to combination 1, while the Sicily time histories refer to combination 2.

Permanent displacements are accumulated in the first 10 s (for the NZ record) and in the first 5-6 s (for the N14 record) of strong motion. Comparison of the Fourier spectra at the foundations and at the grid base show that on the Calabria side significant amplifications occur at frequencies as large as about 3 Hz, and this is consistent with the finding that the largest displacements of the Calabria foundations are produced by the NZ records, which is richer in these frequencies. Conversely, the Sicily side amplifies smaller frequencies (1 – 1.5 Hz), that mostly characterize the N14 record, and this may account for the significant displacements that this record is capable to produce even with the small peak accelerations shown in Figure 66.

		Ponte sullo Stretto di Messina PROGETTO DEFINITIVO		
Seismic analyses for soil-foundation systems, Annex		<i>Codice documento</i> PB0032_F0_ANX	<i>Rev</i> F0	<i>Data</i> 20/06/2011

Table 16. Displacements and rotations at the end of Earthquake N14

location	comb.	shore	horizontal displacements		vertical displacements		rotations	
			longitudinal mm	transversal mm	longitudinal mm	transversal mm	longitudinal °	transversal °
block	1	sicilia	-6.9	-1.6	-0.9	0.7	0.0015	0.0003
tower (column sx)	1	sicilia	-6.4	0.2	-1.7	-1.6	0.0027	0.0018
tower (column dx)	1	sicilia	-6.4	0.7	-1.7	-0.1	0.0027	0.0003
terminal struct. sx	1	sicilia	-11.8	1.6	-0.1	-1.4	0.0043	0.0009
terminal struct. dx	1	sicilia	-9.9	1.6	-1.4	-1.4	-0.0004	0.0009
block	1	calabria	-7.0	0.2	1.1	-0.3	-0.0005	0.0000
tower (column sx)	1	calabria	-30.7	1.8	-8.5	0.0	0.0113	0.0001
tower (column dx)	1	calabria	-30.7	1.8	-8.5	0.2	0.0113	0.0000
terminal struct. sx	1	calabria	-10.3	0.6	-0.6	0.0	0.0009	0.0000
terminal struct. dx	1	calabria	-9.4	0.6	-0.1	0.0	0.0008	0.0000
block	2	sicilia	6.4	1.6	0.5	0.7	-0.0012	0.0003
tower (column sx)	2	sicilia	18.1	-0.2	-3.1	-1.6	0.0017	0.0018
tower (column dx)	2	sicilia	18.1	-0.7	-3.1	-0.1	0.0017	0.0003
terminal struct. sx	2	sicilia	7.5	-1.6	-1.3	-1.4	0.0060	0.0009
terminal struct. dx	2	sicilia	13.6	-1.6	-2.1	-1.4	-0.0099	0.0009
block	2	calabria	-2.8	-0.2	-0.6	-0.3	-0.0003	0.0000
tower (column sx)	2	calabria	-10.8	-1.8	-2.8	0.0	0.0035	0.0001
tower (column dx)	2	calabria	-10.8	-1.8	-2.8	0.2	0.0035	0.0000
terminal struct. sx	2	calabria	-3.3	-0.6	-1.4	0.0	0.0003	0.0000
terminal struct. dx	2	calabria	-2.9	-0.6	-1.2	0.0	0.0005	0.0000
block	3	sicilia	0.9	-3.8	2.0	1.2	0.0014	-0.0007
tower (column sx)	3	sicilia	5.8	-16.3	0.3	-2.3	-0.0038	0.0009
tower (column dx)	3	sicilia	5.8	-16.1	0.3	-1.3	-0.0038	0.0011
terminal struct. sx	3	sicilia	9.5	-10.0	0.6	-1.2	-0.0039	0.0003
terminal struct. dx	3	sicilia	7.9	-10.0	-1.1	-1.2	-0.0005	0.0003
block	3	calabria	-4.1	0.5	0.6	0.4	-0.0001	0.0000
tower (column sx)	3	calabria	-10.0	1.3	-1.9	0.0	0.0027	-0.0002
tower (column dx)	3	calabria	-10.0	1.3	-1.9	-0.2	0.0027	-0.0003
terminal struct. sx	3	calabria	-3.8	-0.4	-0.4	0.3	0.0003	0.0000
terminal struct. dx	3	calabria	-3.5	-0.4	-0.2	0.3	0.0004	0.0000
block	4	sicilia	2.3	3.8	0.6	1.2	0.0007	-0.0007
tower (column sx)	4	sicilia	-3.5	16.3	1.1	-2.3	-0.0037	0.0009
tower (column dx)	4	sicilia	-3.5	16.1	1.1	-1.3	-0.0037	0.0011
terminal struct. sx	4	sicilia	-2.8	10.0	0.3	-1.2	0.0027	0.0003
terminal struct. dx	4	sicilia	-1.8	10.0	0.5	-1.2	-0.0012	0.0003
block	4	calabria	-3.9	-0.2	0.1	0.4	0.0000	0.0000
tower (column sx)	4	calabria	-10.2	-1.3	-2.7	0.0	0.0038	-0.0002
tower (column dx)	4	calabria	-10.2	-1.3	-2.7	-0.2	0.0038	-0.0003
terminal struct. sx	4	calabria	-3.4	0.4	-0.1	0.3	0.0004	0.0000
terminal struct. dx	4	calabria	-3.1	0.4	0.0	0.3	0.0001	0.0000

		Ponte sullo Stretto di Messina PROGETTO DEFINITIVO		
Seismic analyses for soil-foundation systems, Annex	<i>Codice documento</i> PB0032_F0_ANX		<i>Rev</i> F0	<i>Data</i> 20/06/2011

Table 17. Displacements and rotations at the end of Earthquake NZ

location	comb.	shore	horizontal displacements		vertical displacements		rotations	
			longitudinal mm	transversal mm	longitudinal mm	transversal mm	longitudinal °	transversal °
block	1	sicilia	6.1	19.0	4.0	4.4	-0.0029	-0.0006
tower (column sx)	1	sicilia	20.3	-0.2	1.2	1.6	-0.0014	-0.0008
tower (column dx)	1	sicilia	20.3	0.3	1.2	0.5	-0.0014	-0.0005
terminal struct. sx	1	sicilia	20.6	-8.7	6.8	0.9	0.0022	0.0014
terminal struct. dx	1	sicilia	16.6	-8.7	3.0	0.9	0.0078	0.0014
block	1	calabria	-18.1	3.3	-0.5	0.5	-0.0027	0.0001
tower (column sx)	1	calabria	-28.4	0.4	-8.7	-0.7	0.0144	0.0000
tower (column dx)	1	calabria	-28.4	0.3	-8.7	-0.9	0.0144	0.0001
terminal struct. sx	1	calabria	-8.2	-1.7	0.3	-0.5	0.0015	0.0000
terminal struct. dx	1	calabria	-7.3	-1.7	0.6	-0.5	0.0010	0.0000
block	2	sicilia	-3.2	-19.0	-2.8	4.4	-0.0043	-0.0006
tower (column sx)	2	sicilia	7.7	0.2	0.5	1.6	-0.0031	-0.0008
tower (column dx)	2	sicilia	7.7	-0.3	0.5	0.5	-0.0031	-0.0005
terminal struct. sx	2	sicilia	-5.0	8.7	-1.6	0.9	-0.0021	0.0014
terminal struct. dx	2	sicilia	-1.9	8.7	-2.5	0.9	-0.0010	0.0014
block	2	calabria	-21.3	-4.6	0.0	0.4	-0.0035	0.0000
tower (column sx)	2	calabria	-24.7	-0.4	-7.3	-0.7	0.0118	0.0000
tower (column dx)	2	calabria	-24.7	-0.3	-7.3	-0.9	0.0118	0.0001
terminal struct. sx	2	calabria	-6.7	1.7	-0.2	-0.5	0.0010	0.0000
terminal struct. dx	2	calabria	-5.9	1.7	0.5	-0.5	0.0014	0.0000
block	3	sicilia	18.0	7.5	5.1	4.1	-0.0064	0.0003
tower (column sx)	3	sicilia	42.6	19.4	-2.6	0.7	-0.0057	-0.0001
tower (column dx)	3	sicilia	42.6	19.5	-2.6	1.0	-0.0057	0.0002
terminal struct. sx	3	sicilia	36.0	16.2	7.6	0.1	0.0069	0.0003
terminal struct. dx	3	sicilia	39.5	16.2	8.2	0.1	-0.0066	0.0003
block	3	calabria	-7.0	-0.1	3.0	0.6	-0.0014	0.0000
tower (column sx)	3	calabria	-14.6	-3.1	-6.2	0.7	0.0065	0.0000
tower (column dx)	3	calabria	-14.6	-3.1	-6.2	0.4	0.0065	-0.0005
terminal struct. sx	3	calabria	-3.3	-2.1	-1.0	-0.2	0.0004	-0.0001
terminal struct. dx	3	calabria	-2.3	-2.1	-1.1	-0.2	-0.0002	-0.0001
block	4	sicilia	-21.5	-7.5	2.3	4.1	0.0006	0.0003
tower (column sx)	4	sicilia	-13.1	-19.4	3.1	0.7	0.0012	-0.0001
tower (column dx)	4	sicilia	-13.1	-19.5	3.1	1.0	0.0012	0.0002
terminal struct. sx	4	sicilia	-18.9	-16.2	5.6	0.1	0.0043	0.0003
terminal struct. dx	4	sicilia	-17.2	-16.2	4.0	0.1	-0.0029	0.0003
block	4	calabria	-17.3	-1.0	0.9	0.2	-0.0017	0.0000
tower (column sx)	4	calabria	-20.7	3.1	-6.6	0.7	0.0082	0.0000
tower (column dx)	4	calabria	-20.7	3.1	-6.6	0.4	0.0082	-0.0005
terminal struct. sx	4	calabria	-9.0	2.1	0.7	-0.2	0.0011	-0.0001
terminal struct. dx	4	calabria	-8.0	2.1	0.9	-0.2	0.0000	-0.0001

		Ponte sullo Stretto di Messina PROGETTO DEFINITIVO		
Seismic analyses for soil-foundation systems, Annex	<i>Codice documento</i> PB0032_F0_ANX		<i>Rev</i> F0	<i>Data</i> 20/06/2011

Table 18. Maximum accelerations computed during Earthquake N14

location	comb.	shore	max horiz. acceleration		max vert. acceleration	
			longitudinal	transversal	longitudinal	transversal
			g	g	g	g
base	1	sicilia	0.122	0.094	0.071	0.071
block	1	sicilia	0.139	0.098	0.110	0.100
tower (column sx)	1	sicilia	0.139	0.093	0.116	0.107
tower (column dx)	1	sicilia	0.139	0.081	0.116	0.105
terminal struct. sx	1	sicilia	0.159	0.083	0.137	0.127
terminal struct. dx	1	sicilia	0.191	0.083	0.141	0.127
base	1	calabria	0.178	0.104	0.084	0.084
block	1	calabria	0.216	0.107	0.112	0.124
tower (column sx)	1	calabria	0.251	0.174	0.121	0.084
tower (column dx)	1	calabria	0.251	0.163	0.121	0.081
terminal struct. sx	1	calabria	0.229	0.167	0.119	0.101
terminal struct. dx	1	calabria	0.224	0.167	0.125	0.101
base	2	sicilia	0.122	0.094	0.071	0.071
block	2	sicilia	0.151	0.098	0.090	0.100
tower (column sx)	2	sicilia	0.167	0.093	0.137	0.107
tower (column dx)	2	sicilia	0.167	0.081	0.137	0.105
terminal struct. sx	2	sicilia	0.154	0.083	0.156	0.127
terminal struct. dx	2	sicilia	0.189	0.083	0.132	0.127
base	2	calabria	0.178	0.104	0.084	0.084
block	2	calabria	0.218	0.107	0.113	0.124
tower (column sx)	2	calabria	0.259	0.174	0.099	0.084
tower (column dx)	2	calabria	0.259	0.163	0.099	0.081
terminal struct. sx	2	calabria	0.236	0.167	0.106	0.101
terminal struct. dx	2	calabria	0.222	0.167	0.110	0.101
base	3	sicilia	0.094	0.122	0.071	0.071
block	3	sicilia	0.121	0.130	0.110	0.093
tower (column sx)	3	sicilia	0.120	0.100	0.123	0.109
tower (column dx)	3	sicilia	0.120	0.097	0.123	0.094
terminal struct. sx	3	sicilia	0.159	0.095	0.136	0.119
terminal struct. dx	3	sicilia	0.143	0.095	0.133	0.119
base	3	calabria	0.104	0.178	0.084	0.084
block	3	calabria	0.146	0.200	0.100	0.119
tower (column sx)	3	calabria	0.176	0.237	0.096	0.080
tower (column dx)	3	calabria	0.176	0.244	0.096	0.092
terminal struct. sx	3	calabria	0.169	0.279	0.106	0.110
terminal struct. dx	3	calabria	0.171	0.279	0.105	0.110
base	4	sicilia	0.094	0.122	0.071	0.071
block	4	sicilia	0.126	0.130	0.103	0.093
tower (column sx)	4	sicilia	0.115	0.100	0.133	0.109
tower (column dx)	4	sicilia	0.115	0.097	0.133	0.094
terminal struct. sx	4	sicilia	0.143	0.095	0.142	0.119
terminal struct. dx	4	sicilia	0.175	0.095	0.153	0.119
base	4	calabria	0.104	0.178	0.084	0.084
block	4	calabria	0.154	0.199	0.136	0.118
tower (column sx)	4	calabria	0.163	0.237	0.083	0.080
tower (column dx)	4	calabria	0.163	0.244	0.083	0.092
terminal struct. sx	4	calabria	0.177	0.279	0.087	0.110
terminal struct. dx	4	calabria	0.171	0.279	0.084	0.110

		Ponte sullo Stretto di Messina PROGETTO DEFINITIVO		
Seismic analyses for soil-foundation systems, Annex		<i>Codice documento</i> PB0032_F0_ANNX	<i>Rev</i> F0	<i>Data</i> 20/06/2011

Table 19. Maximum accelerations computed during Earthquake NZ

location	comb.	shore	max horiz. acceleration		max vert. acceleration	
			longitudinal	transversal	longitudinal	transversal
			g	g	g	g
base	1	sicilia	0.226	0.207	0.096	0.096
block	1	sicilia	0.182	0.166	0.143	0.184
tower (column sx)	1	sicilia	0.169	0.132	0.169	0.171
tower (column dx)	1	sicilia	0.169	0.142	0.169	0.156
terminal struct. sx	1	sicilia	0.228	0.128	0.209	0.195
terminal struct. dx	1	sicilia	0.273	0.128	0.178	0.195
base	1	calabria	0.306	0.287	0.134	0.109
block	1	calabria	0.387	0.217	0.214	0.182
tower (column sx)	1	calabria	0.457	0.305	0.223	0.186
tower (column dx)	1	calabria	0.457	0.330	0.223	0.198
terminal struct. sx	1	calabria	0.423	0.400	0.181	0.271
terminal struct. dx	1	calabria	0.422	0.400	0.170	0.271
base	2	sicilia	0.226	0.207	0.096	0.096
block	2	sicilia	0.175	0.166	0.155	0.184
tower (column sx)	2	sicilia	0.222	0.132	0.180	0.171
tower (column dx)	2	sicilia	0.222	0.142	0.180	0.156
terminal struct. sx	2	sicilia	0.242	0.128	0.183	0.195
terminal struct. dx	2	sicilia	0.231	0.128	0.188	0.195
base	2	calabria	0.306	0.287	0.134	0.109
block	2	calabria	0.385	0.221	0.161	0.185
tower (column sx)	2	calabria	0.415	0.305	0.225	0.186
tower (column dx)	2	calabria	0.415	0.330	0.225	0.198
terminal struct. sx	2	calabria	0.365	0.400	0.227	0.271
terminal struct. dx	2	calabria	0.360	0.400	0.207	0.271
base	3	sicilia	0.207	0.226	0.096	0.096
block	3	sicilia	0.217	0.167	0.178	0.183
tower (column sx)	3	sicilia	0.187	0.134	0.173	0.166
tower (column dx)	3	sicilia	0.187	0.146	0.173	0.196
terminal struct. sx	3	sicilia	0.241	0.137	0.200	0.193
terminal struct. dx	3	sicilia	0.215	0.137	0.200	0.193
base	3	calabria	0.306	0.287	0.134	0.109
block	3	calabria	0.280	0.237	0.163	0.184
tower (column sx)	3	calabria	0.363	0.404	0.240	0.201
tower (column dx)	3	calabria	0.363	0.401	0.240	0.201
terminal struct. sx	3	calabria	0.398	0.456	0.196	0.266
terminal struct. dx	3	calabria	0.358	0.456	0.177	0.266
base	4	sicilia	0.207	0.226	0.096	0.096
block	4	sicilia	0.216	0.167	0.128	0.183
tower (column sx)	4	sicilia	0.210	0.134	0.181	0.166
tower (column dx)	4	sicilia	0.210	0.146	0.181	0.196
terminal struct. sx	4	sicilia	0.237	0.137	0.205	0.193
terminal struct. dx	4	sicilia	0.224	0.137	0.196	0.193
base	4	calabria	0.306	0.287	0.134	0.109
block	4	calabria	0.287	0.244	0.193	0.186
tower (column sx)	4	calabria	0.395	0.404	0.215	0.201
tower (column dx)	4	calabria	0.395	0.401	0.215	0.201
terminal struct. sx	4	calabria	0.329	0.456	0.167	0.266
terminal struct. dx	4	calabria	0.329	0.456	0.176	0.266

		Ponte sullo Stretto di Messina PROGETTO DEFINITIVO		
Seismic analyses for soil-foundation systems, Annex	<i>Codice documento</i> PB0032_F0_ANX	<i>Rev</i> F0	<i>Data</i> 20/06/2011	

5 REFERENCES

- Baldi, G. Bellotti, R. Ghionna, V., Jamiolkowski, M. and Pasqualini, E. (1985). *Penetration Resistance and Liquefaction of Sands*. Proc. XI ICSMFE, San Francisco, V.4, pp.1891-1896
- Bardet J.P., Ichii, K., and Lin, C.H. (2000). *EERA. A computer program for Equivalent-linear Earthquake site Response Analyses of layered soil deposits*. University of Southern California, Dept. of Civil Engineering.
- Berezantzev W.G. (1964). *Calculation of foundation basis*. Construction Literature, Leningrad, U.S.S.R.
- Croce P., Flora A., Modoni G. (2004) *Jet grouting. Tecnica, progetto e controllo*. Hevelius Edizioni, Benevento
- Cubrinovski M. e Ishihara K. (1999). *Empirical Correlation between SPT N-value and Relative Density of Sandy Soils*. Soils and Foundations. 5: 61-71.
- Gazetas G. (1991). *Foundation vibrations*. In: Foundation Engineering Handbook, 2nd edition, H.-Y. Fang, ed., Van Nostrand Reinhold, New York, 553-593.
- Gerrard C.M. & Harrison W.J. (1970) *Circular loads applied to a cross-anisotropic half space*, CSIRO, Aust. Div. App. Geomech., Tech. Paper No. 8
- Itasca (2005). *FLAC: Fast Lagrangian Analysis of Continua v.5.0 User's Manual*. ITASCA, USA.
- Jamiolkowski et al. (1991) Jamiolkowski, M., Leroueil, S., and Lo Presti, D. C. F. (1991). *Design parameters from theory to practice*. Theme lecture, Proc., Geo-Coast'91, 1-41.
- Joyner, W.B., and Chen, A.T.F. (1975). *Calculation of nonlinear ground response in earthquakes*. Bulletin of the Seismological Society of America, 65(5), 1315-1336.
- Lysmer J., Kuhlemeyer R.L. (1969) *Finite dynamic model for infinite media*. Journal of Engineering Mechanics, 95(EM4), 859-877.
- Mansur, C.I. e Kaufman, R.I. (1962). *Dewatering*, Cap.3 in Foundation Engineering. McGraw Hill, N.Y.
- Masing, G. (1926). *Eigenspannungen und Verfertigung bim Messing*. Proceedings 2nd Int. Congress on Applied Mechanics, Zurich.

		Ponte sullo Stretto di Messina PROGETTO DEFINITIVO		
Seismic analyses for soil-foundation systems, Annex	<i>Codice documento</i> PB0032_F0_ANX	<i>Rev</i> F0	<i>Data</i> 20/06/2011	

Mesri G. (1993). *Aging of soils*. Aging Symp., Sociedad Mexicana de Mecanica de Suelos, Mexico City, Mexico, 1, 1-29



Schmertmann, J.H. (1978). *Guidelines for Cone Penetration Test Performance and Design*. Report HWA-TS-78-209, US Dept. of Transportation, Federal Highway Administration, Washington, D.C.

Schnabel, P.B., Lysmer, J., and Seed, H.B. (1972). *SHAKE, a computer program for earthquake response analysis of horizontally layered sites*. Report: Earthquake Engineering research Center, University of California, Berkeley.

Seed, H.B., and Idriss, I.M. (1970). *Soil moduli and damping factors for dynamic analysis*. Report No. EERC 70-10, University of California, Berkeley.

Tanaka Y., Kudo Y., Yoshida Y. & Ikemi M. (1987). *A study on the mechanical properties of sandy gravel – dynamic properties of reconstituted samples*. Central Research Institute of Electric Power Industry, Report U87019.

Tanaka Y., Kudo Y., Yoshida Y. & Ikemi M. (1987). *A study on the mechanical properties of sandy gravel – dynamic properties of reconstituted samples*. Central Research Institute of Electric Power Industry, Report U87019.

		Ponte sullo Stretto di Messina PROGETTO DEFINITIVO		
Seismic analyses for soil-foundation systems, Annex	<i>Codice documento</i> PB0032_F0_ANX	<i>Rev</i> F0	<i>Data</i> 20/06/2011	

6 FIGURES

		Ponte sullo Stretto di Messina PROGETTO DEFINITIVO		
		Seismic analyses for soil-foundation systems, Annex	Codice documento PB0032_F0_ANX	Rev F0

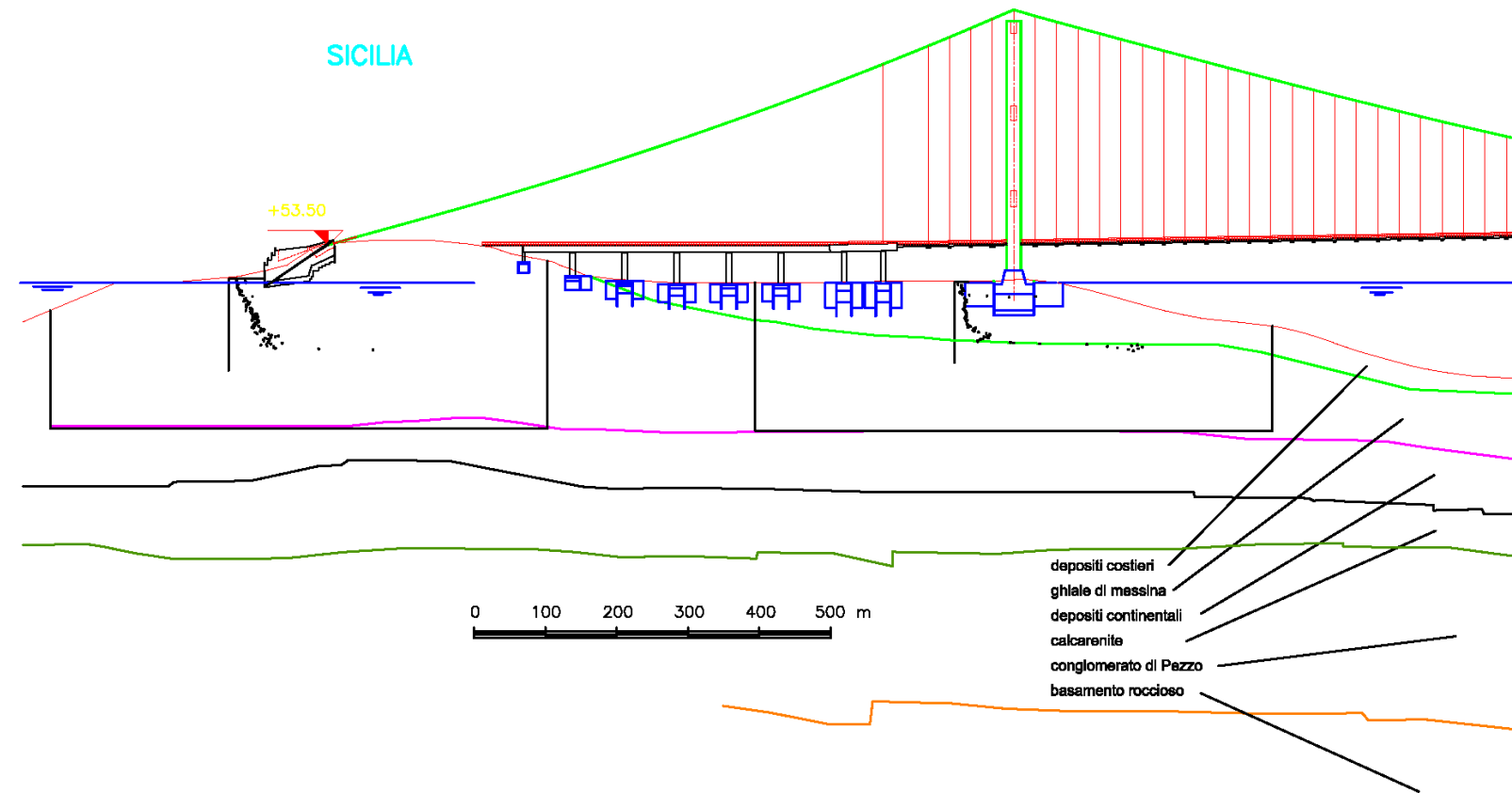


Figure 1: Soil profile on Sicily shore of Messina Strait

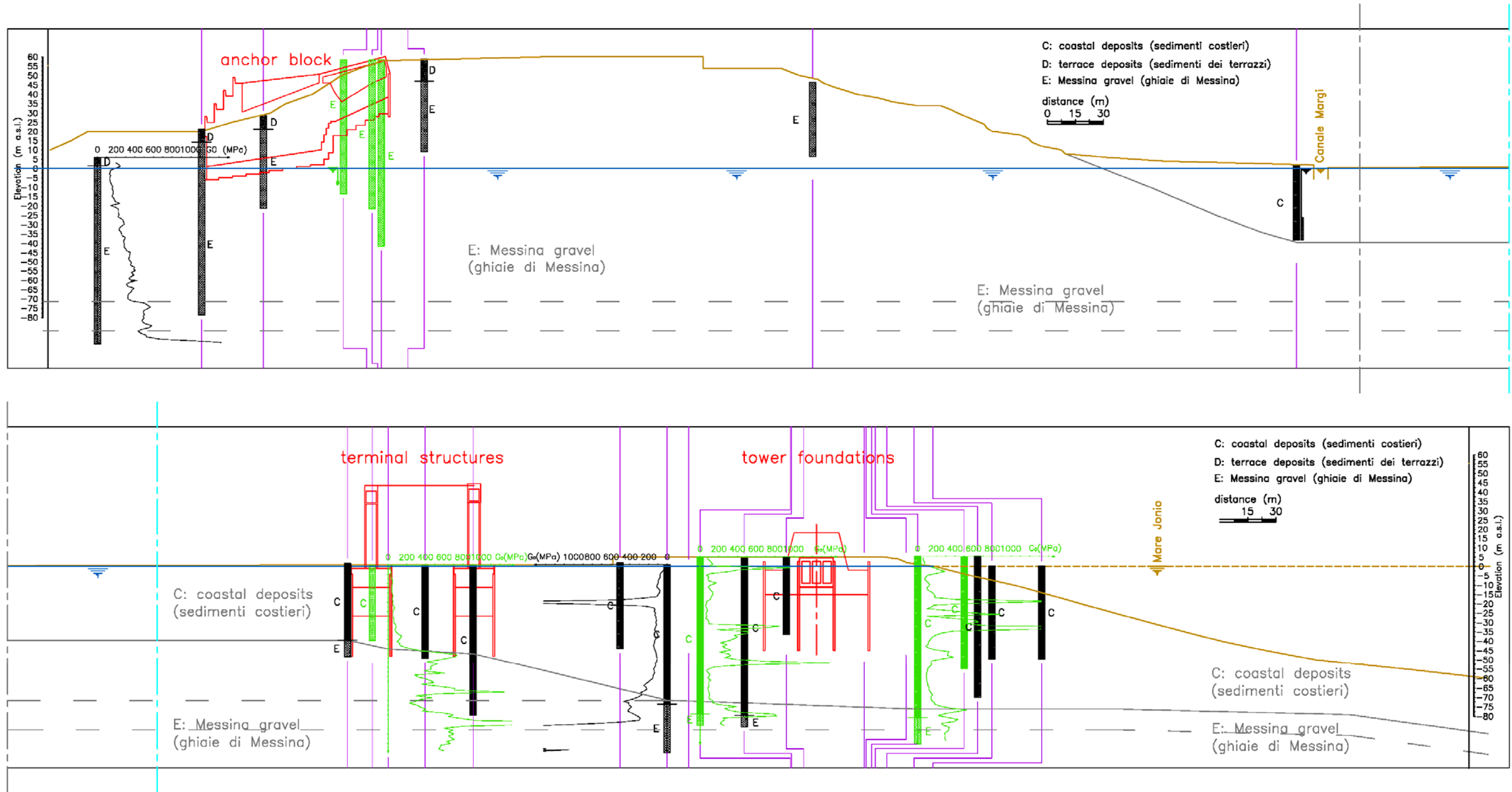


Figure 2: Sicilia shore - longitudinal section: global view

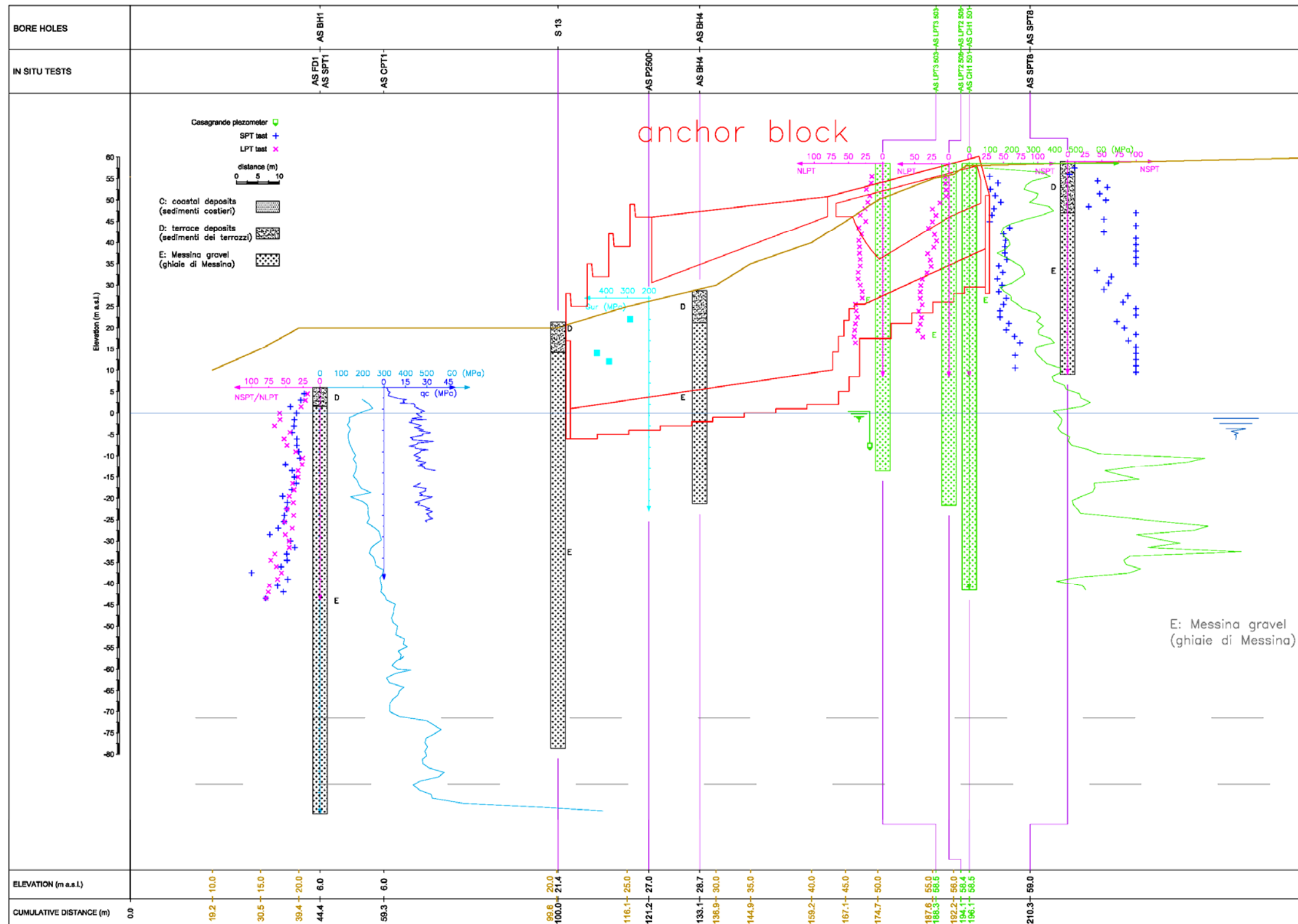


Figure 3: Sicilia shore - longitudinal section at the anchor block

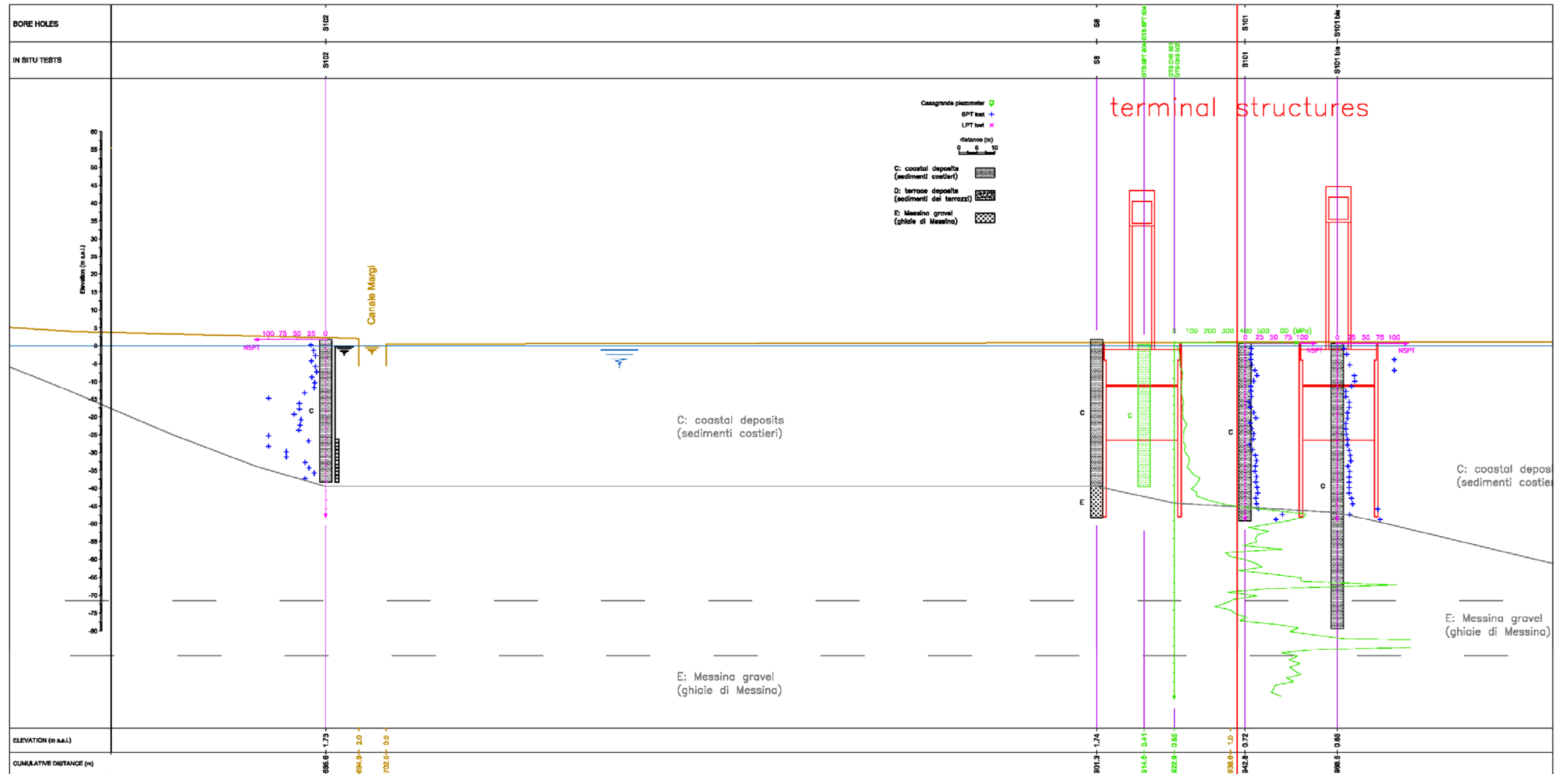


Figure 4: Sicilia shore - longitudinal section at the terminal structures

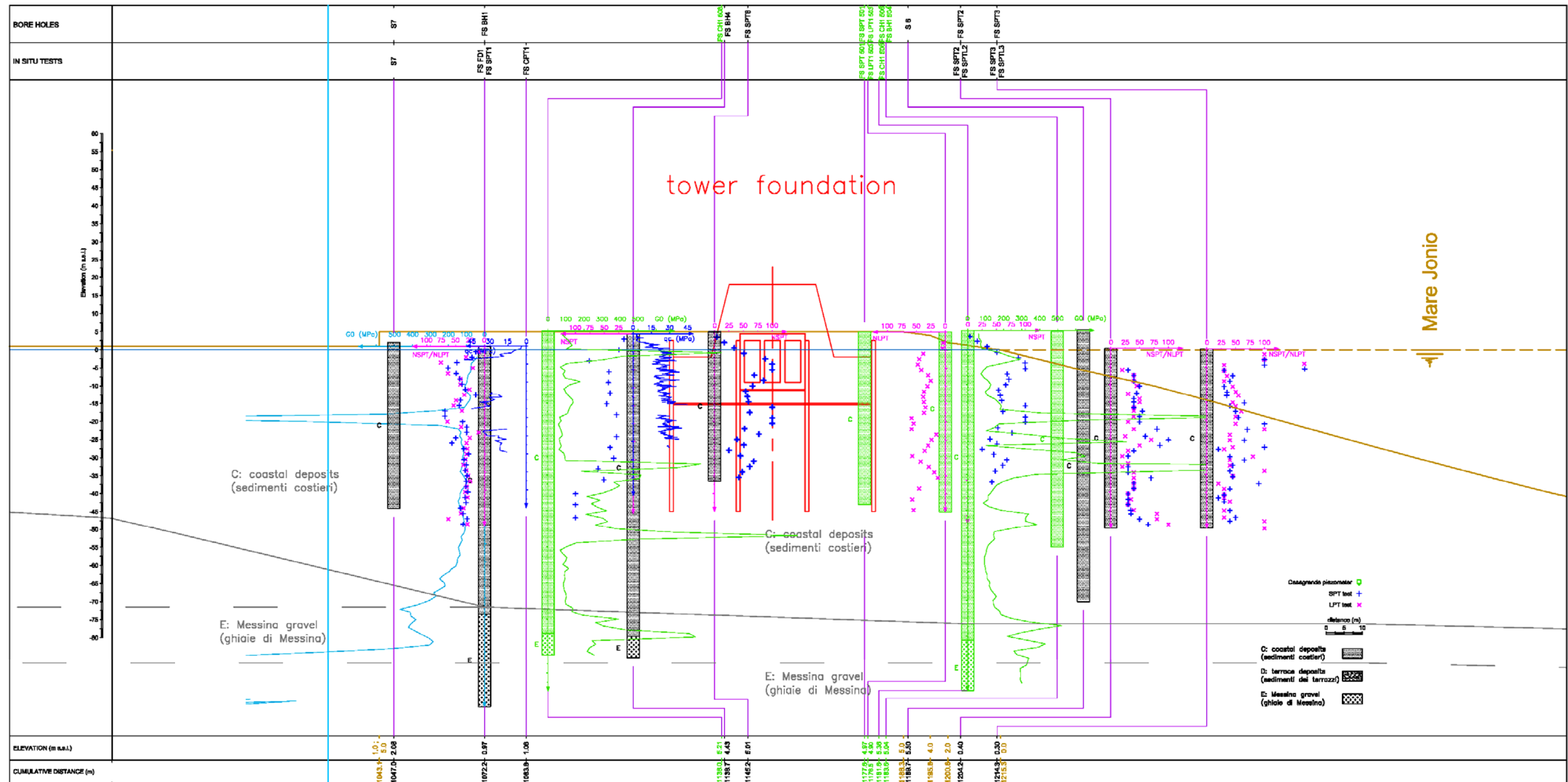




Figure 5: Sicilia shore - longitudinal section at the tower foundation

		Ponte sullo Stretto di Messina PROGETTO DEFINITIVO		
Seismic analyses for soil-foundation systems, Annex	Codice documento PB0032_F0_ANX	Rev F0	Data 20/06/2011	

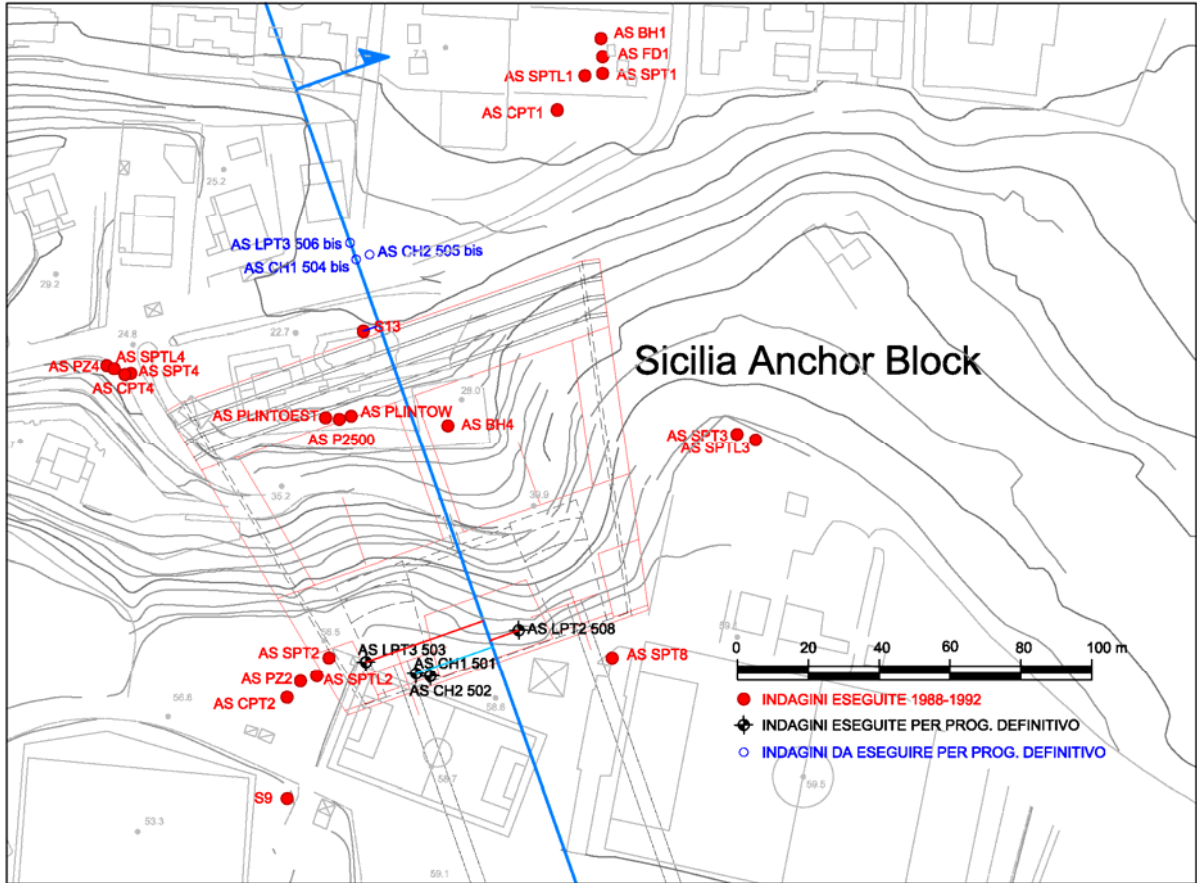


Figure 6: Sicilia shore - plan view of Anchor Block

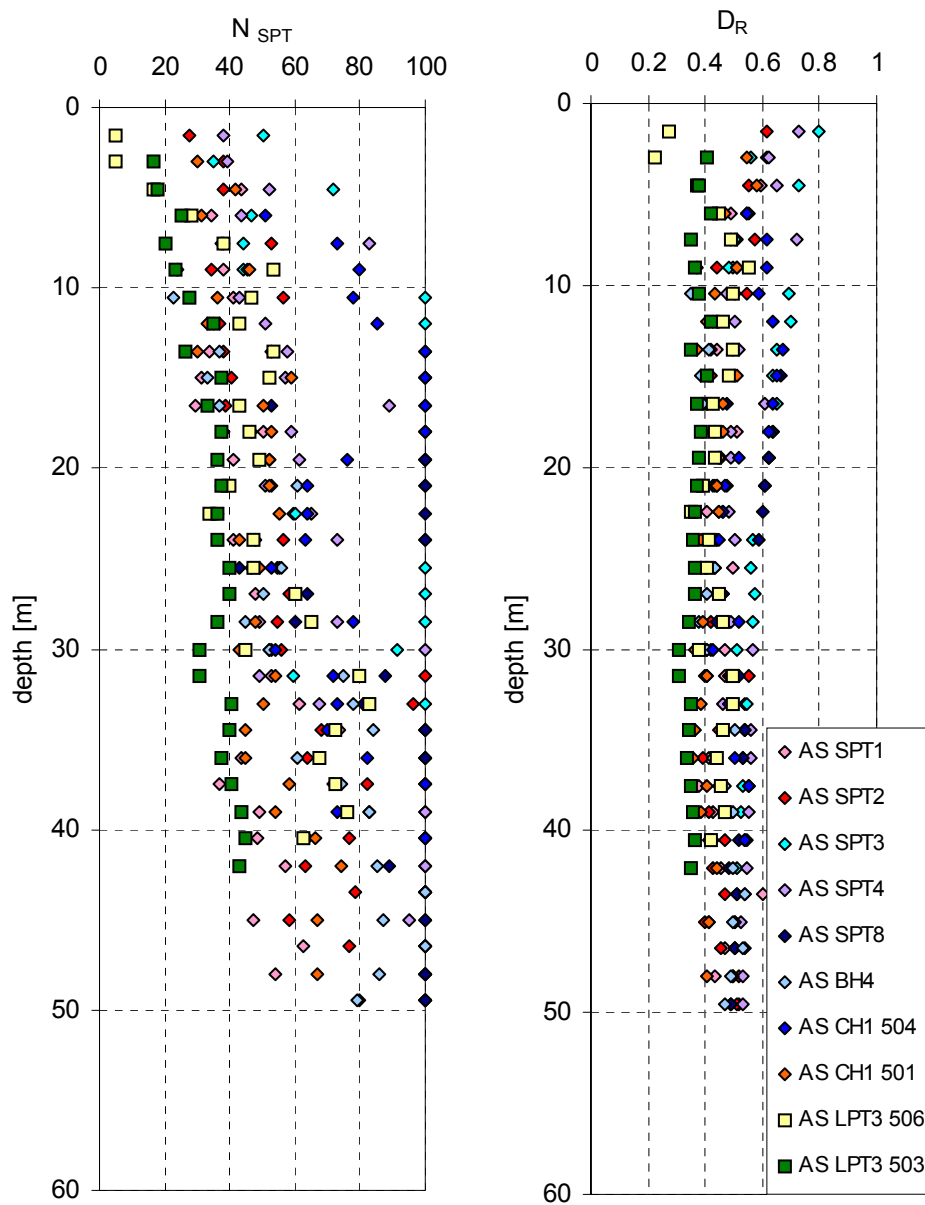




Figure 7: Sicilia Anchor Block - relative density from SPT and LPT test results

		Ponte sullo Stretto di Messina PROGETTO DEFINITIVO		
Seismic analyses for soil-foundation systems, Annex	Codice documento <i>PB0032_F0_ANX</i>	Rev <i>F0</i>	Data <i>20/06/2011</i>	

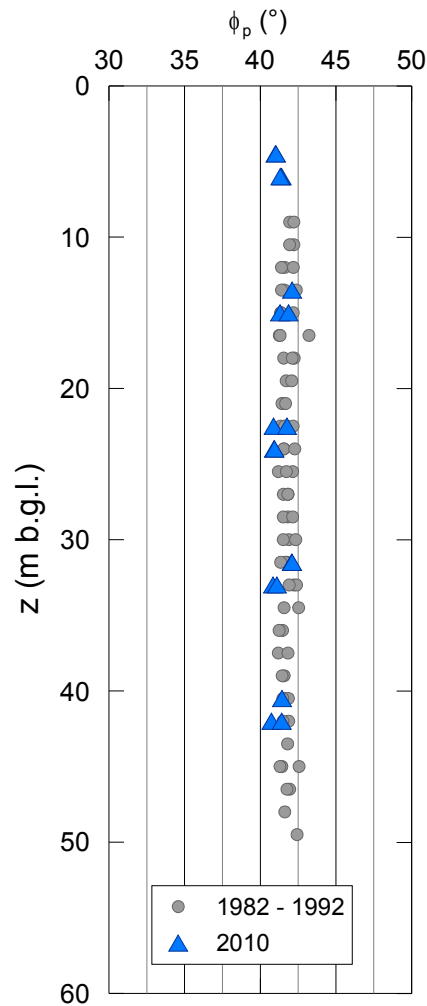




Figure 8: Sicilia Anchor Block - angle of peak shearing resistance from SPT and LPT results

		Ponte sullo Stretto di Messina PROGETTO DEFINITIVO		
Seismic analyses for soil-foundation systems, Annex	<i>Codice documento</i> PB0032_F0_ANX	<i>Rev</i> F0	<i>Data</i> 20/06/2011	

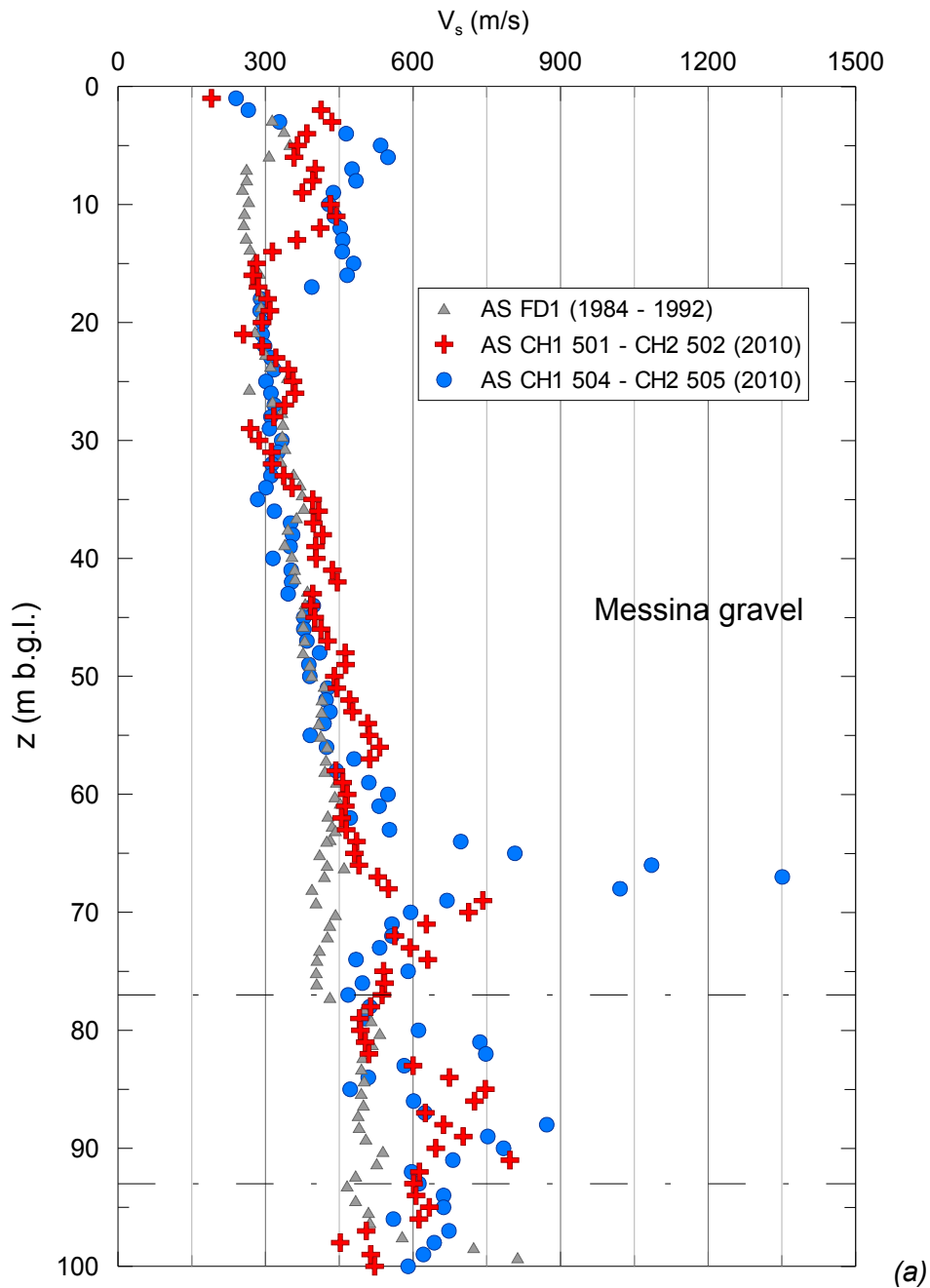


Figure 9: Sicilia Anchor Block - (a) V_s and (b) G_0 profiles from cross-hole tests (continues)

		Ponte sullo Stretto di Messina PROGETTO DEFINITIVO		
Seismic analyses for soil-foundation systems, Annex	Codice documento <i>PB0032_F0_ANX</i>	Rev <i>F0</i>	Data <i>20/06/2011</i>	

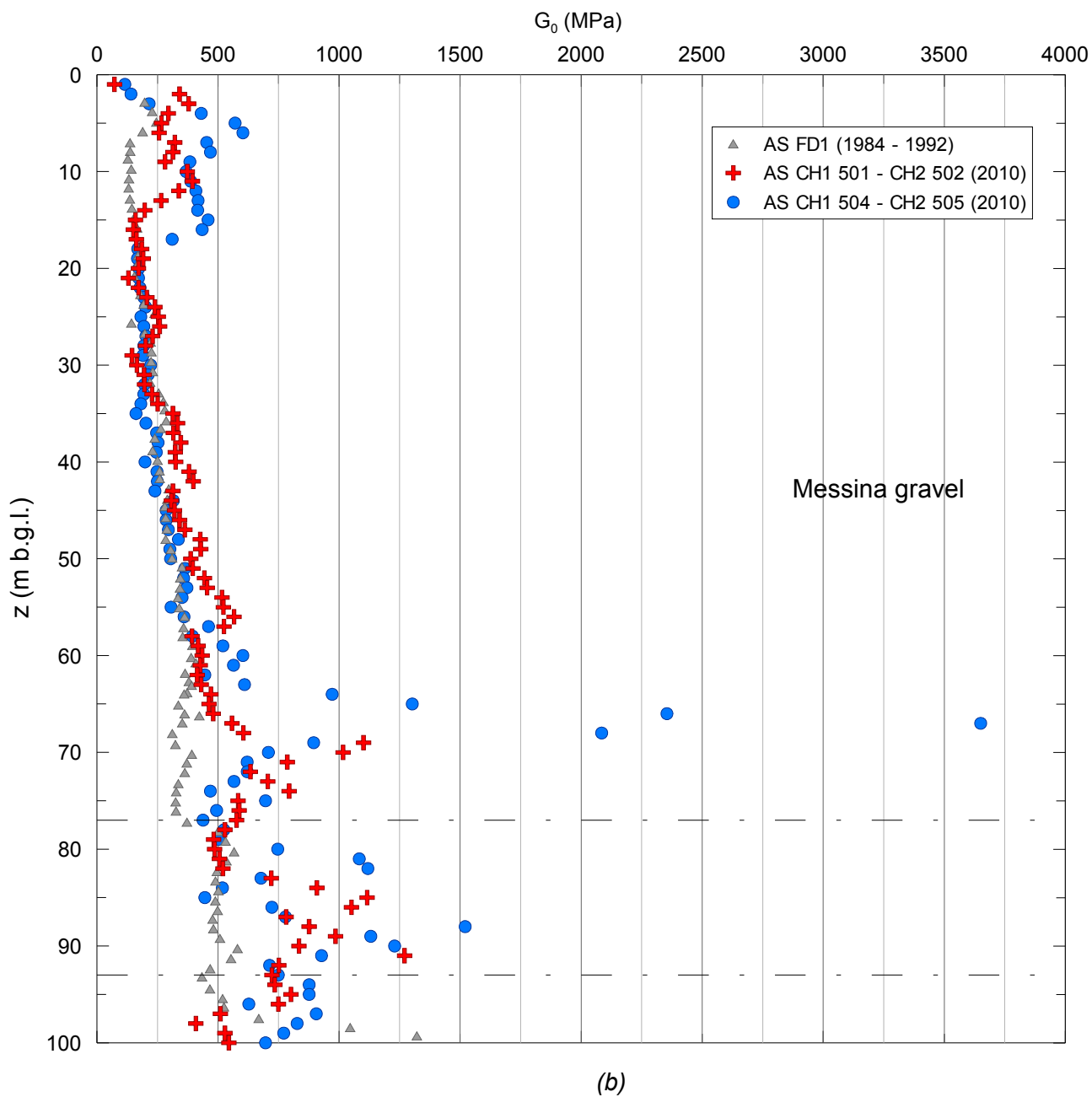
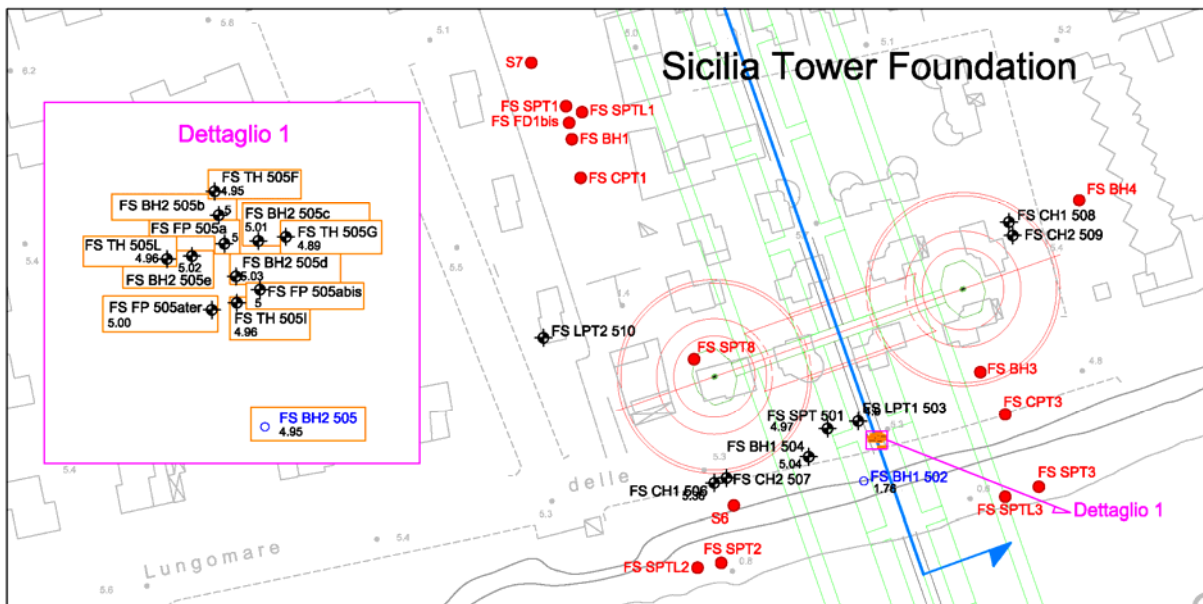
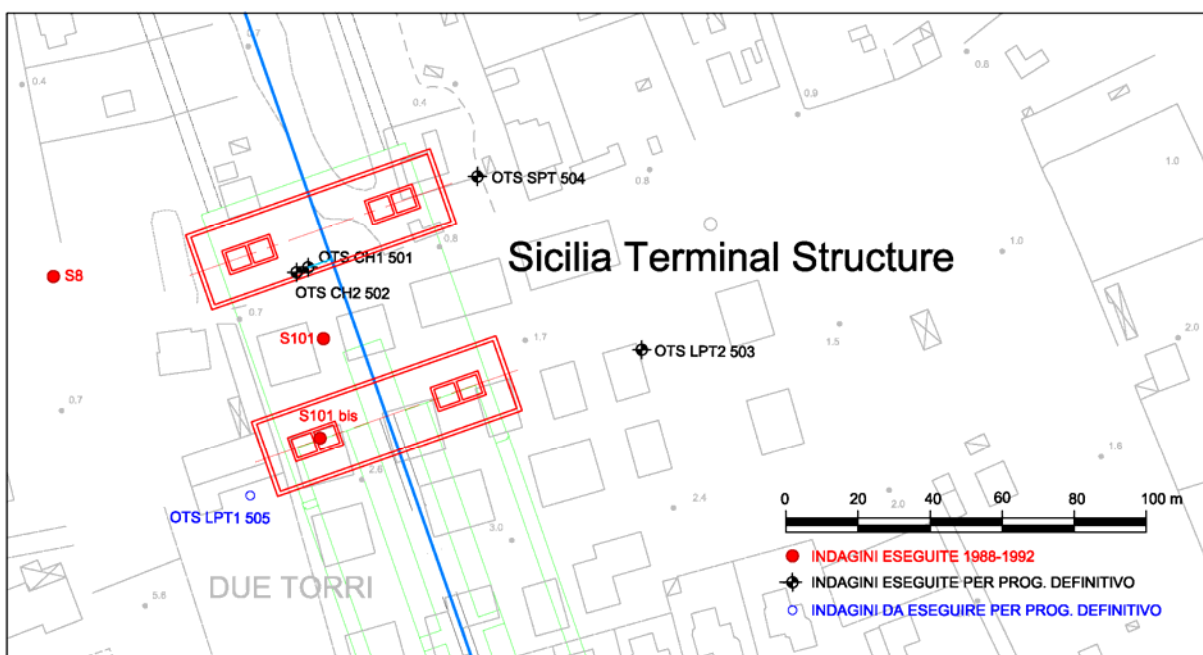


Figure 9: Sicilia Anchor Block - (a) V_s and (b) G_0 profiles from cross-hole tests

		Ponte sullo Stretto di Messina PROGETTO DEFINITIVO		
Seismic analyses for soil-foundation systems, Annex	Codice documento PB0032_F0_ANX	Rev F0	Data 20/06/2011	



(a)



(b)

Figure 10: Sicilia shore - plan view of Tower and of the Terminal Structure and boreholes location

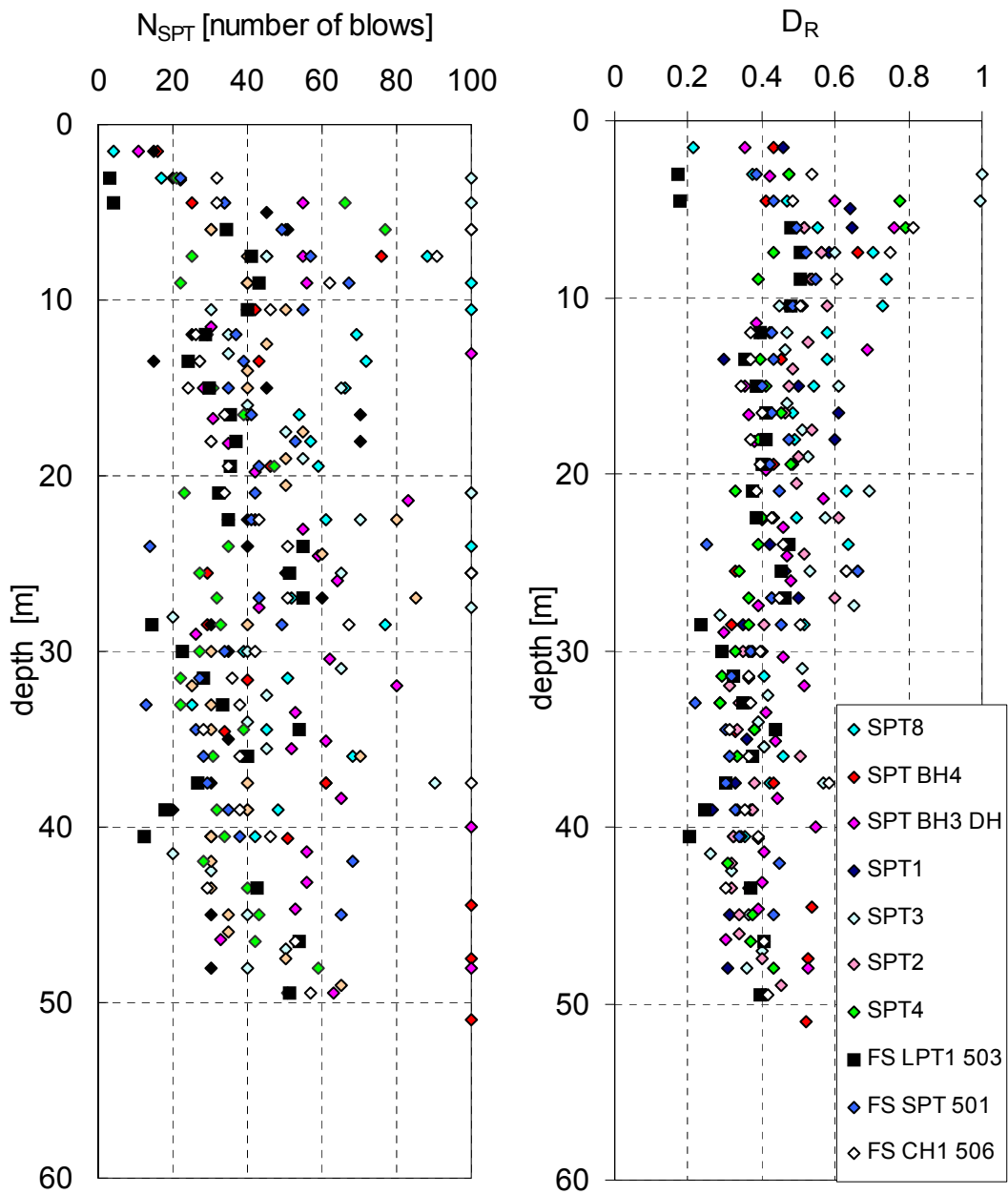




Figure 11: Sicilia Tower - relative density from SPT and LPT test results

		Ponte sullo Stretto di Messina PROGETTO DEFINITIVO		
Seismic analyses for soil-foundation systems, Annex	Codice documento <i>PB0032_F0_ANX</i>	Rev <i>F0</i>	Data <i>20/06/2011</i>	

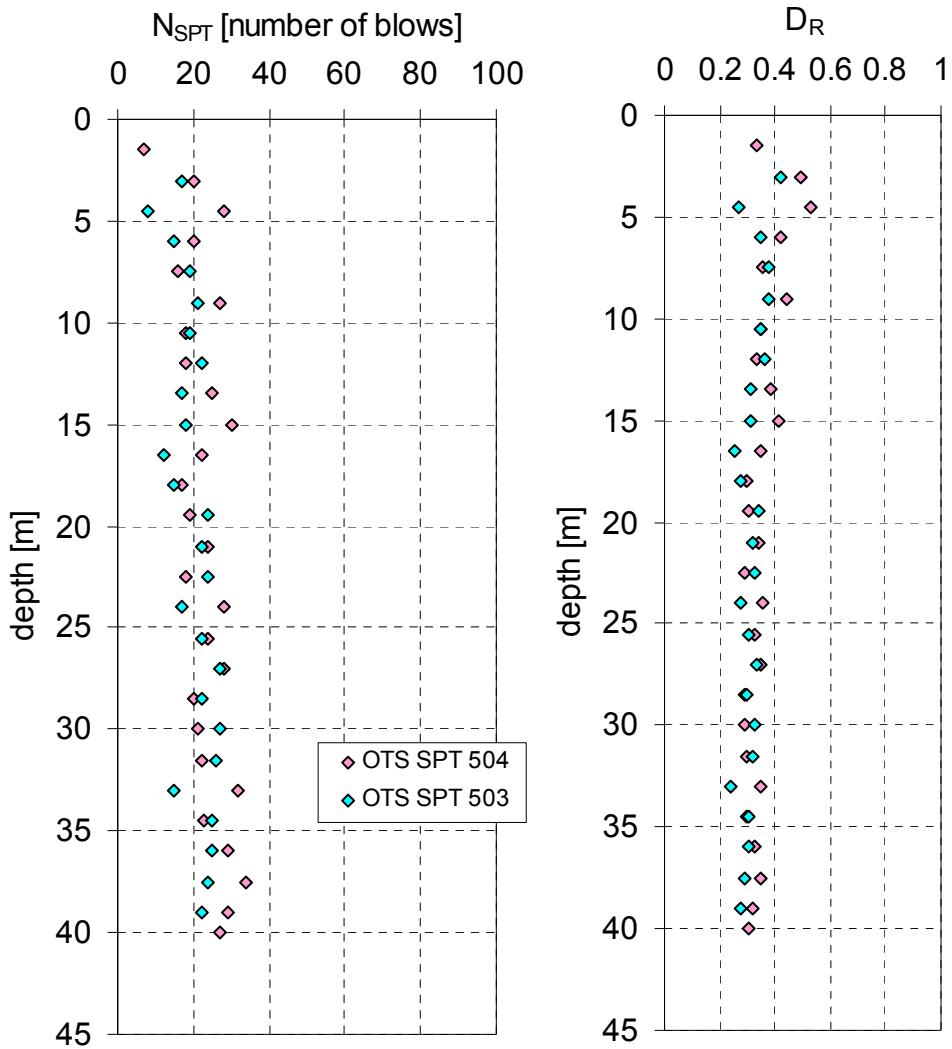




Figure 12: Sicilia Terminal Structure - relative density from SPT and LPT test results

		Ponte sullo Stretto di Messina PROGETTO DEFINITIVO		
Seismic analyses for soil-foundation systems, Annex	<i>Codice documento</i> PB0032_F0_ANX	<i>Rev</i> F0	<i>Data</i> 20/06/2011	

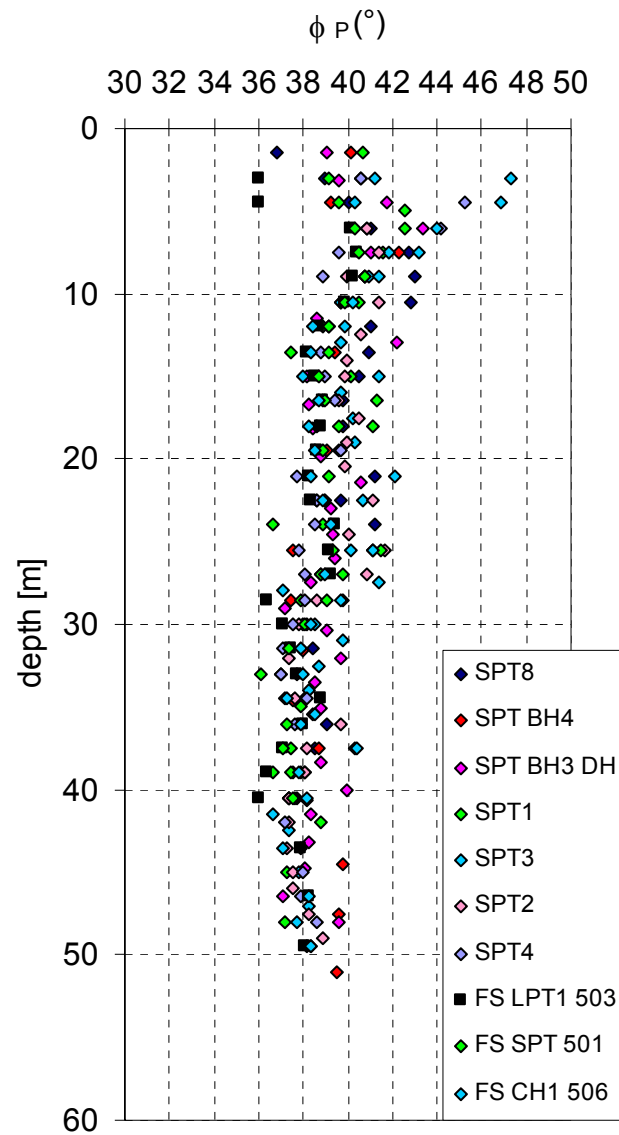


Figure 13: Sicilia Tower - angle of peak shearing resistance from SPT and LPT results

		Ponte sullo Stretto di Messina PROGETTO DEFINITIVO		
Seismic analyses for soil-foundation systems, Annex	Codice documento <i>PB0032_F0_ANX</i>	Rev <i>F0</i>	Data <i>20/06/2011</i>	

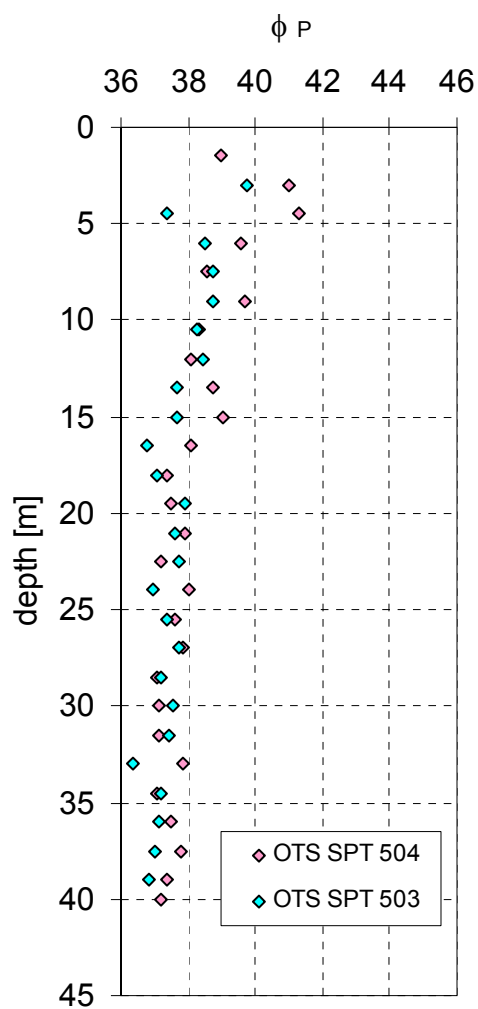


Figure 14: Sicilia Terminal Structure - angle of peak shearing resistance from SPT and LPT results

		Ponte sullo Stretto di Messina PROGETTO DEFINITIVO		
Seismic analyses for soil-foundation systems, Annex	Codice documento <i>PB0032_F0_ANX</i>	Rev <i>F0</i>	Data <i>20/06/2011</i>	

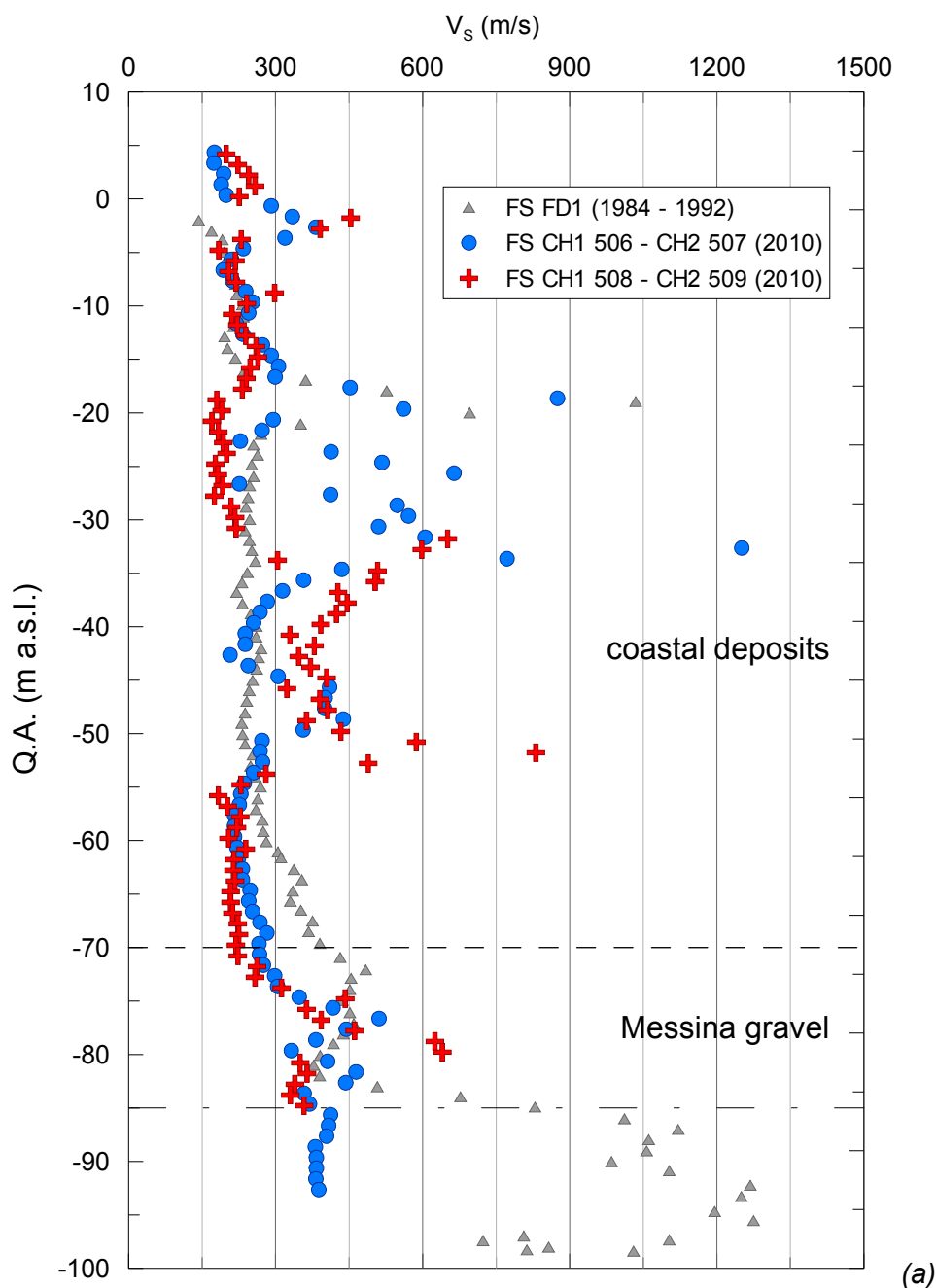


Figure 15: Sicilia Tower – (a) V_s and (b) G_0 profiles from cross-hole tests (continues)

		Ponte sullo Stretto di Messina PROGETTO DEFINITIVO		
Seismic analyses for soil-foundation systems, Annex	Codice documento <i>PB0032_F0_ANX</i>	Rev <i>F0</i>	Data <i>20/06/2011</i>	

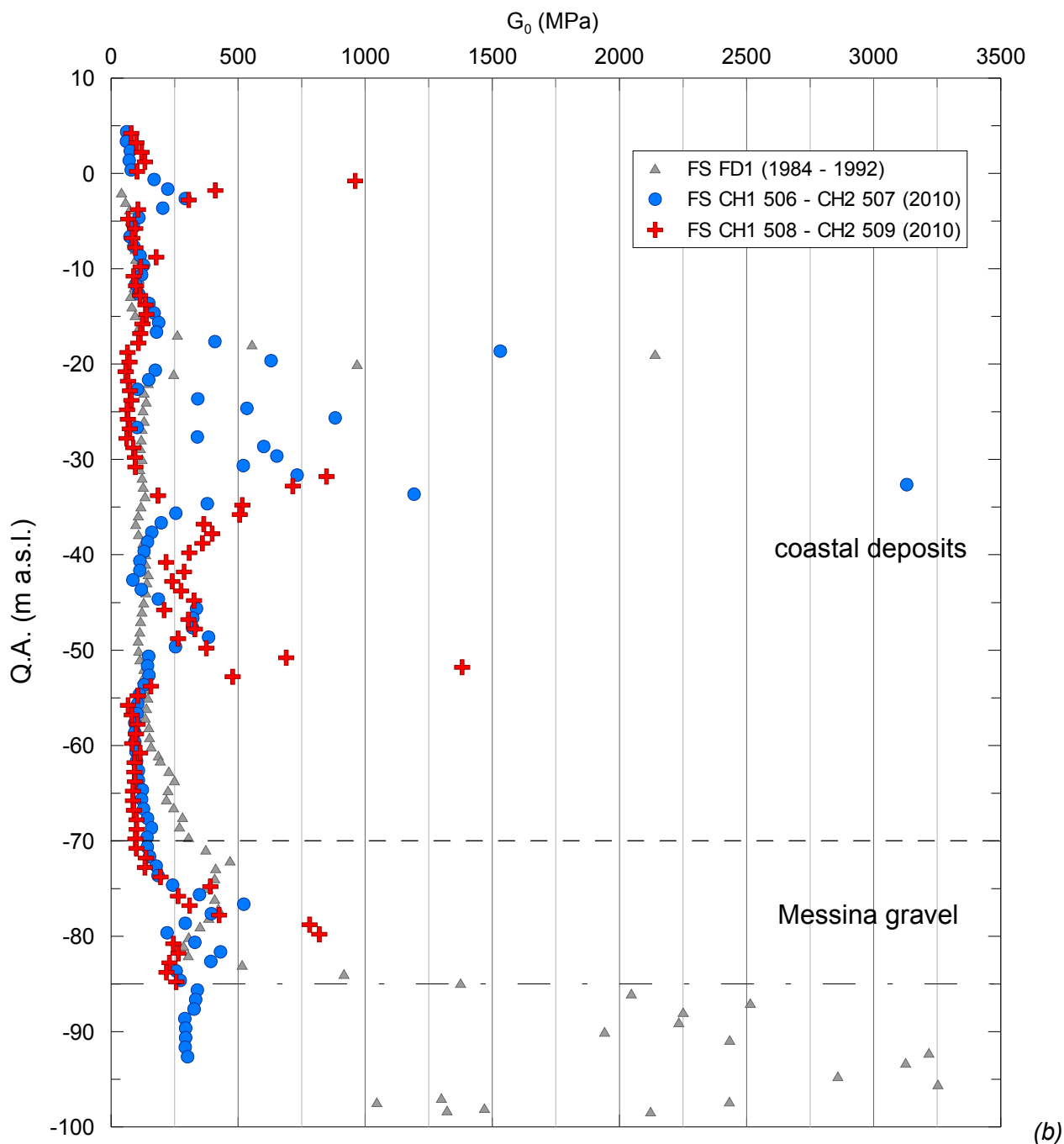




Figure 15: Sicilia Tower – (a) V_s and (b) G_0 profiles from cross-hole tests)

		Ponte sullo Stretto di Messina PROGETTO DEFINITIVO		
Seismic analyses for soil-foundation systems, Annex	Codice documento <i>PB0032_F0_ANX</i>	Rev <i>F0</i>	Data <i>20/06/2011</i>	

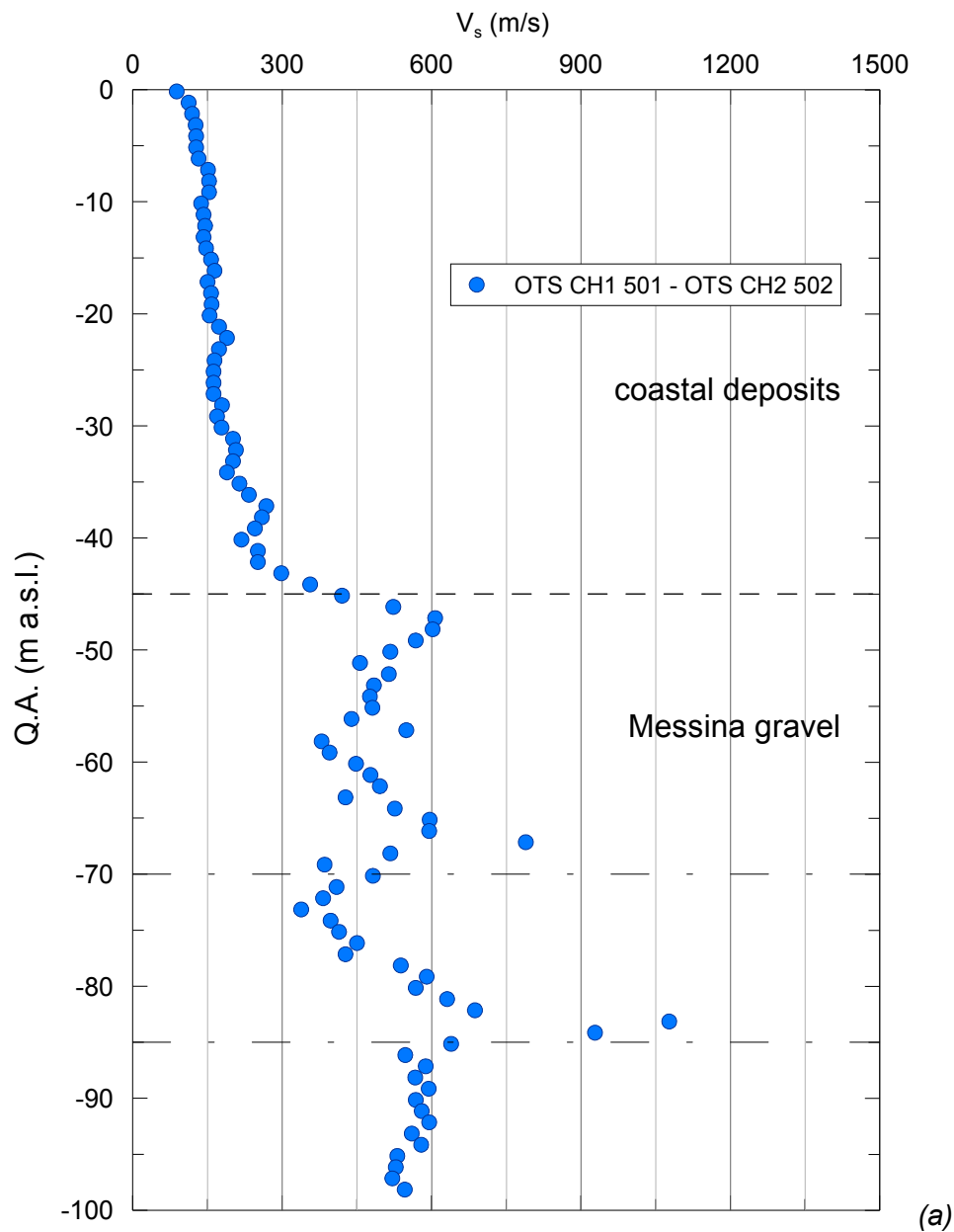


Figure 16: Sicilia Terminal Structure - (a) V_s and (b) G_0 profiles from cross-hole tests (continues)

		Ponte sullo Stretto di Messina PROGETTO DEFINITIVO		
Seismic analyses for soil-foundation systems, Annex	<i>Codice documento</i> PB0032_F0_ANX	<i>Rev</i> F0	<i>Data</i> 20/06/2011	

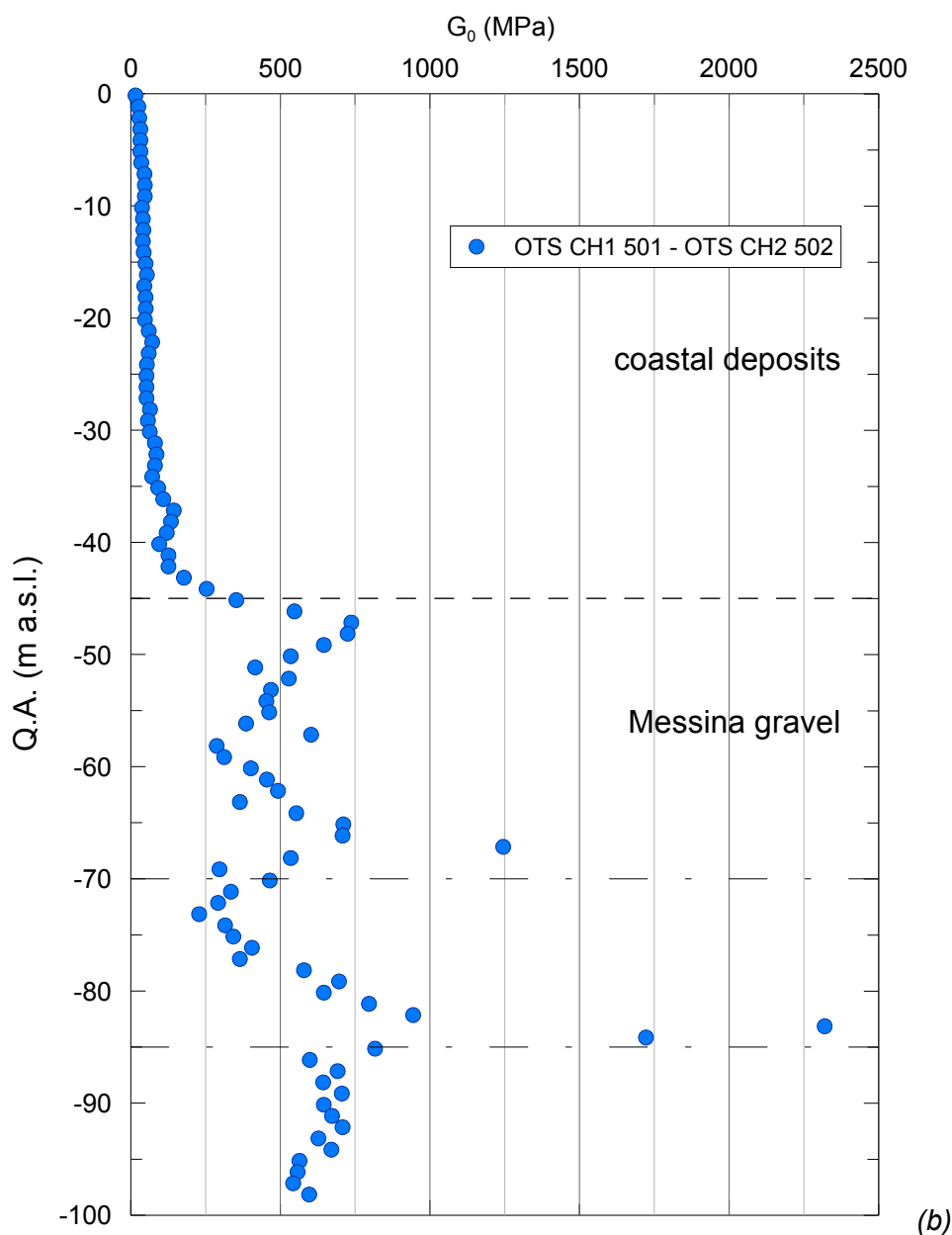


Figure 16: Sicilia Terminal Structure - (a) V_s and (b) G_0 profiles from cross-hole tests

		Ponte sullo Stretto di Messina PROGETTO DEFINITIVO		
Seismic analyses for soil-foundation systems, Annex	<i>Codice documento</i> PB0032_F0_ANX	<i>Rev</i> F0	<i>Data</i> 20/06/2011	

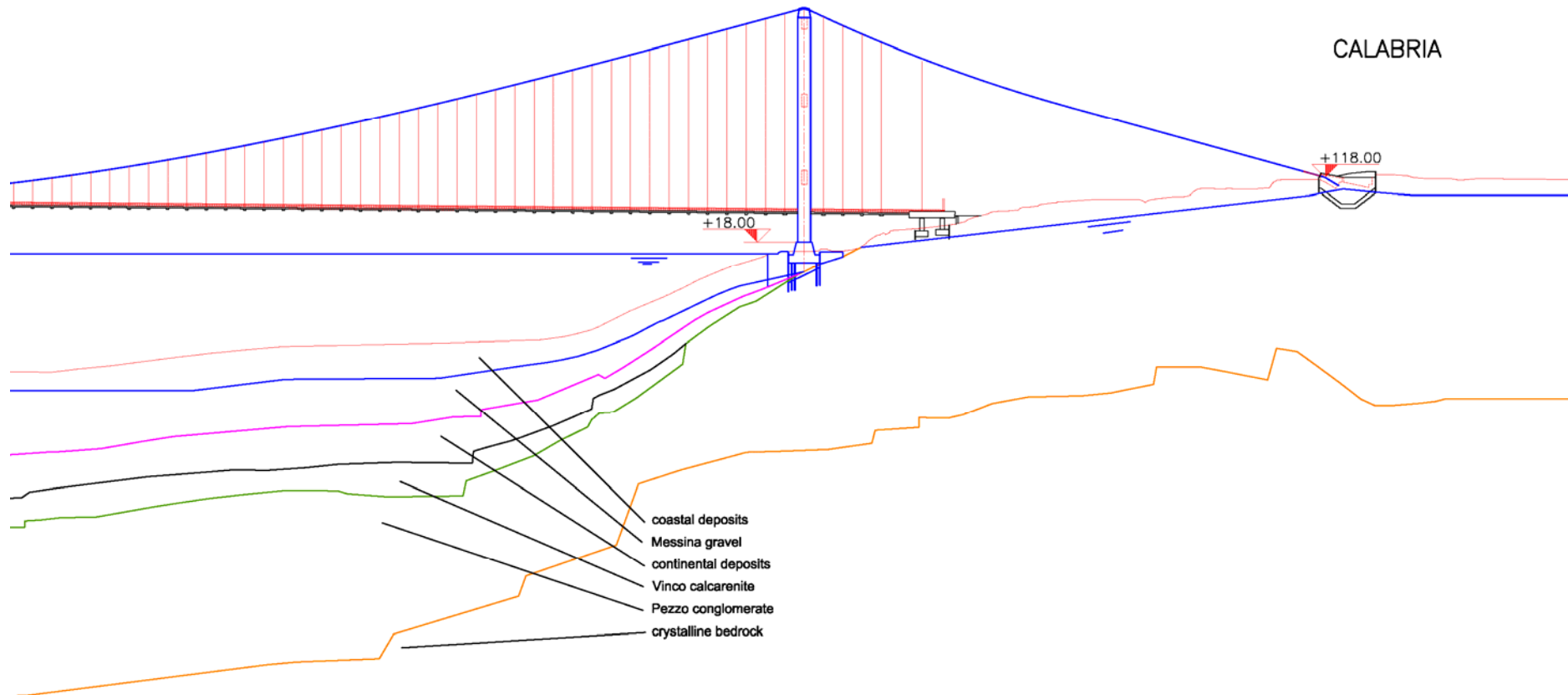


Figure 17: Soil profile on the Calabria shore of Messina Strait

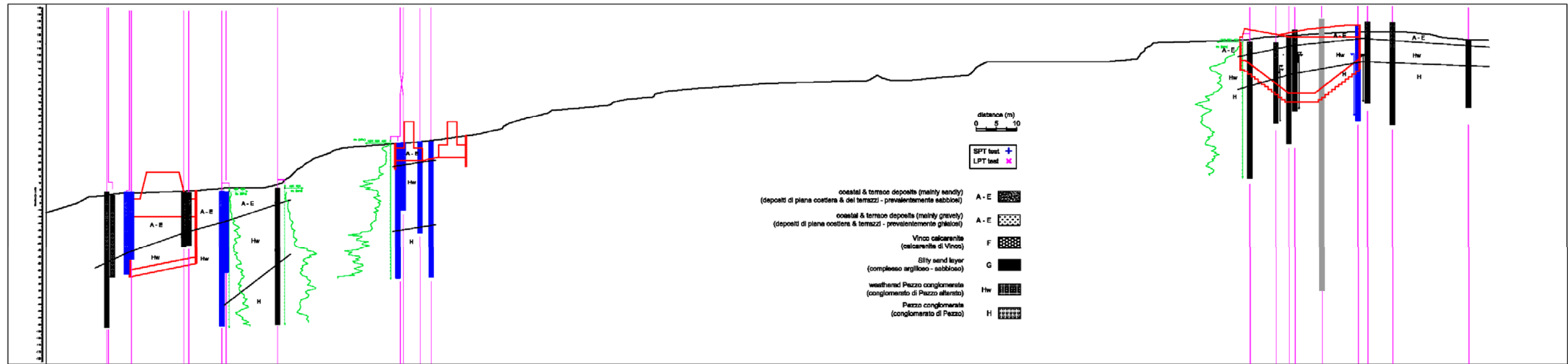


Figure 18: Calabria shore - geotechnical longitudinal section: global view

CALABRIA LONGITUDINAL SECTION - TOWER AND TERMINAL STRUCTURE

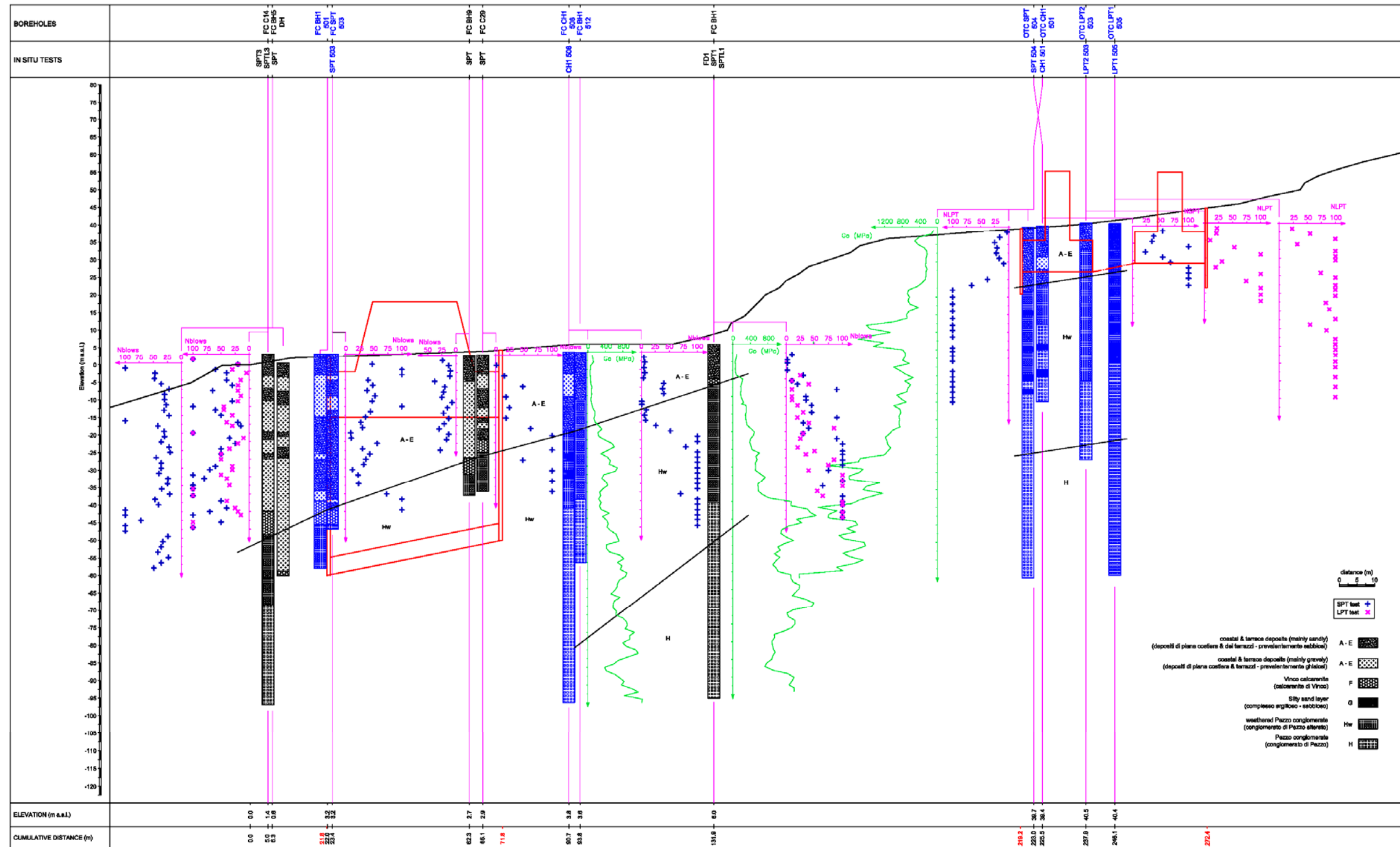


Figure 19: Calabria shore - geotechnical longitudinal section at the tower and the terminal structure

CALABRIA LONGITUDINAL SECTION - ANCHOR BLOCK

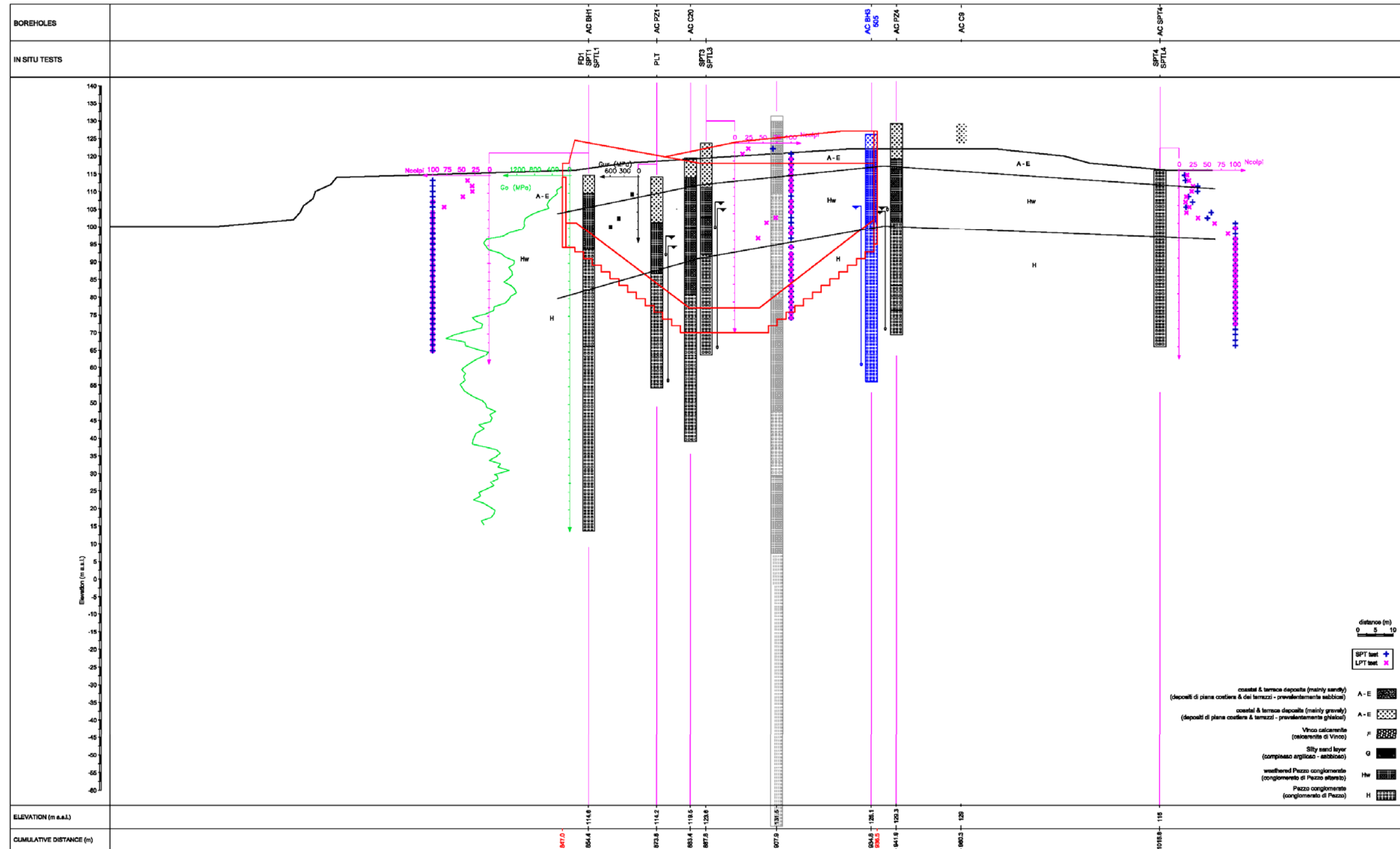


Figure 20: Calabria shore - geotechnical longitudinal section at the anchor block

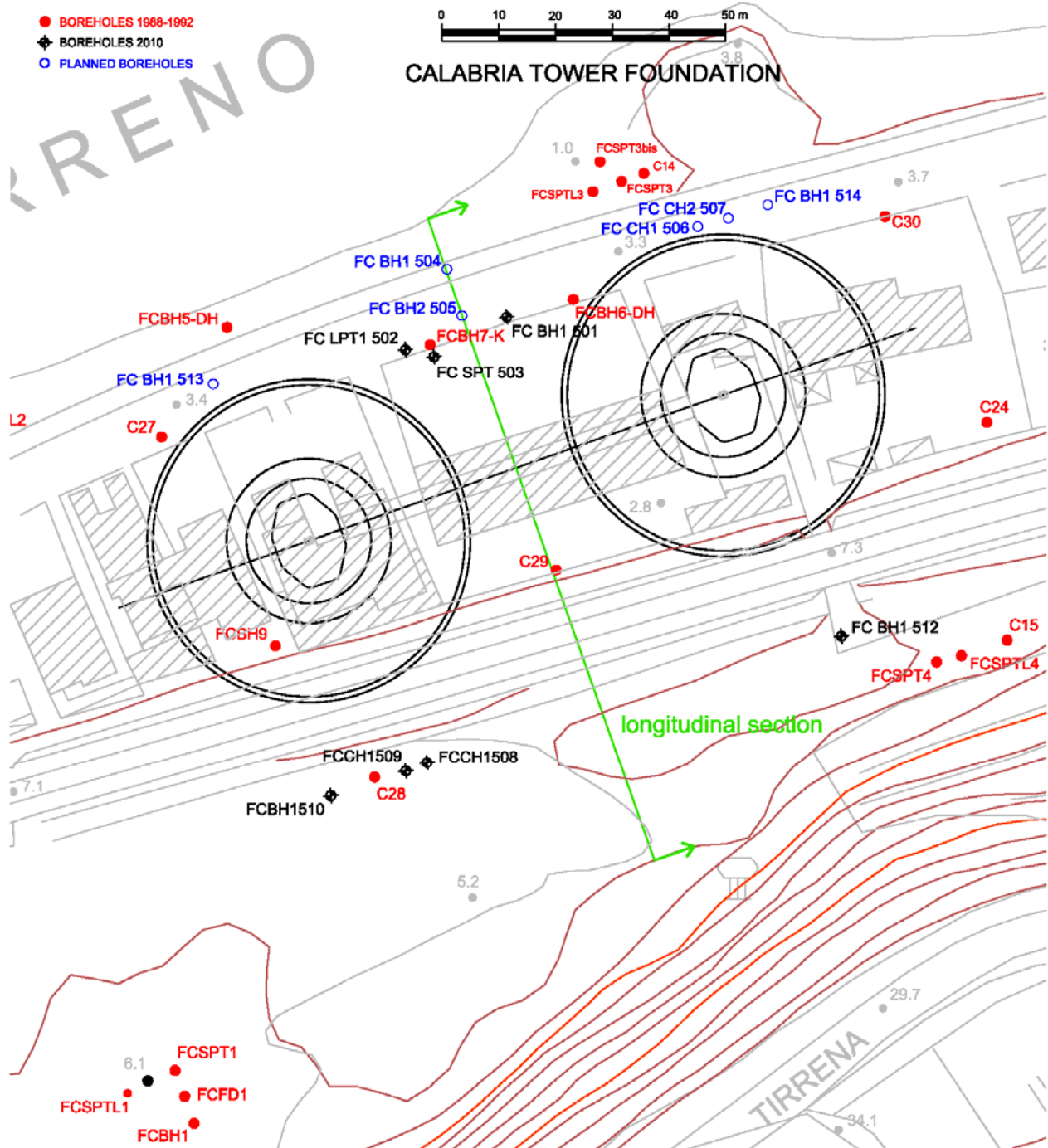


Figure 21: Calabria shore - plan view of Tower and boreholes location

		Ponte sullo Stretto di Messina PROGETTO DEFINITIVO		
Seismic analyses for soil-foundation systems, Annex		Codice documento PB0032_F0_ANX	Rev F0	Data 20/06/2011

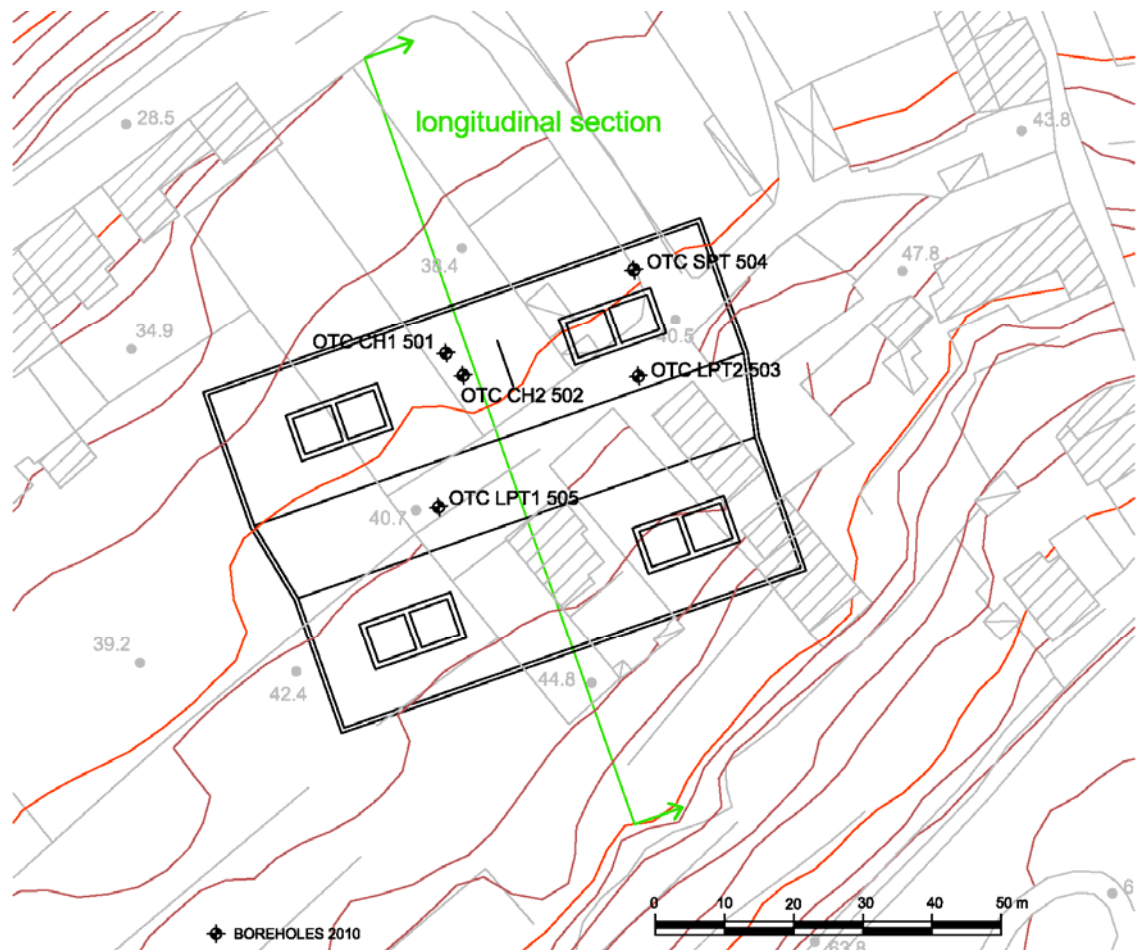


Figure 22: Calabria shore - plan view of Terminal Structure and boreholes location

		Ponte sullo Stretto di Messina PROGETTO DEFINITIVO		
Seismic analyses for soil-foundation systems, Annex		Codice documento PB0032_F0_ANX	Rev F0	Data 20/06/2011

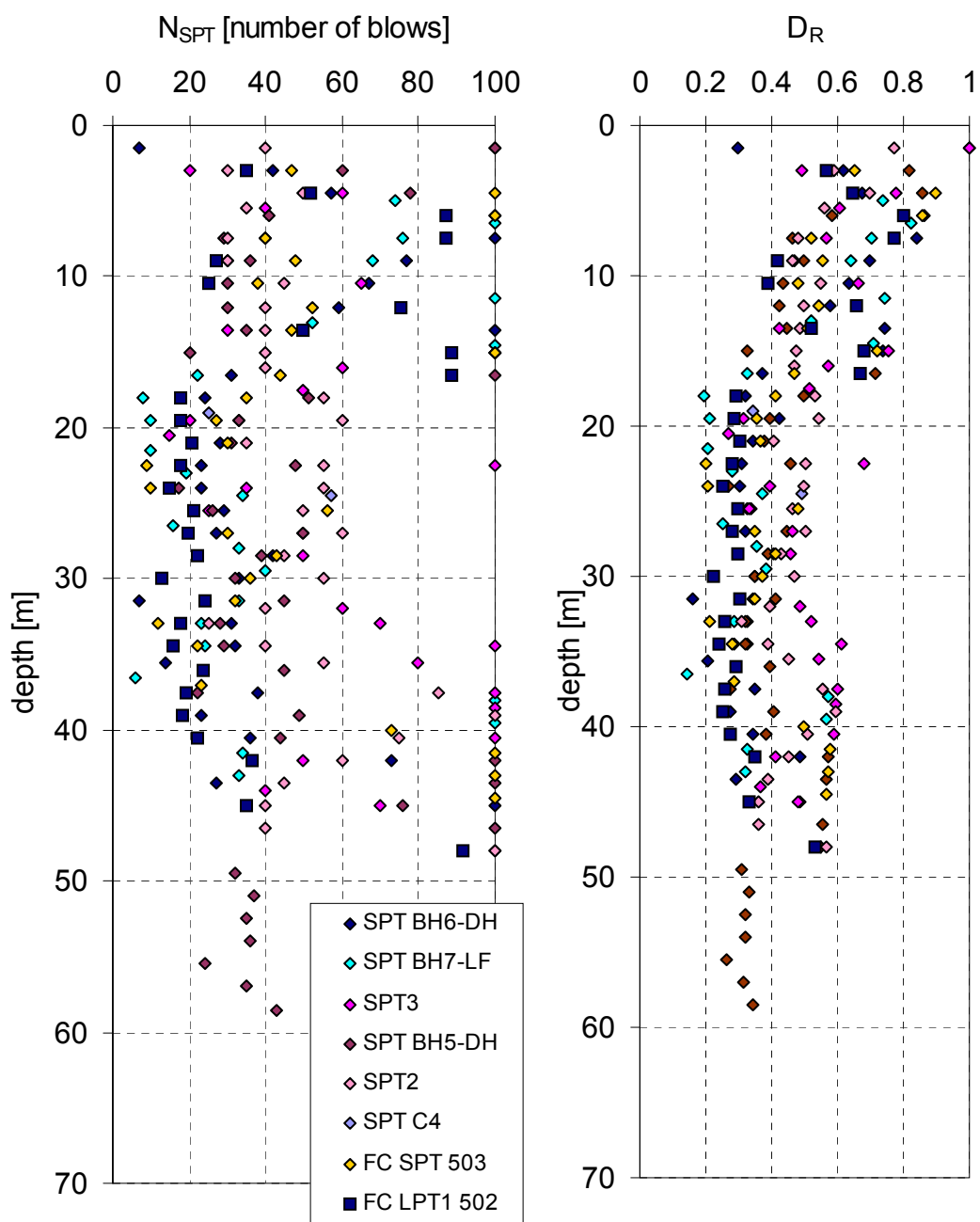




Figure 23: Calabria Tower (Northern side), coastal deposits - relative density from SPT and LPT results

		Ponte sullo Stretto di Messina PROGETTO DEFINITIVO		
Seismic analyses for soil-foundation systems, Annex	<i>Codice documento</i> PB0032_F0_ANX	<i>Rev</i> F0	<i>Data</i> 20/06/2011	

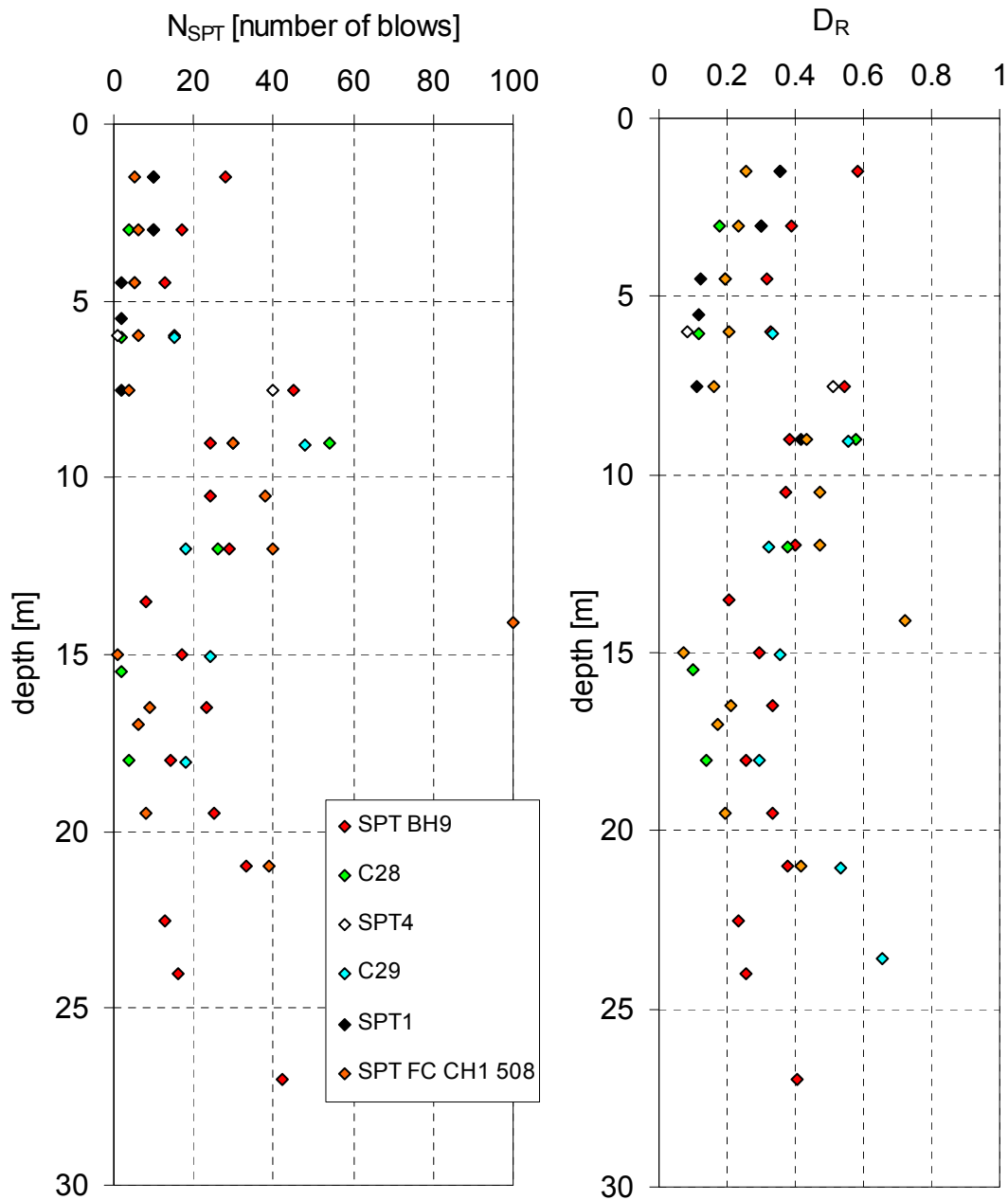




Figure 24: Calabria Tower (Southern side), coastal deposits - relative density from SPT results

		Ponte sullo Stretto di Messina PROGETTO DEFINITIVO		
Seismic analyses for soil-foundation systems, Annex	Codice documento <i>PB0032_F0_ANX</i>	Rev <i>F0</i>	Data <i>20/06/2011</i>	

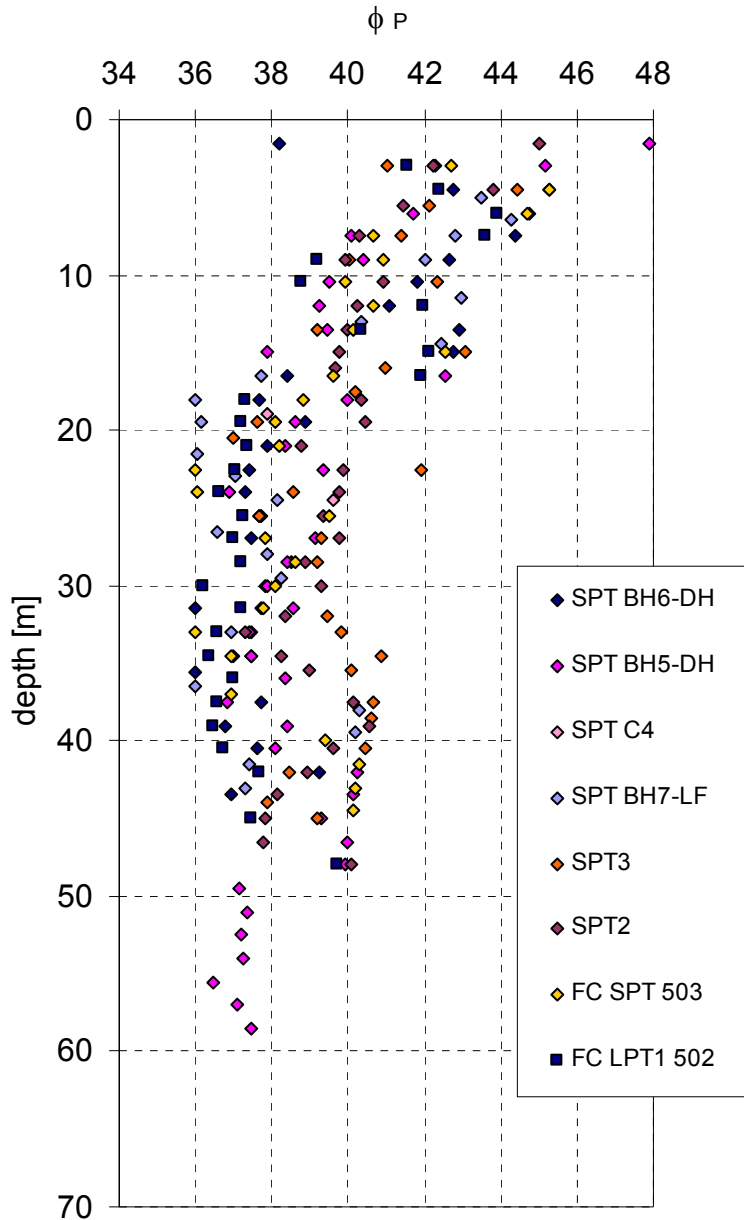


Figure 25: Calabria Tower (Northern side), coastal deposits - angle of peak shearing resistance from SPT and LPT results

		Ponte sullo Stretto di Messina PROGETTO DEFINITIVO		
Seismic analyses for soil-foundation systems, Annex	<i>Codice documento</i> PB0032_F0_ANX	<i>Rev</i> F0	<i>Data</i> 20/06/2011	

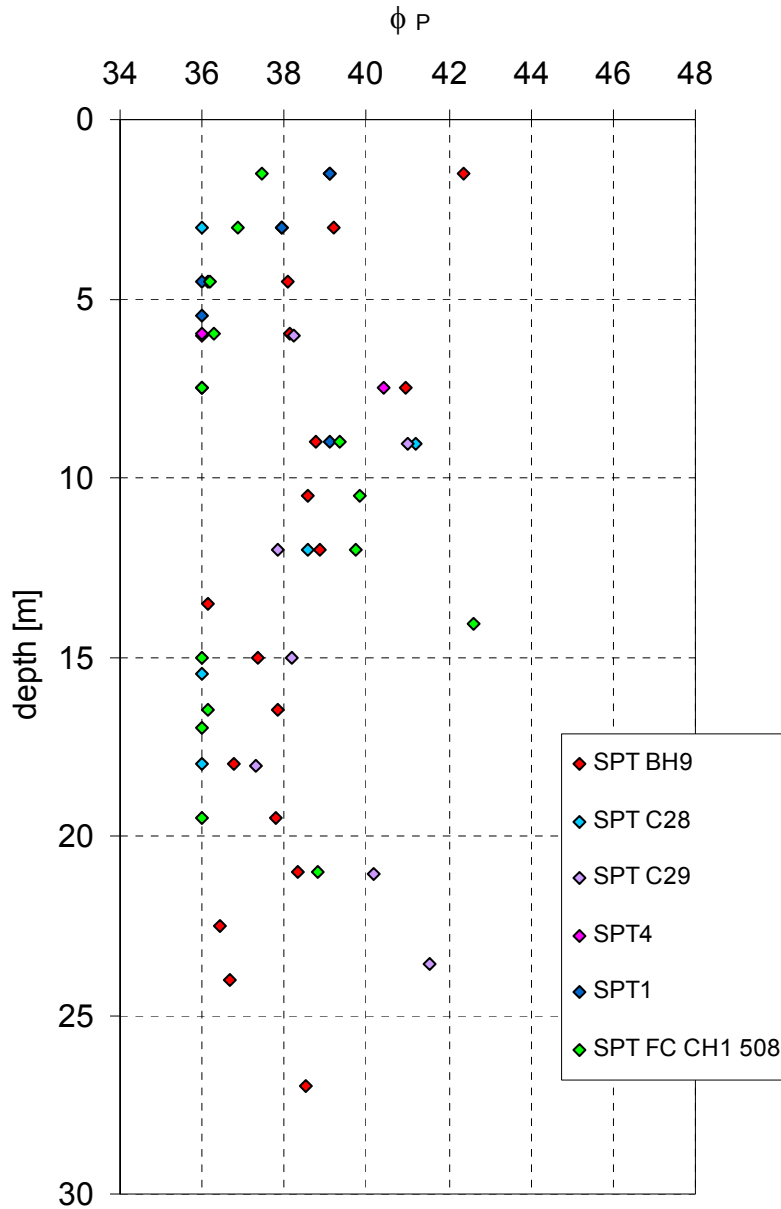


Figure 26: Calabria Tower (Southern side), coastal deposits - angle of peak shearing resistance from SPT results

		Ponte sullo Stretto di Messina PROGETTO DEFINITIVO		
Seismic analyses for soil-foundation systems, Annex	Codice documento <i>PB0032_F0_ANX</i>	Rev <i>F0</i>	Data <i>20/06/2011</i>	

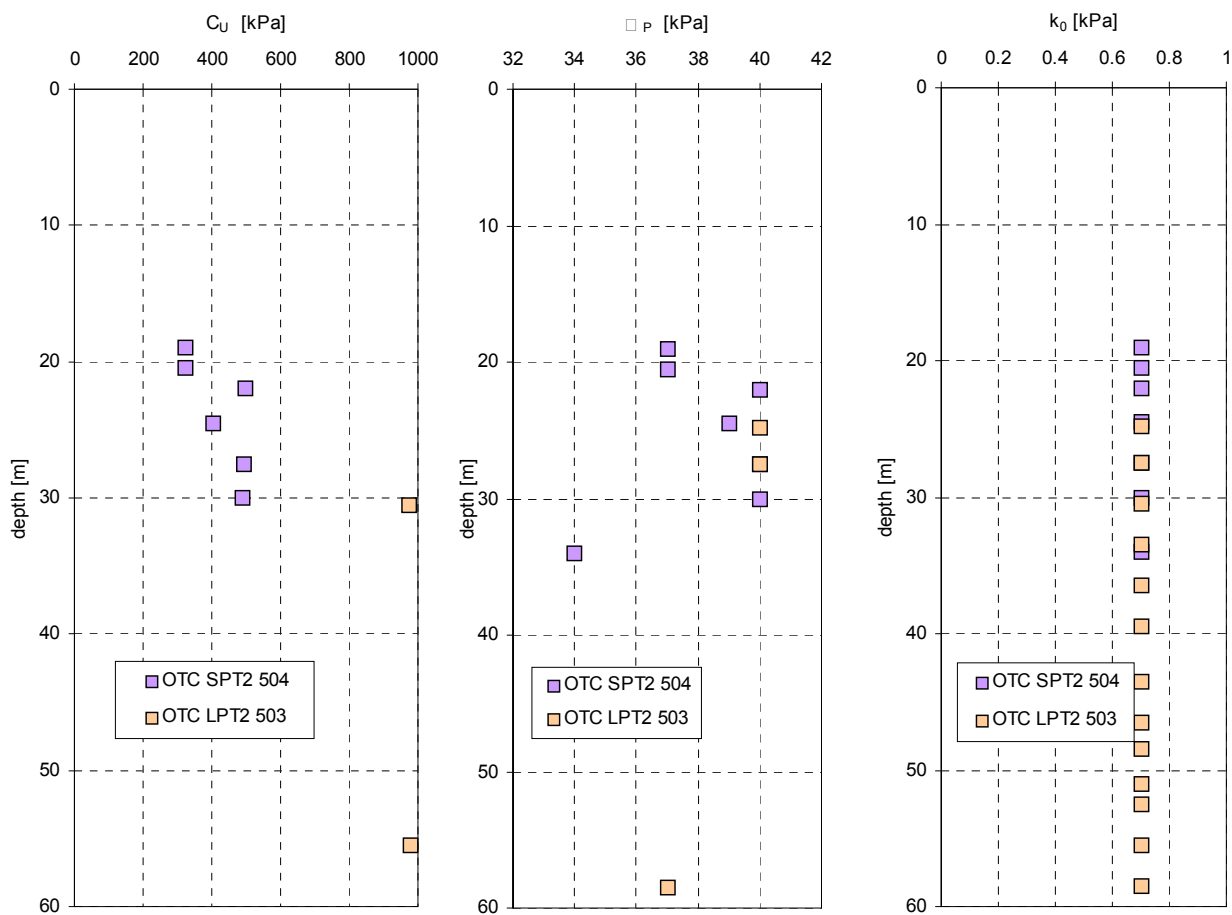


Figure 27: Calabria Terminal Structure: Pezzo Conglomerate - c , p and K_0 profiles from dilatometer test

		Ponte sullo Stretto di Messina PROGETTO DEFINITIVO		
Seismic analyses for soil-foundation systems, Annex	<i>Codice documento</i> PB0032_F0_ANX	<i>Rev</i> F0	<i>Data</i> 20/06/2011	

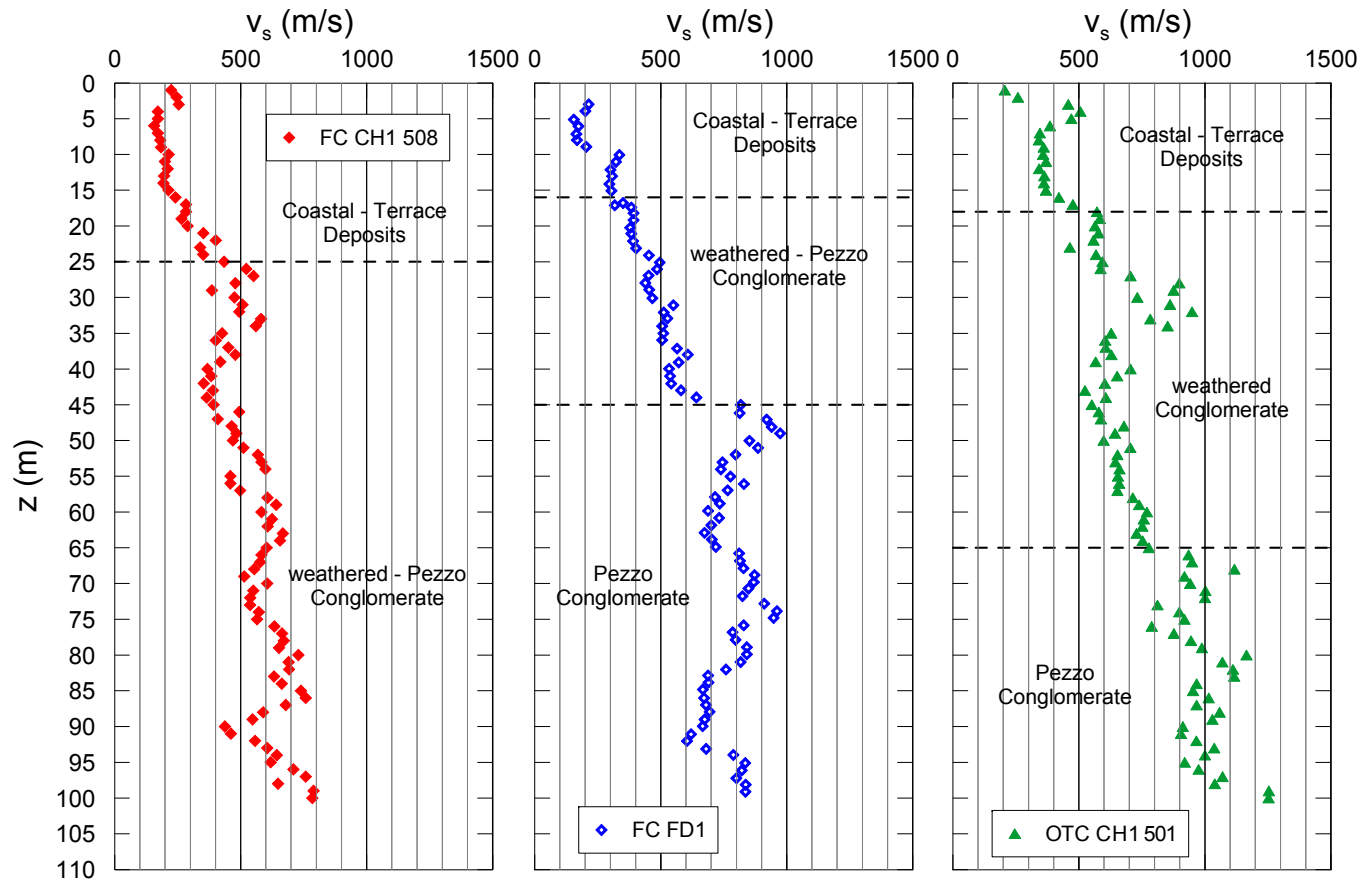


Figure 28: Calabria Tower and Terminal Structure site - v_s profile from cross-hole tests

		Ponte sullo Stretto di Messina PROGETTO DEFINITIVO		
Seismic analyses for soil-foundation systems, Annex	<i>Codice documento</i> PB0032_F0_ANX	<i>Rev</i> F0	<i>Data</i> 20/06/2011	

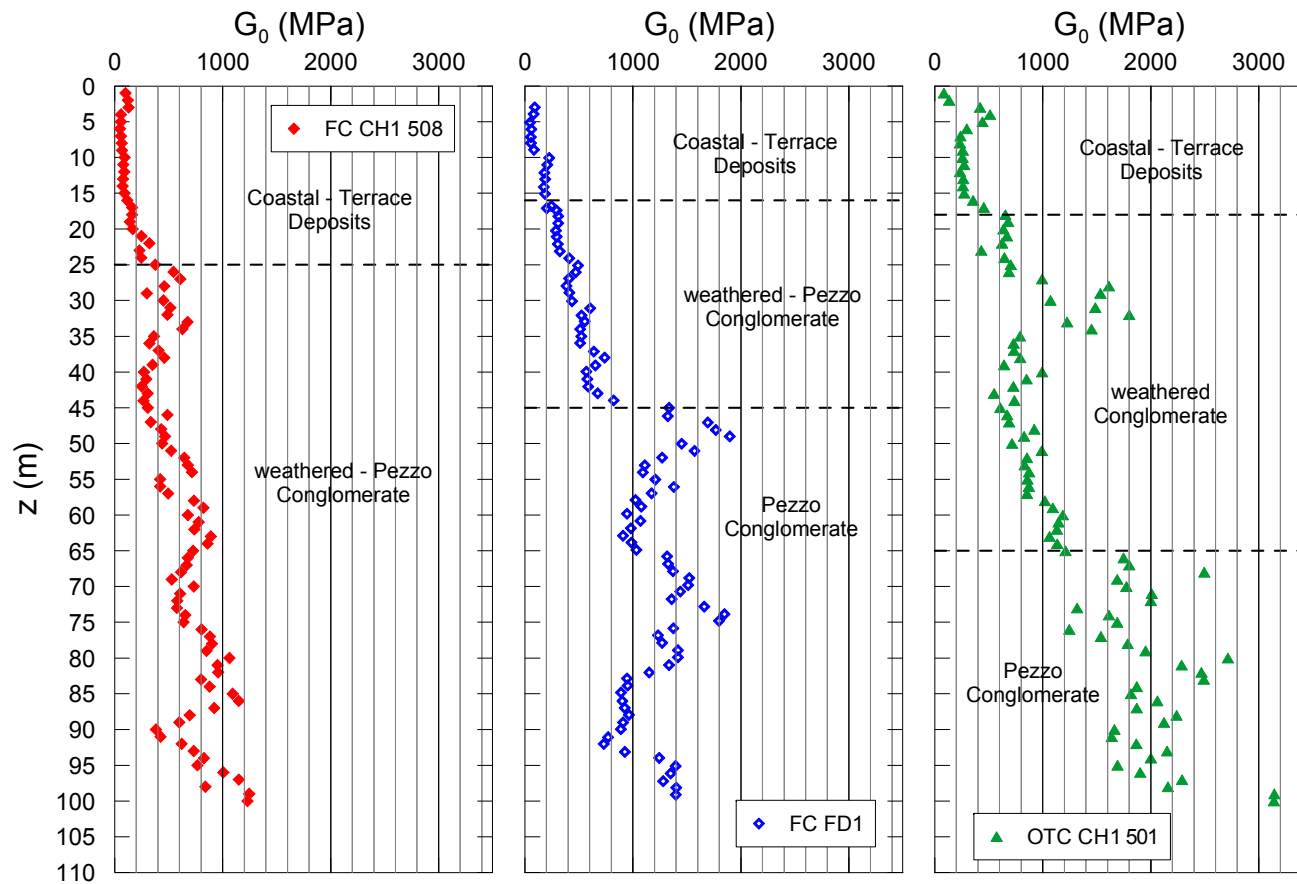


Figure 29: Calabria Tower and Terminal Structure site - G_0 profile from cross-hole tests

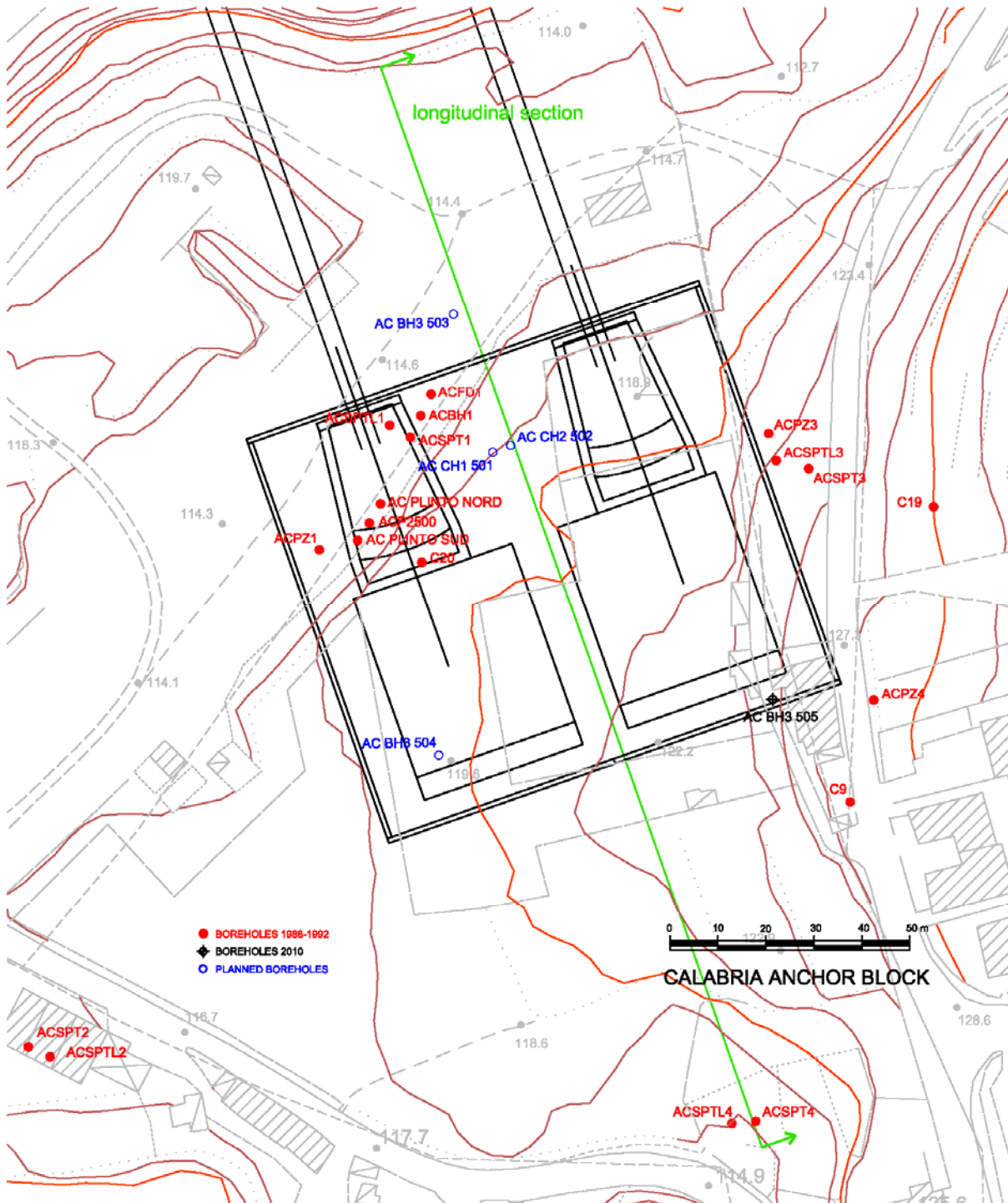


Figure 30: Calabria shore - plan view of Anchor Block

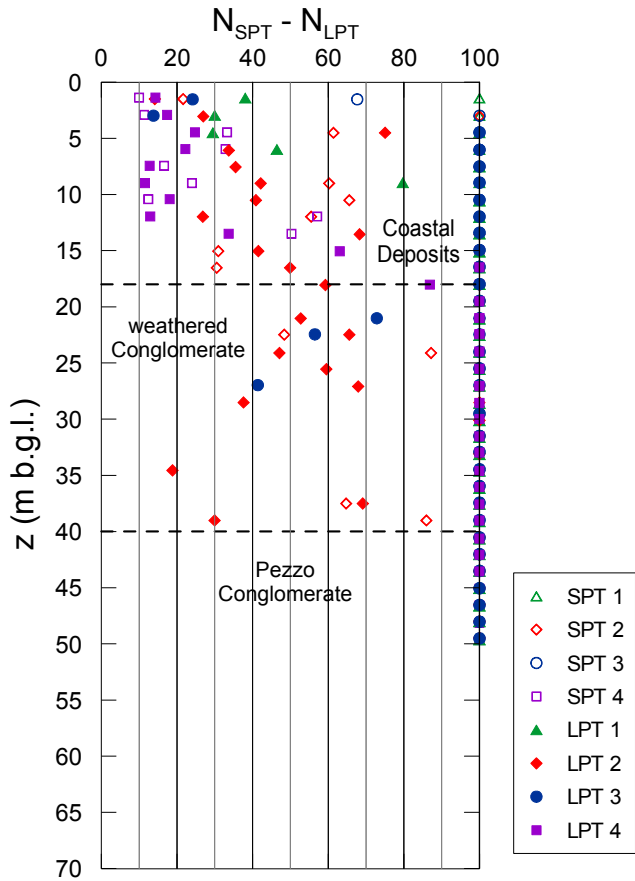




Figure 31: Calabria Anchor Block – SPT and LPT test results

		Ponte sullo Stretto di Messina PROGETTO DEFINITIVO	
Seismic analyses for soil-foundation systems, Annex	<i>Codice documento</i> PB0032_F0_ANX	<i>Rev</i> F0	<i>Data</i> 20/06/2011

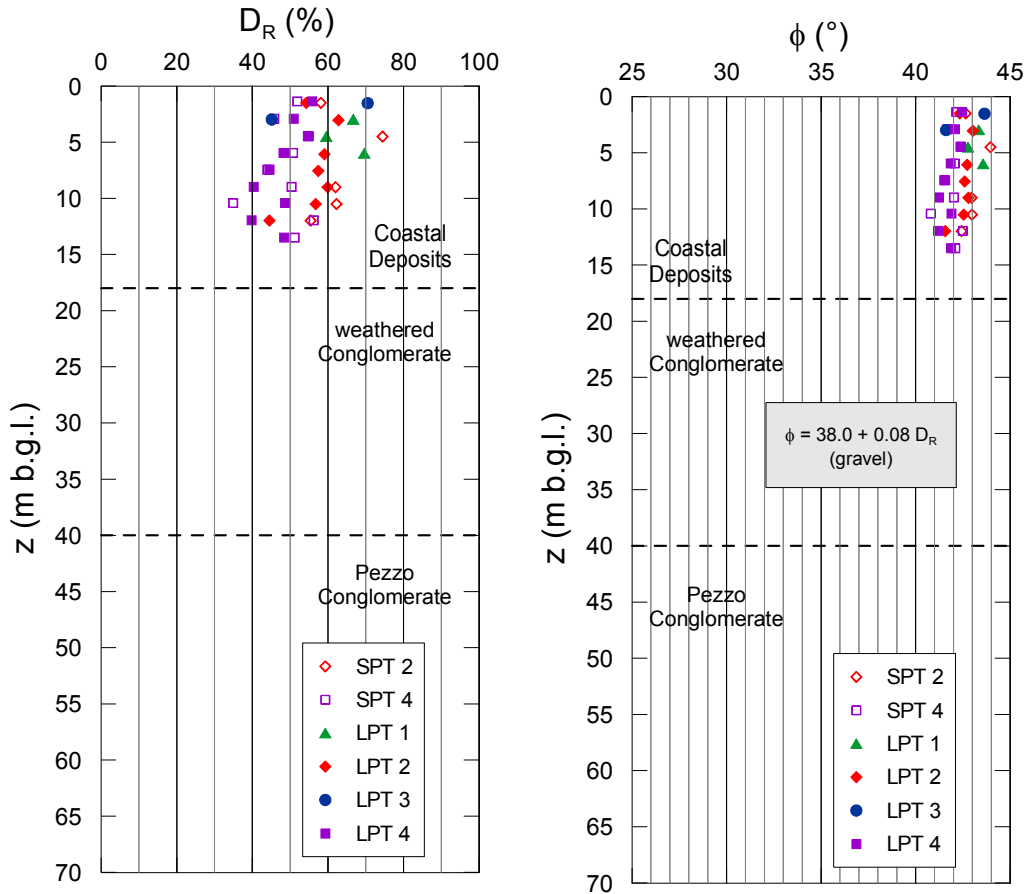


Figure 32: Calabria Anchor Block – relative density and angle of shearing resistance

		Ponte sullo Stretto di Messina PROGETTO DEFINITIVO	
Seismic analyses for soil-foundation systems, Annex	<i>Codice documento</i> PB0032_F0_ANX	<i>Rev</i> F0	<i>Data</i> 20/06/2011

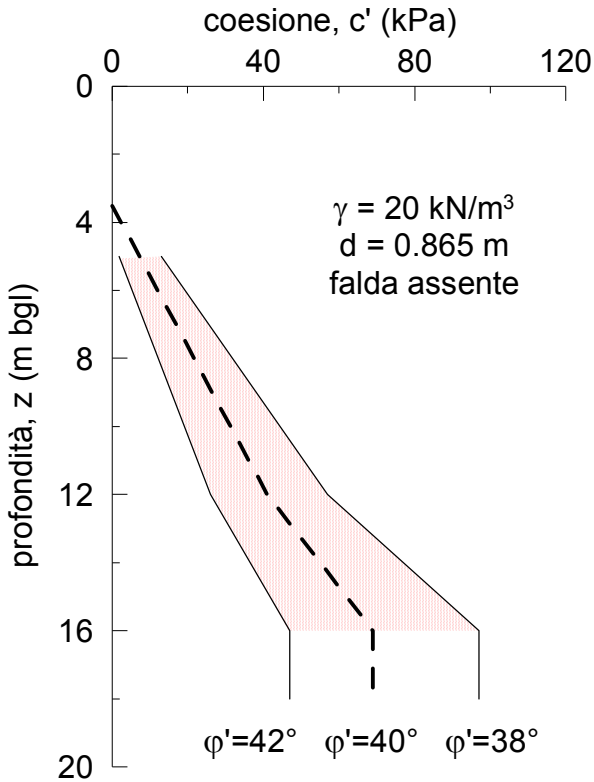


Figure 33: Calabria Anchor Block – c' profile from large diameter plate loading test

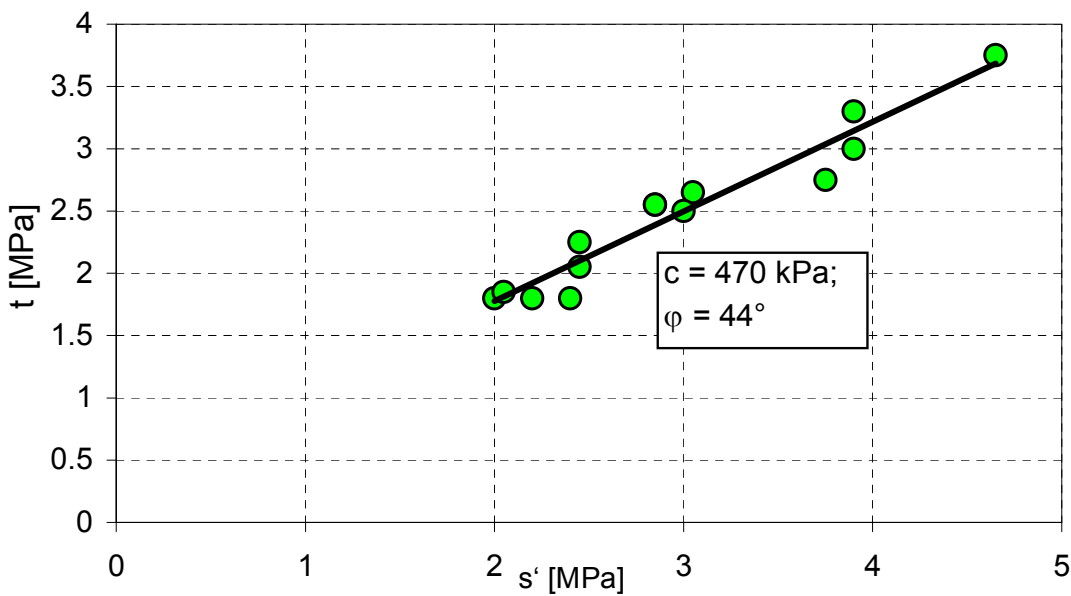


Figure 34: Calabria Anchor Block – results of TX tests (borehole AC BH3 505)

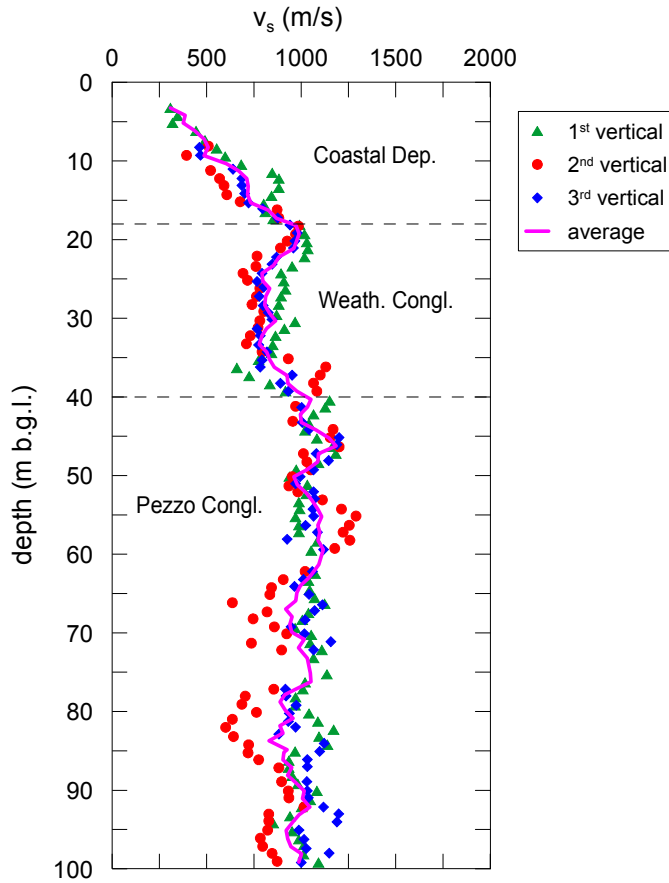


Figure 35: Calabria Anchor Block – v_s profile from cross-hole test

		Ponte sullo Stretto di Messina PROGETTO DEFINITIVO		
Seismic analyses for soil-foundation systems, Annex	<i>Codice documento</i> PB0032_F0_ANX	<i>Rev</i> F0	<i>Data</i> 20/06/2011	

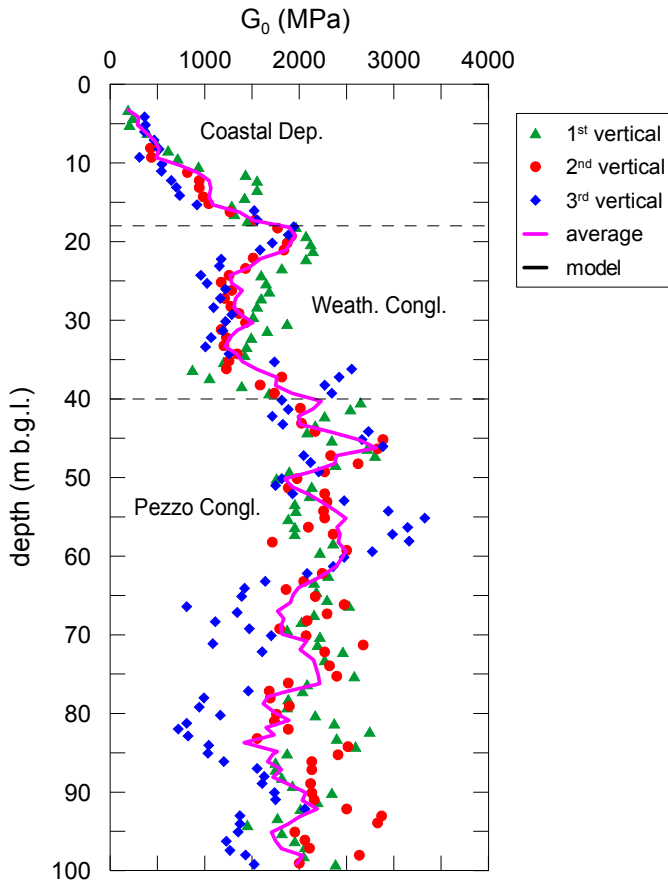




Figure 36: Calabria Anchor Block – G_0 profile from cross-hole test

		Ponte sullo Stretto di Messina PROGETTO DEFINITIVO		
Seismic analyses for soil-foundation systems, Annex		<i>Codice documento</i> PB0032_F0_ANX	<i>Rev</i> F0	<i>Data</i> 20/06/2011

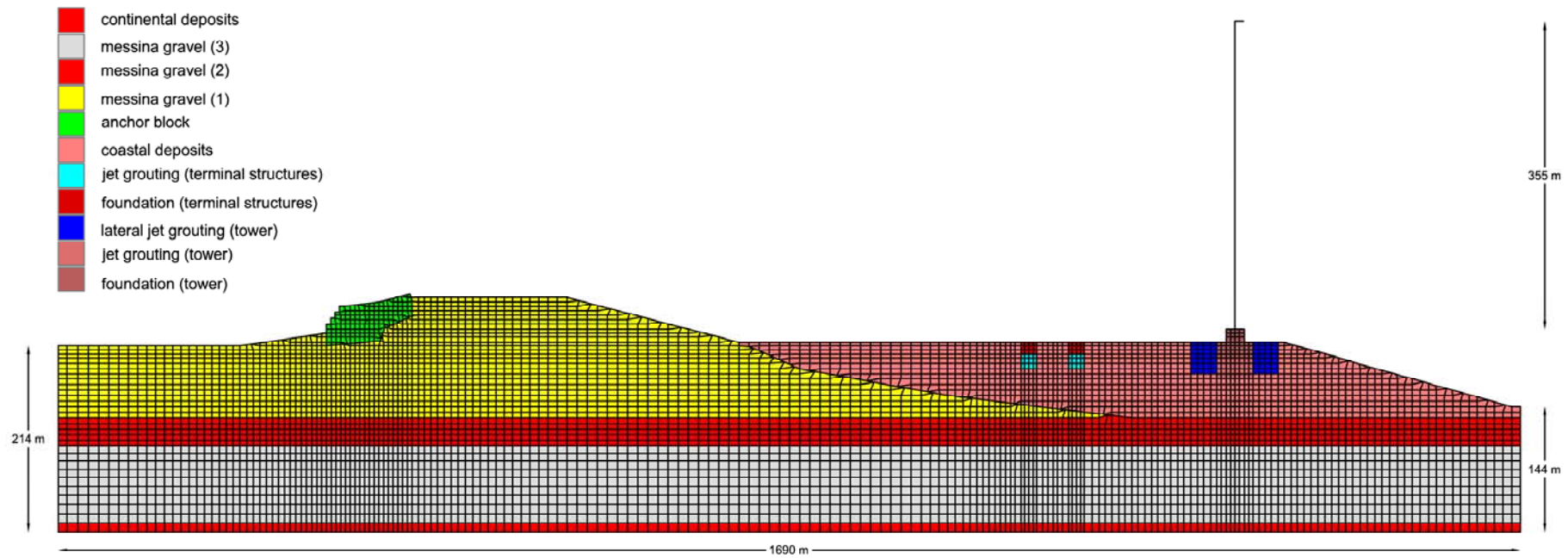


Figure 37: FD model: longitudinal section of the Sicilia shore

		Ponte sullo Stretto di Messina PROGETTO DEFINITIVO	
Seismic analyses for soil-foundation systems, Annex	<i>Codice documento</i> PB0032_F0_ANX	<i>Rev</i> F0	<i>Data</i> 20/06/2011

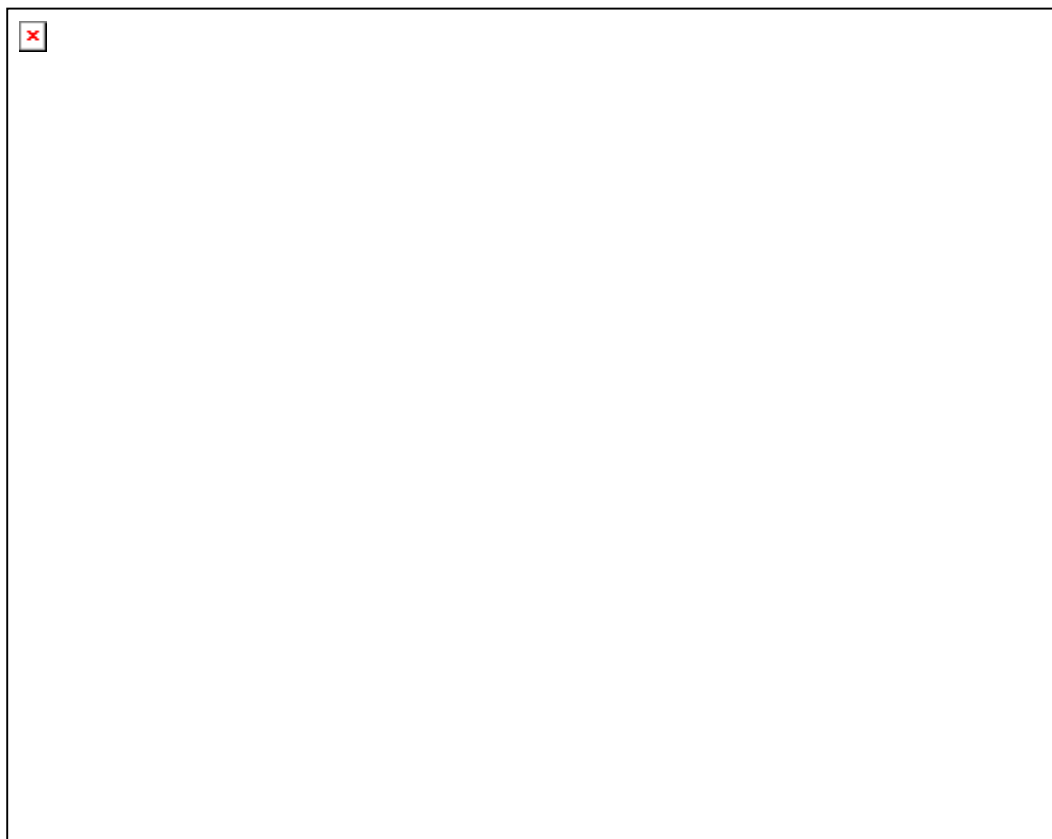


Figure 38: FD model: transversal section of the Sicilia tower



Figure 39: FD model: transversal section of the Sicilia anchor block

		Ponte sullo Stretto di Messina PROGETTO DEFINITIVO		
Seismic analyses for soil-foundation systems, Annex	<i>Codice documento</i> PB0032_F0_ANX	<i>Rev</i> F0	<i>Data</i> 20/06/2011	

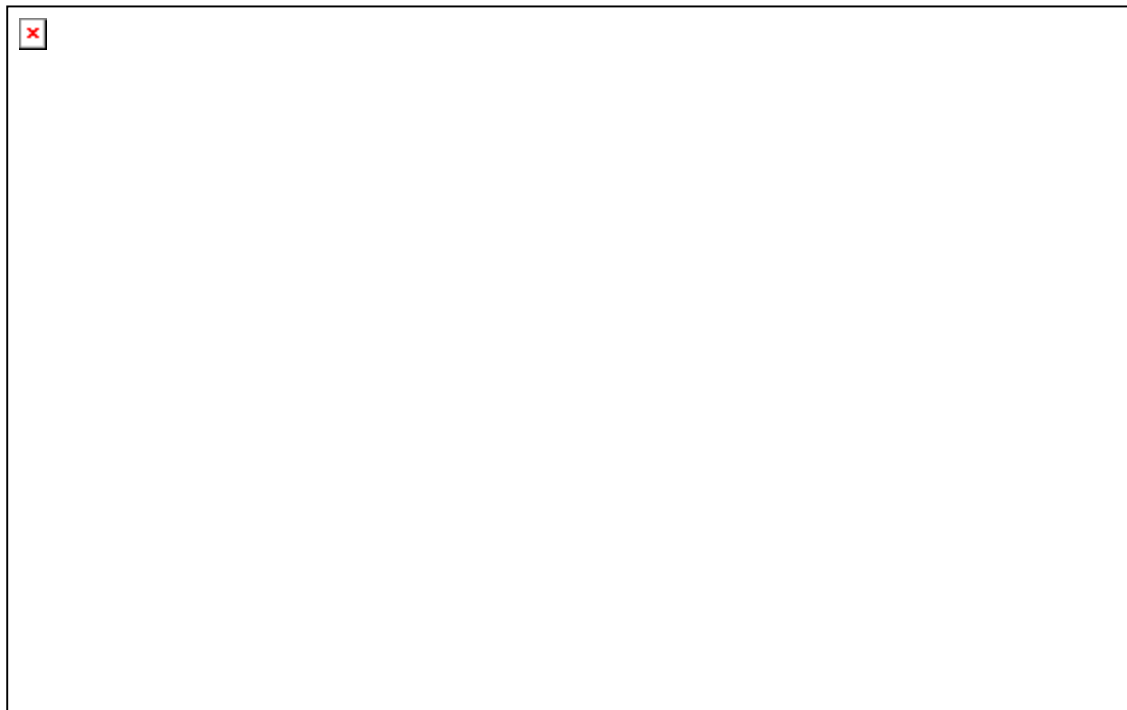


Figure 40: FD model: transversal section of the Sicilia terminal structure

		Ponte sullo Stretto di Messina PROGETTO DEFINITIVO		
Seismic analyses for soil-foundation systems, Annex	<i>Codice documento</i> PB0032_F0_ANX	<i>Rev</i> F0	<i>Data</i> 20/06/2011	

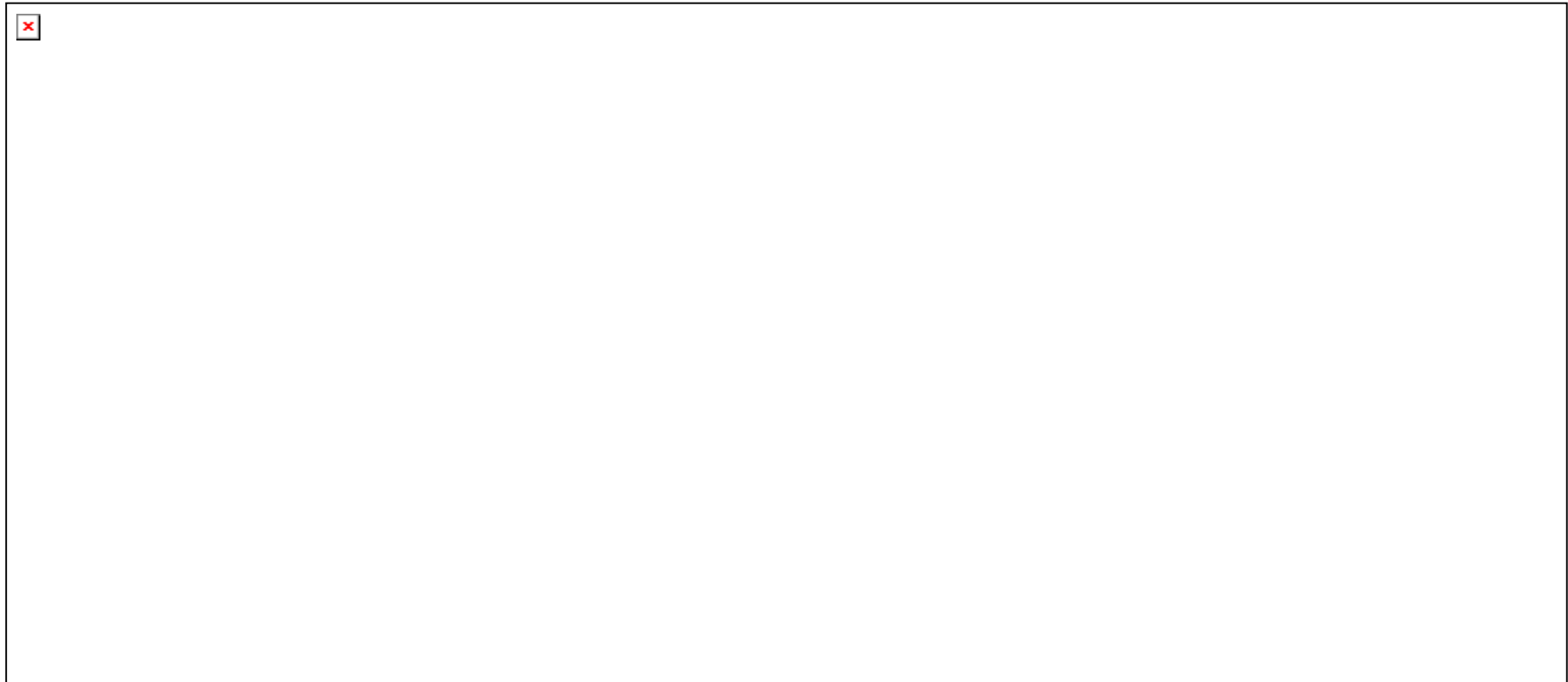


Figure 41: FD model: longitudinal section of the Calabria shore



		Ponte sullo Stretto di Messina PROGETTO DEFINITIVO		
Seismic analyses for soil-foundation systems, Annex	<i>Codice documento</i> PB0032_F0_ANX	<i>Rev</i> F0	<i>Data</i> 20/06/2011	



Figure 42: FD model: transversal section of the Calabria Tower

		Ponte sullo Stretto di Messina PROGETTO DEFINITIVO	
Seismic analyses for soil-foundation systems, Annex	<i>Codice documento</i> PB0032_F0_ANX	<i>Rev</i> F0	<i>Data</i> 20/06/2011

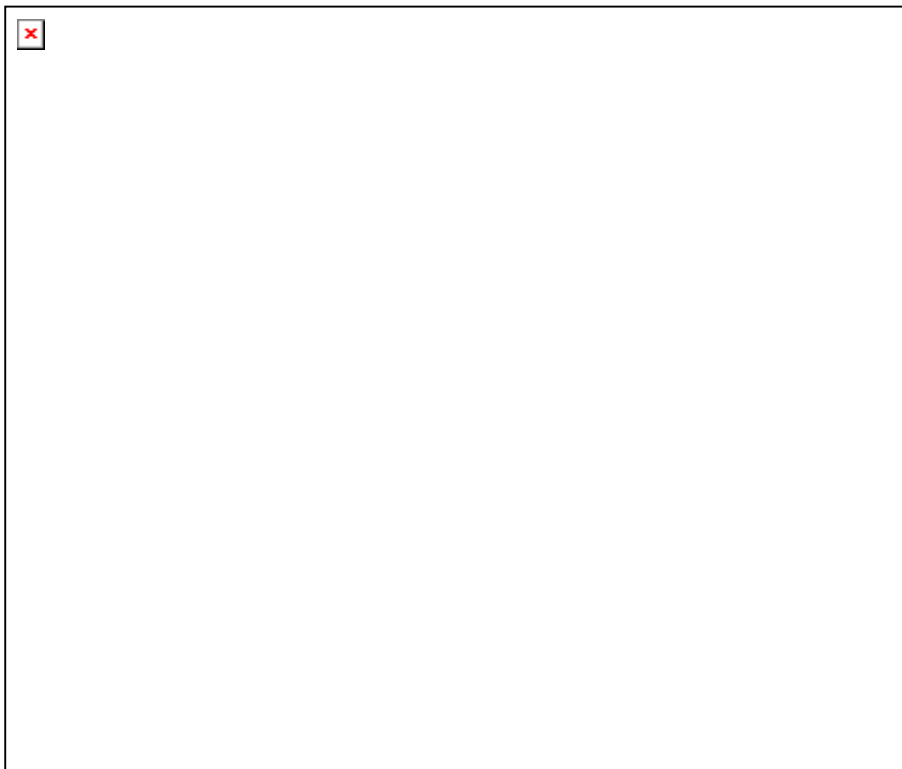


Figure 43: *FD model: transversal section of the Calabria anchor block*

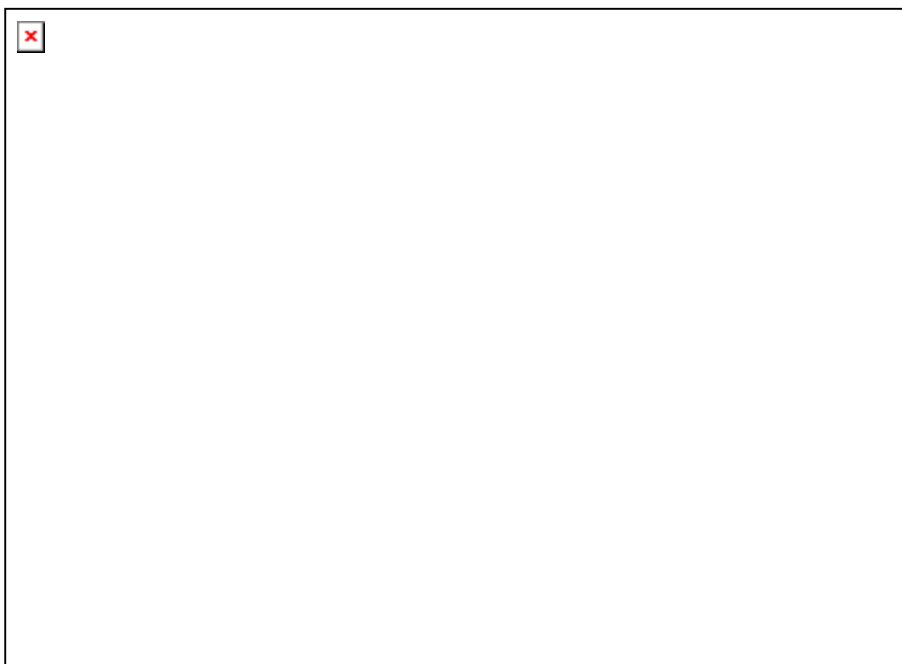


Figure 44: *FD model: transversal section of the Calabria terminal structure*

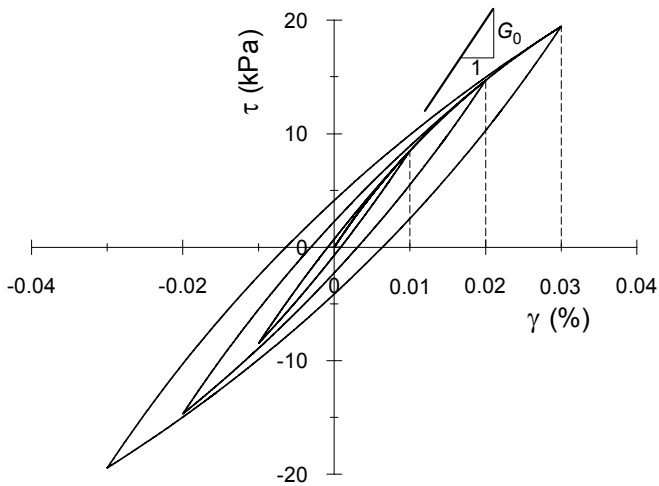


Figure 45: Typical stress-strain response of the hysteretic soil model

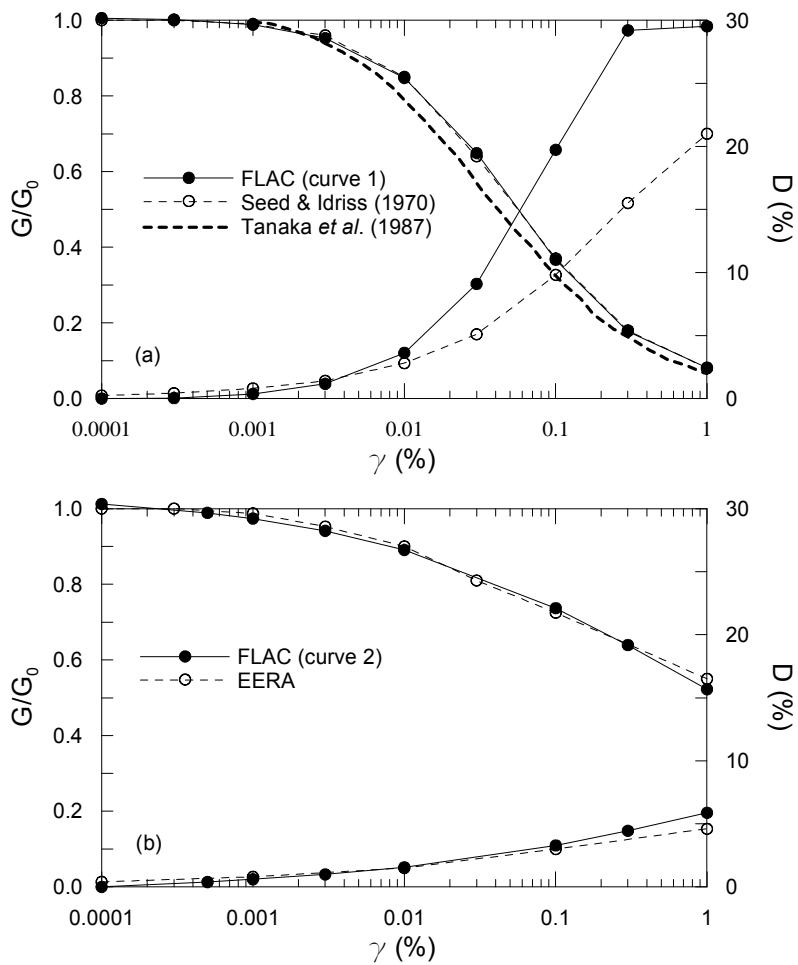


Figure 46: Calibration of the hysteretic model

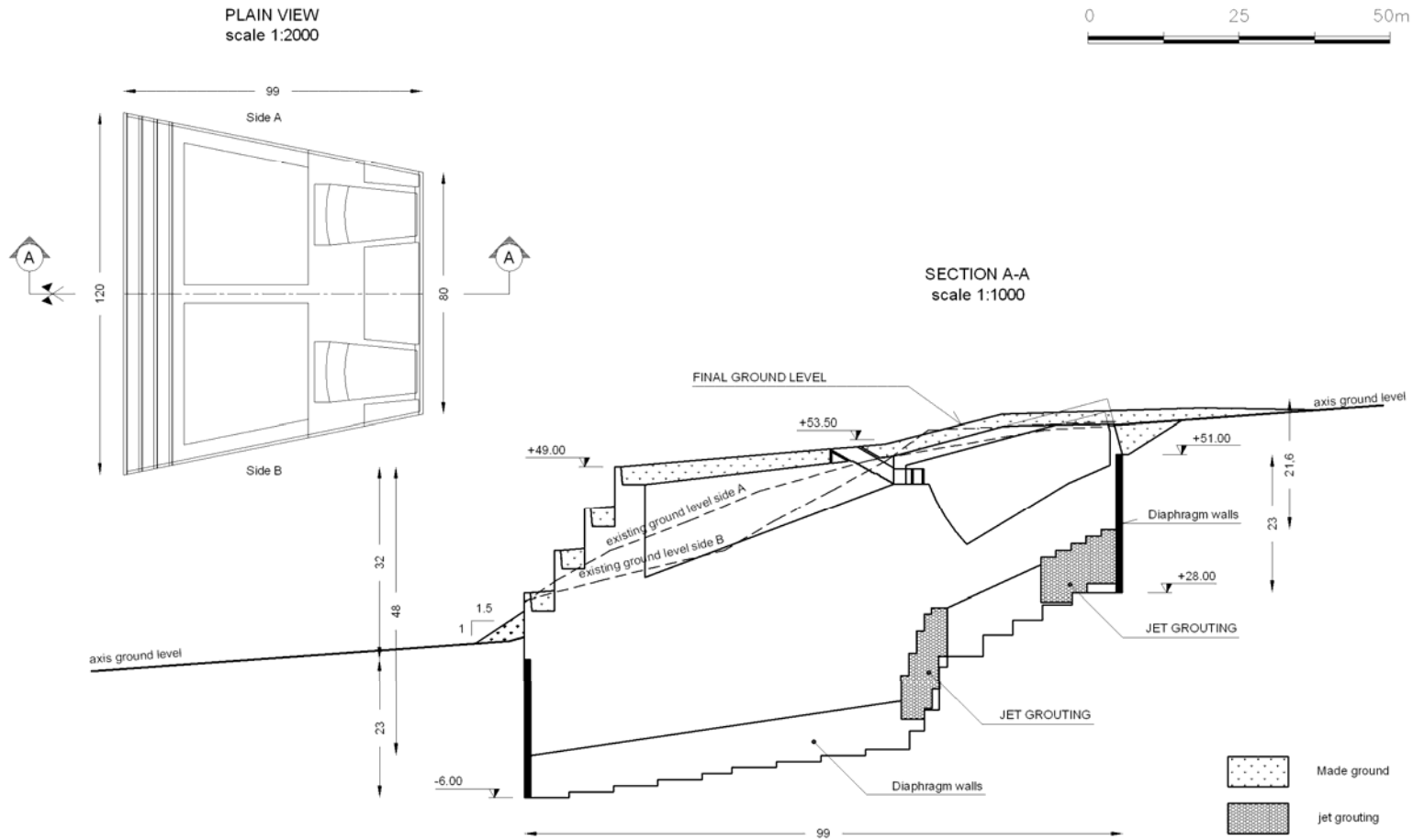




Figure 47: Plan view and cross section of Sicily anchor block

		Ponte sullo Stretto di Messina PROGETTO DEFINITIVO		
Seismic analyses for soil-foundation systems, Annex		<i>Codice documento</i> PB0032_F0_ANX	<i>Rev</i> F0	<i>Data</i> 20/06/2011

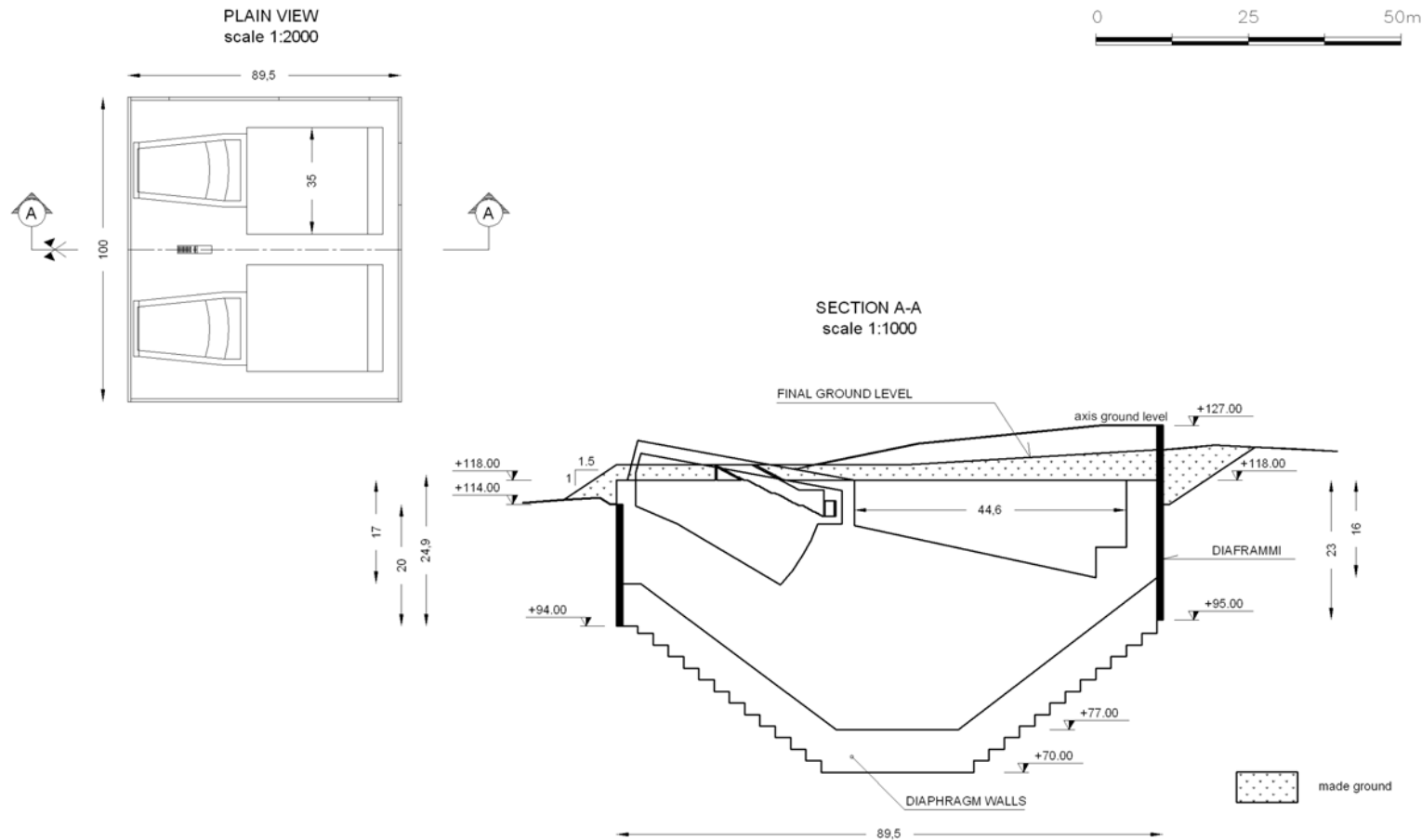


Figure 48: Plan view and cross section of Calabria Anchor Block

TRANSVERSAL MODEL

LONGITUDINAL MODEL

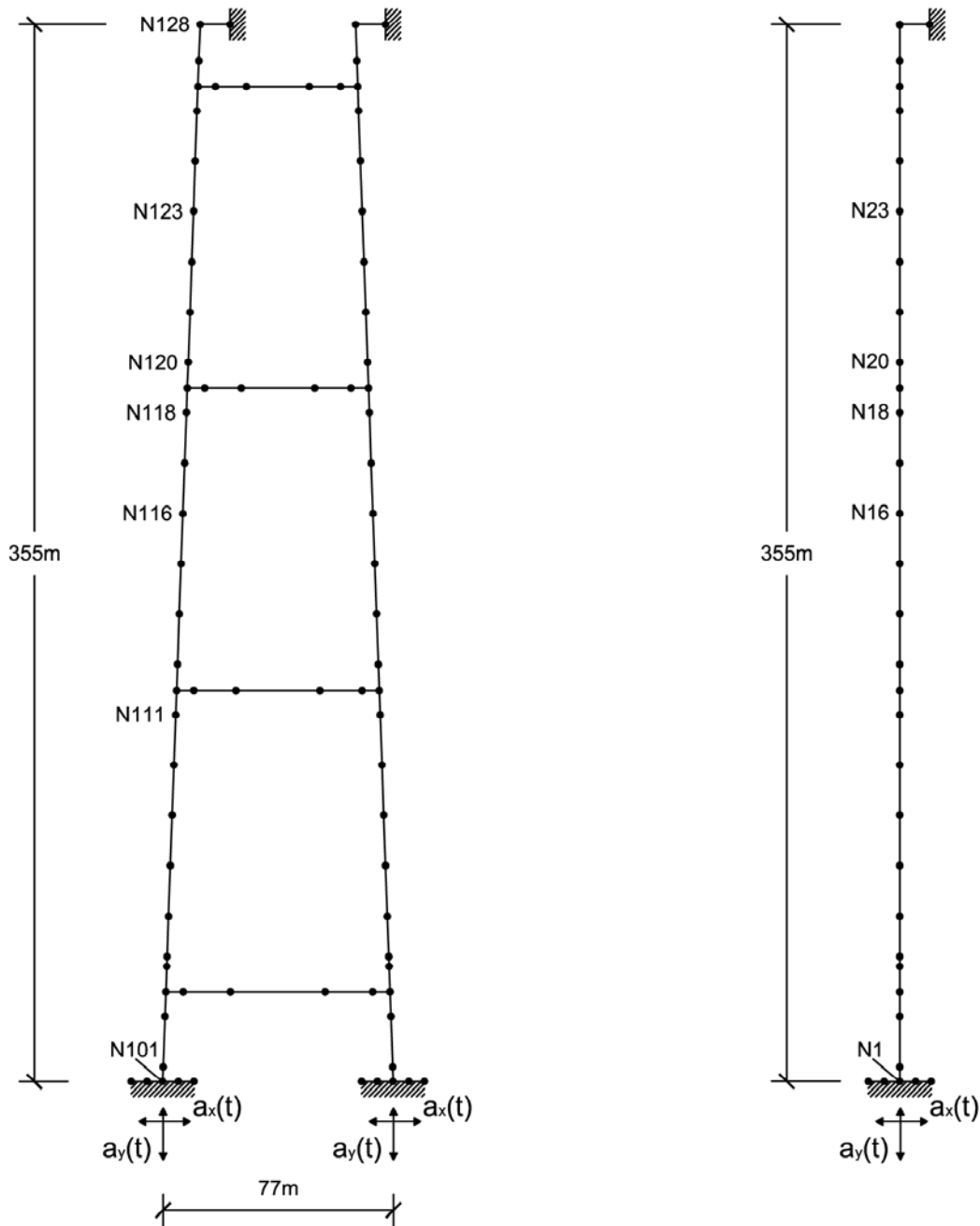


Figure 49. Longitudinal and transversal model of the two towers

		Ponte sullo Stretto di Messina PROGETTO DEFINITIVO		
Seismic analyses for soil-foundation systems, Annex		<i>Codice documento</i> PB0032_F0_ANX	<i>Rev</i> F0	<i>Data</i> 20/06/2011

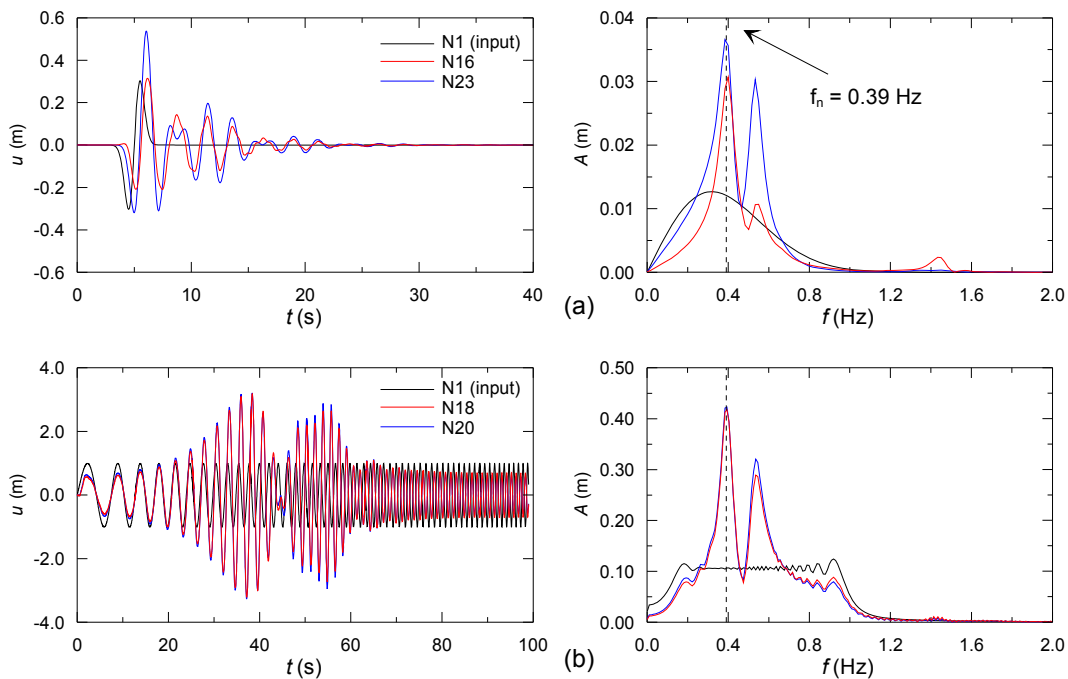


Figure 50. Longitudinal model of the Sicilia tower. Dynamic response for a wavelet (a) and a sweep sine (b) input motion

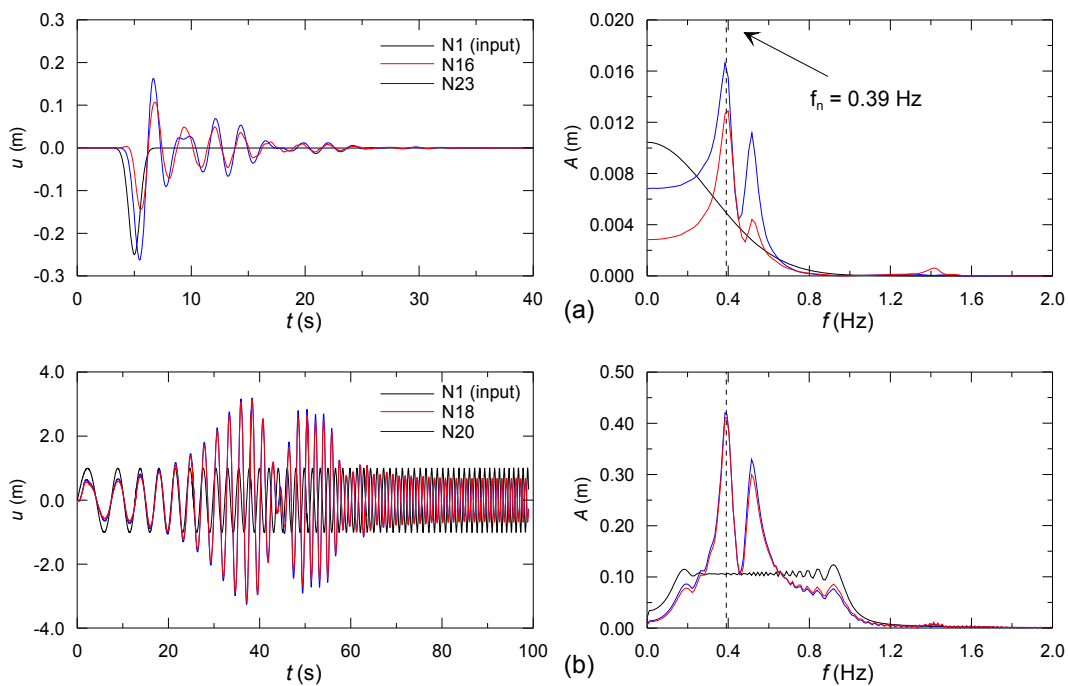


Figure 51. Longitudinal model of the Calabria tower. Dynamic response for a wavelet (a) and a sweep sine (b) input motion

		Ponte sullo Stretto di Messina PROGETTO DEFINITIVO		
Seismic analyses for soil-foundation systems, Annex		<i>Codice documento</i> PB0032_F0_ANX	<i>Rev</i> F0	<i>Data</i> 20/06/2011

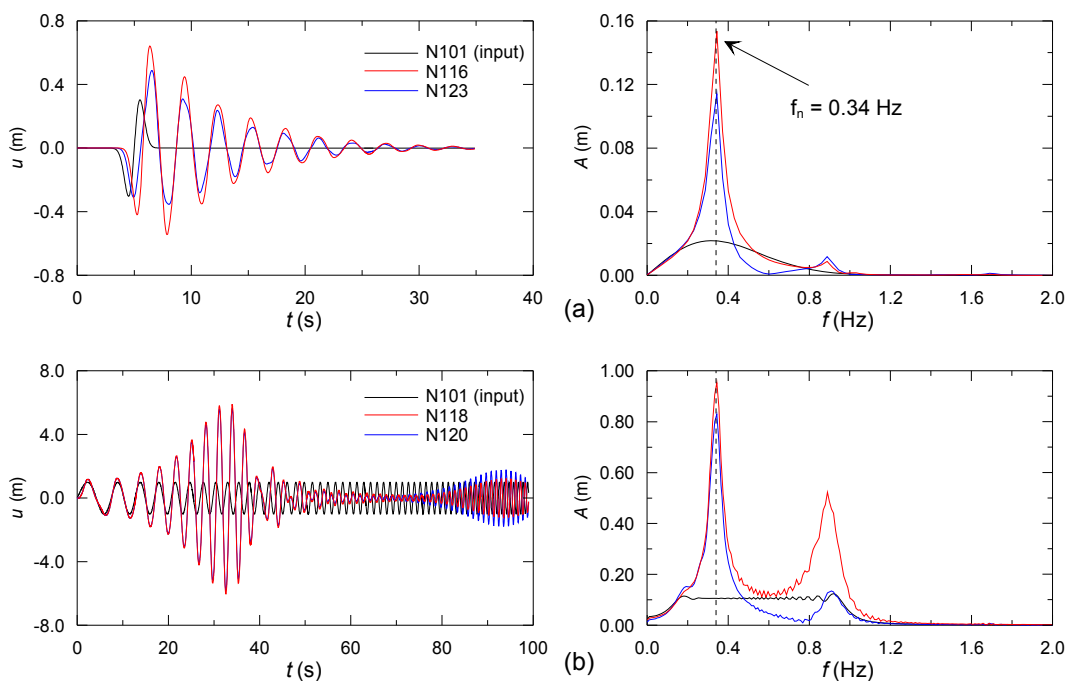


Figure 52. Transversal model of the Sicilia tower. Dynamic response for a wavelet (a) and a sweep sine (b) input motion

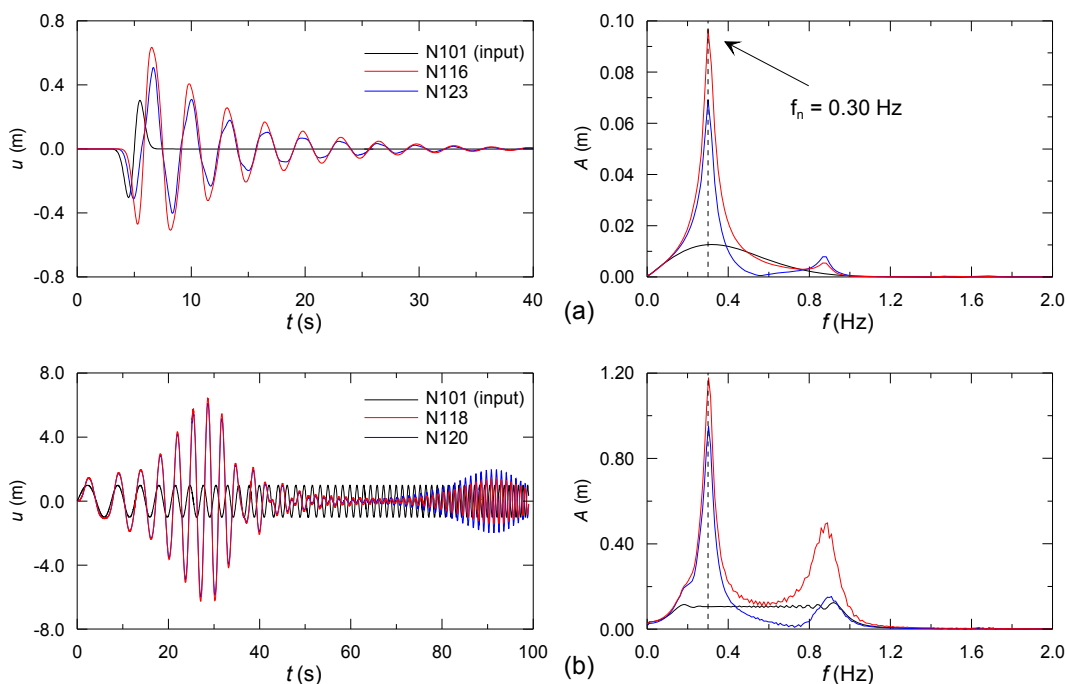


Figure 53. Transversal model of the Calabria tower. Dynamic response for a wavelet (a) and a sweep sine (b) input motion

		Ponte sullo Stretto di Messina PROGETTO DEFINITIVO	
Seismic analyses for soil-foundation systems, Annex	<i>Codice documento</i> PB0032_F0_ANX	<i>Rev</i> F0	<i>Data</i> 20/06/2011

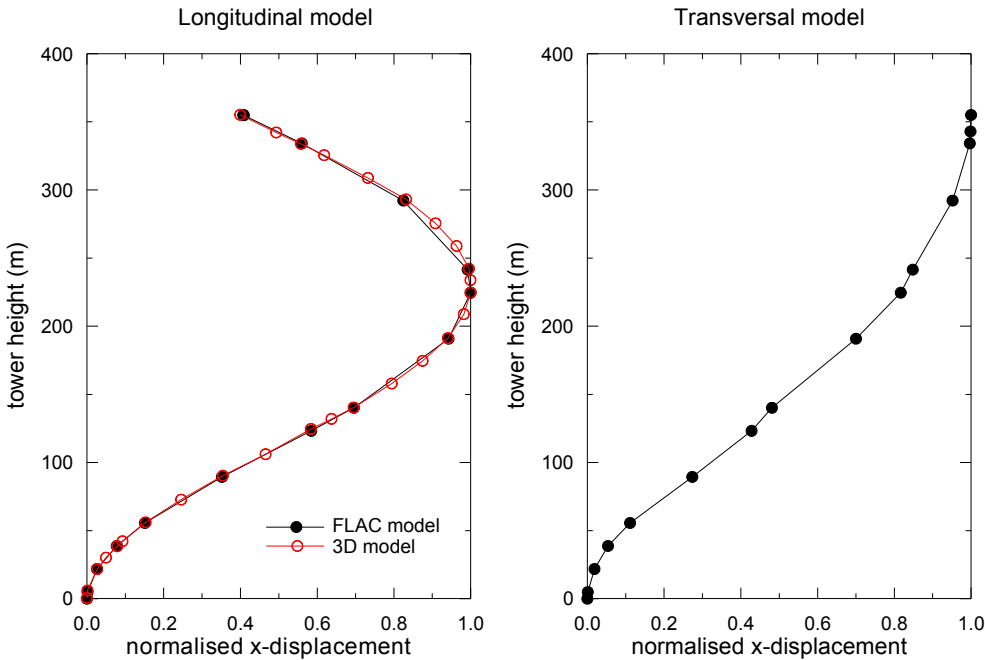


Figure 54. Normalised mode shape of the Sicilia tower for the longitudinal and transversal model. Comparison between 3D and FLAC model

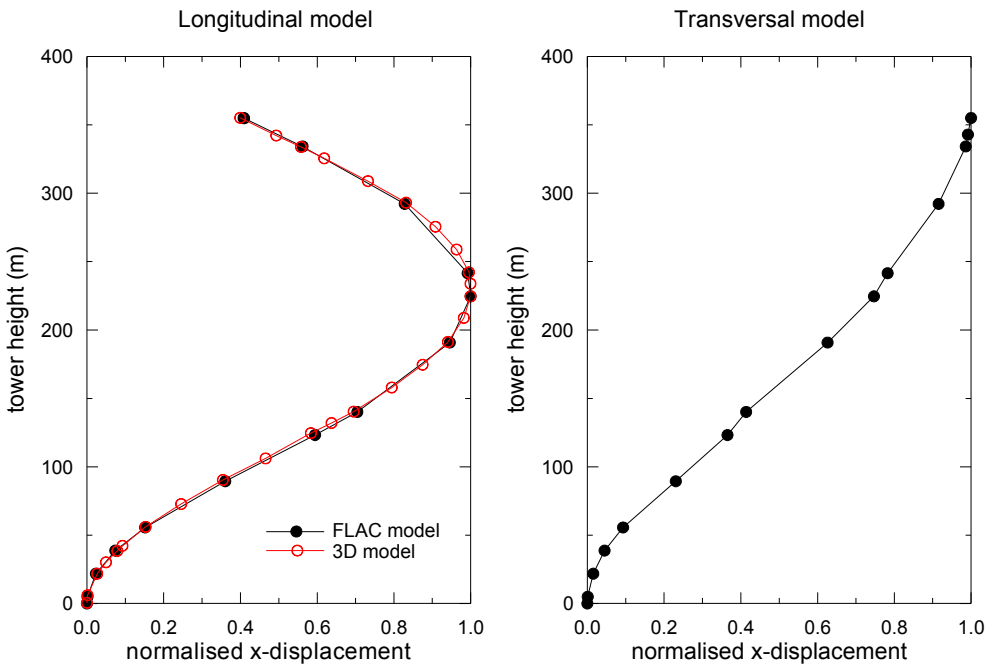


Figure 55. Normalised mode shape of the Calabria tower for the longitudinal and transversal model. Comparison between 3D and FLAC model

		Ponte sullo Stretto di Messina PROGETTO DEFINITIVO	
Seismic analyses for soil-foundation systems, Annex	<i>Codice documento</i> PB0032_F0_ANX	<i>Rev</i> F0	<i>Data</i> 20/06/2011

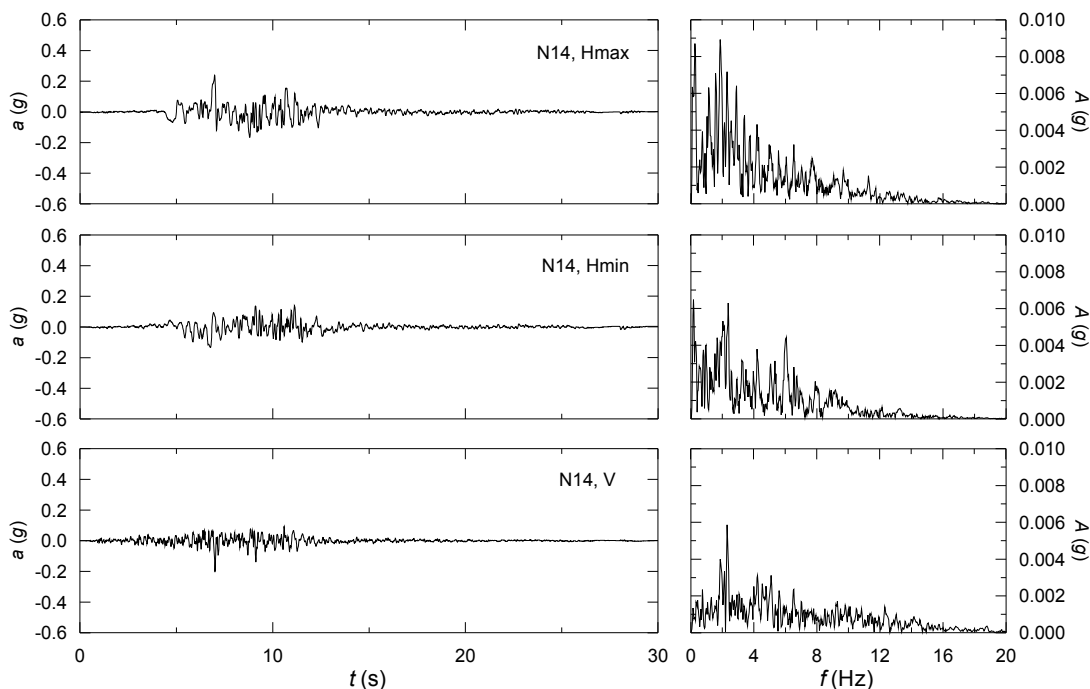


Figure 56. Earthquake N14. Time histories and Fourier spectra of the three components of the recorded signal

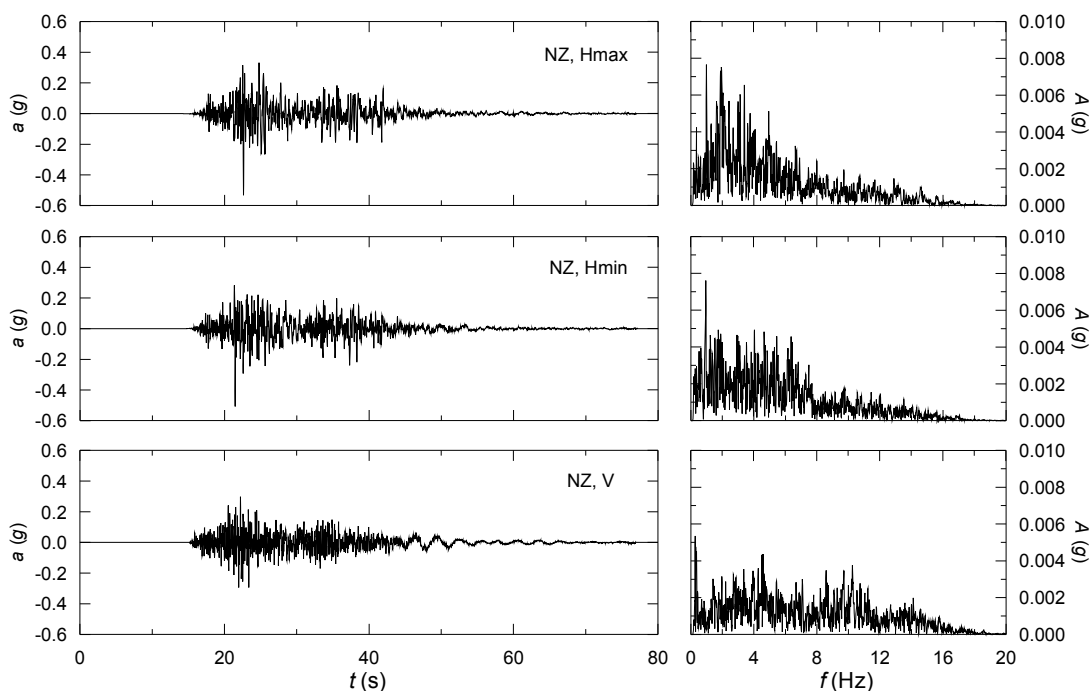




Figure 57. Earthquake NZ. Time histories and Fourier spectra of the three components of the recorded signal

		Ponte sullo Stretto di Messina PROGETTO DEFINITIVO		
Seismic analyses for soil-foundation systems, Annex	<i>Codice documento</i> PB0032_F0_ANX	<i>Rev</i> F0	<i>Data</i> 20/06/2011	

SICILIA

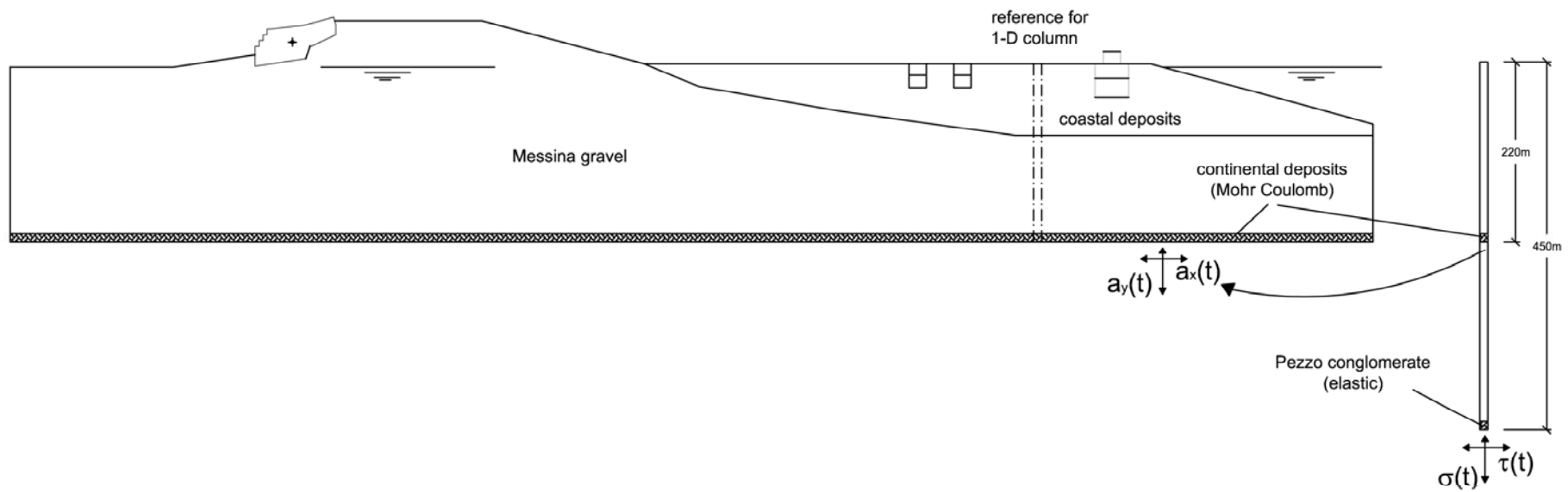




Figure 58. Scheme of the deconvolution analysis for the Sicilia shore.

		Ponte sullo Stretto di Messina PROGETTO DEFINITIVO		
Seismic analyses for soil-foundation systems, Annex		<i>Codice documento</i> PB0032_F0_ANX	<i>Rev</i> F0	<i>Data</i> 20/06/2011

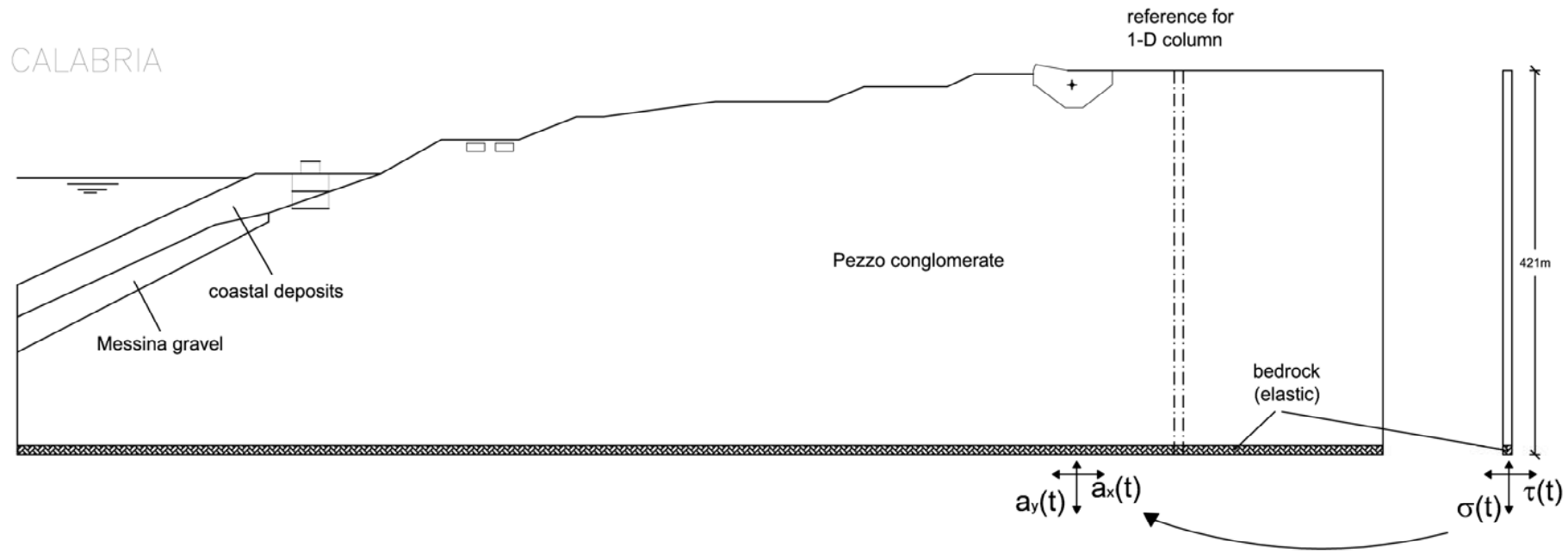


Figure 59. Scheme of the deconvolution analysis for the Calabria shore.

		Ponte sullo Stretto di Messina PROGETTO DEFINITIVO	
Seismic analyses for soil-foundation systems, Annex	<i>Codice documento</i> PB0032_F0_ANX	<i>Rev</i> F0	<i>Data</i> 20/06/2011

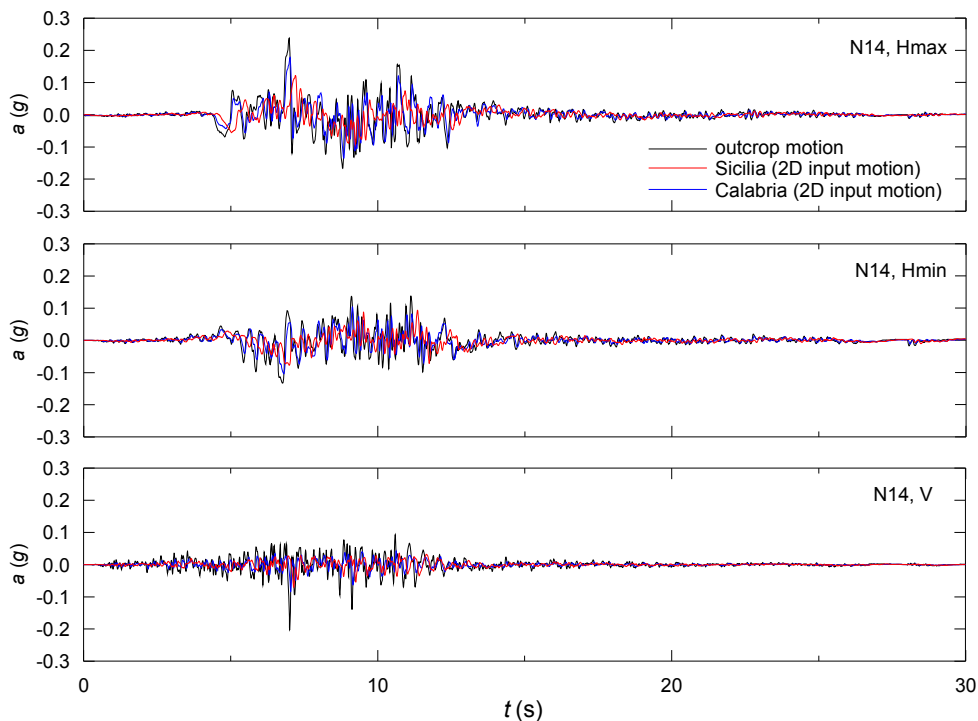


Figure 60. Design earthquake N14. Acceleration time histories computed from the deconvolution analysis at the reference depth for the base of the mesh in the 2D analyses

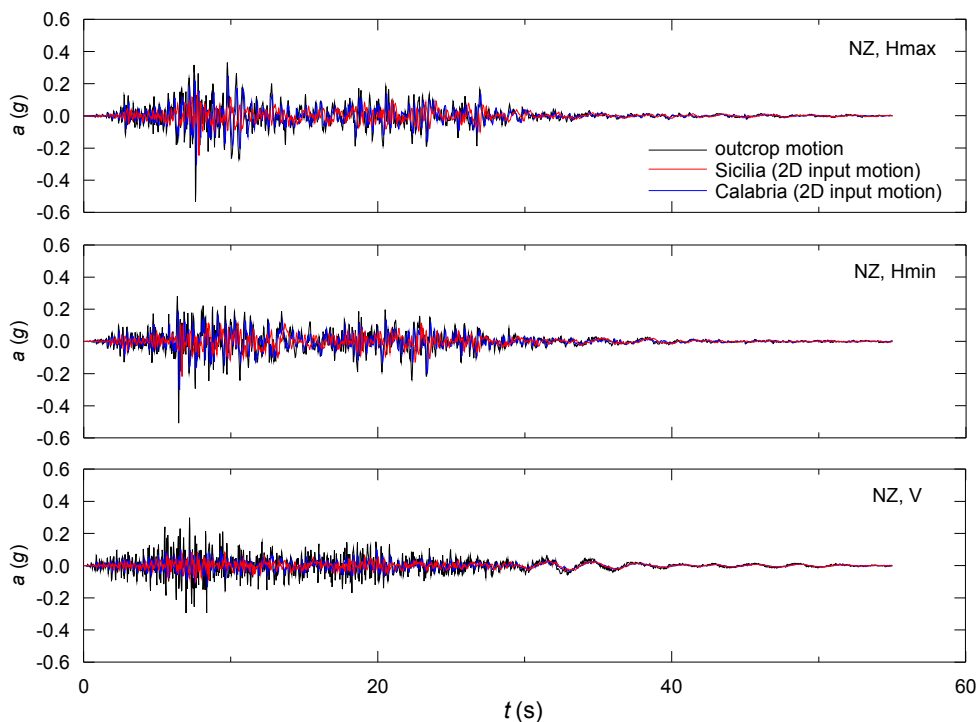


Figure 61. Design earthquake NZ. Acceleration time histories computed from the deconvolution analysis at the reference depth for the base of the mesh in the 2D analyses

		Ponte sullo Stretto di Messina PROGETTO DEFINITIVO		
Seismic analyses for soil-foundation systems, Annex		<i>Codice documento</i> PB0032_F0_ANX	<i>Rev</i> F0	<i>Data</i> 20/06/2011

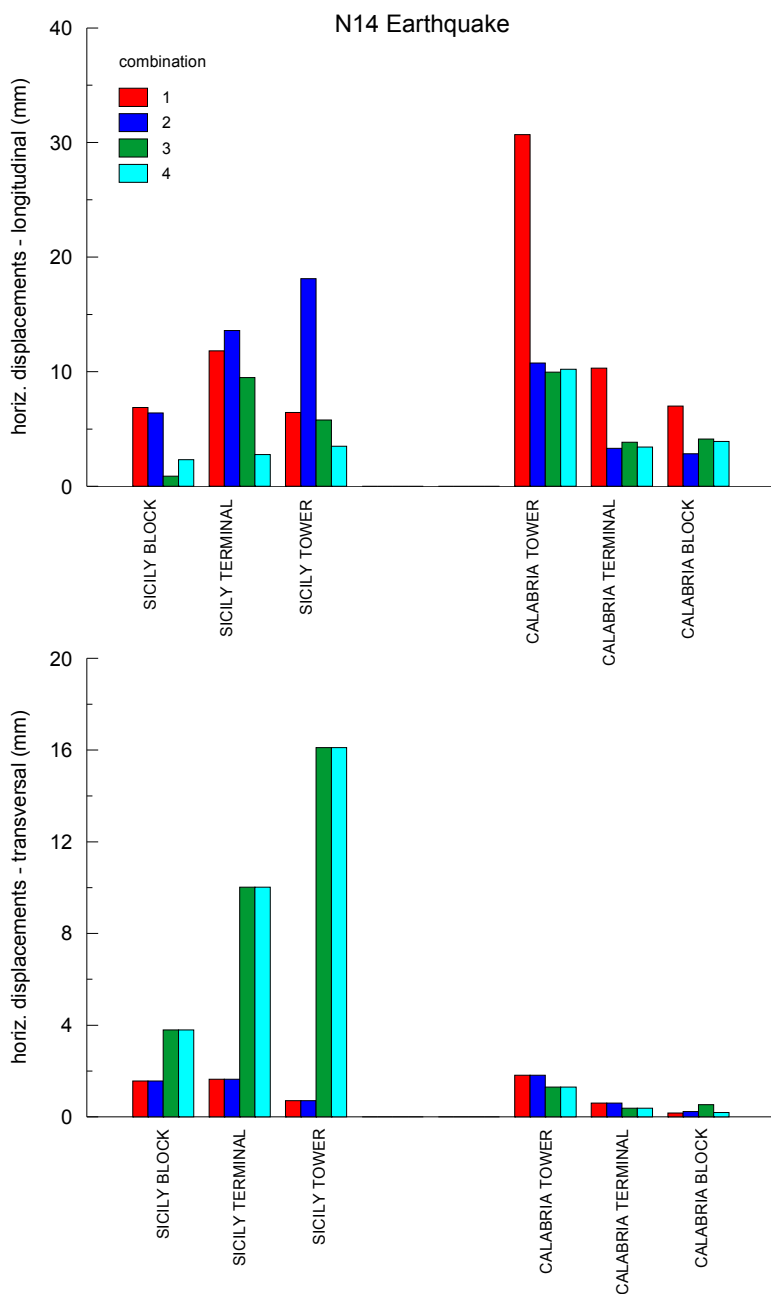



Figure 62. Permanent horizontal displacements produced by the N14 record

		Ponte sullo Stretto di Messina PROGETTO DEFINITIVO		
Seismic analyses for soil-foundation systems, Annex		<i>Codice documento</i> PB0032_F0_ANX	<i>Rev</i> F0	<i>Data</i> 20/06/2011

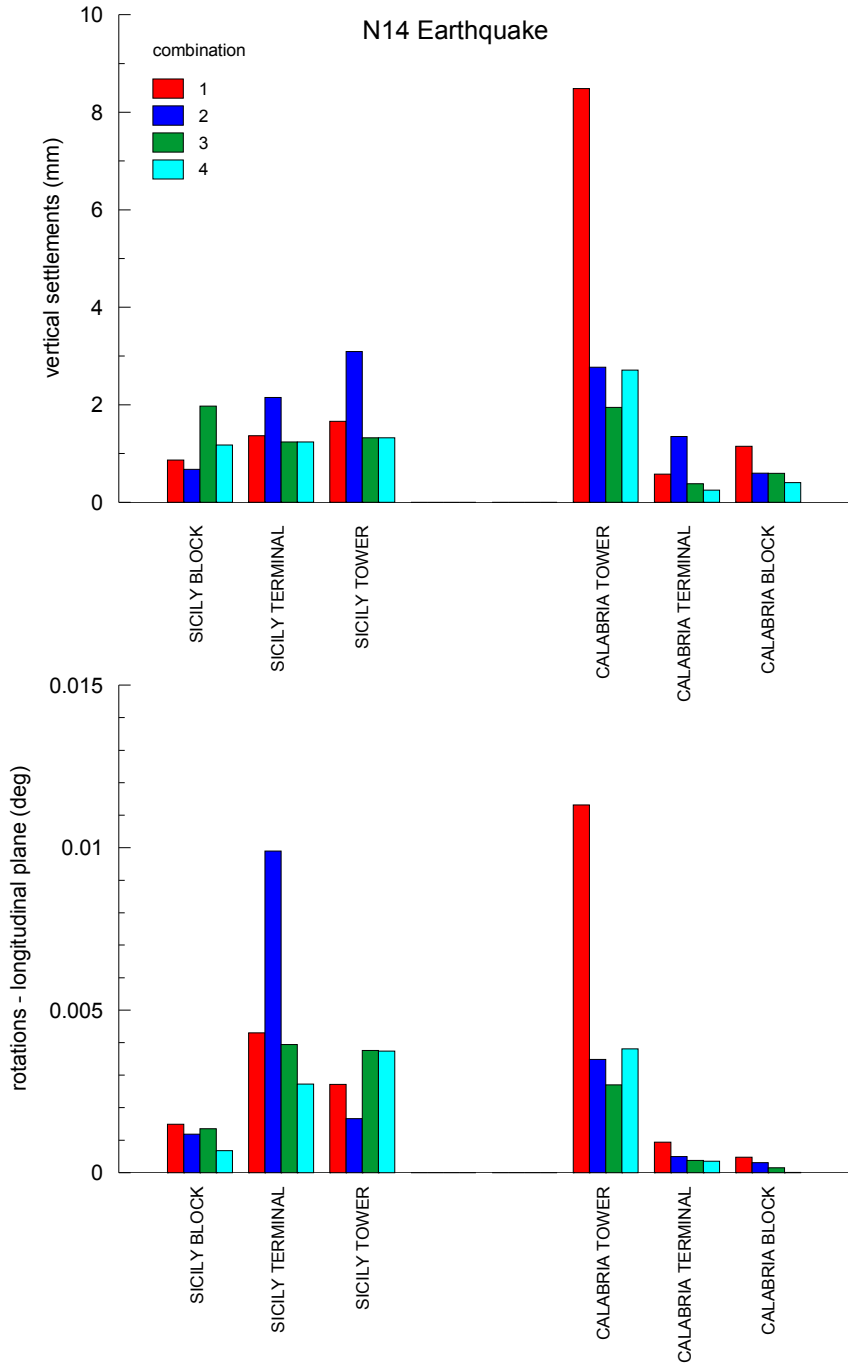


Figure 63. Permanent settlements and rotations produced by the N14 record

		Ponte sullo Stretto di Messina PROGETTO DEFINITIVO	
Seismic analyses for soil-foundation systems, Annex		<i>Codice documento</i> PB0032_F0_ANX	<i>Rev</i> F0 <i>Data</i> 20/06/2011

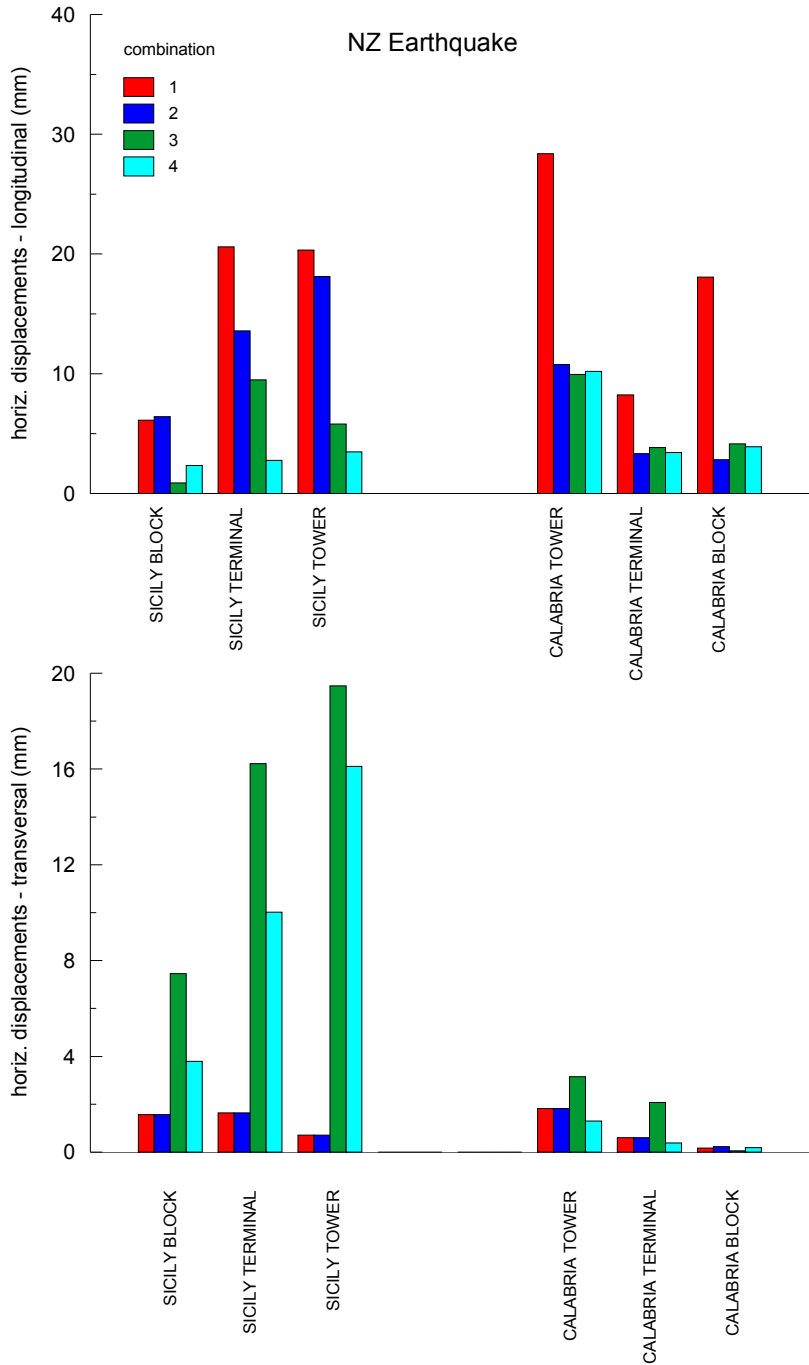




Figure 64. Permanent horizontal displacements produced by the NZ record

		Ponte sullo Stretto di Messina PROGETTO DEFINITIVO		
Seismic analyses for soil-foundation systems, Annex		<i>Codice documento</i> PB0032_F0_ANX	<i>Rev</i> F0	<i>Data</i> 20/06/2011

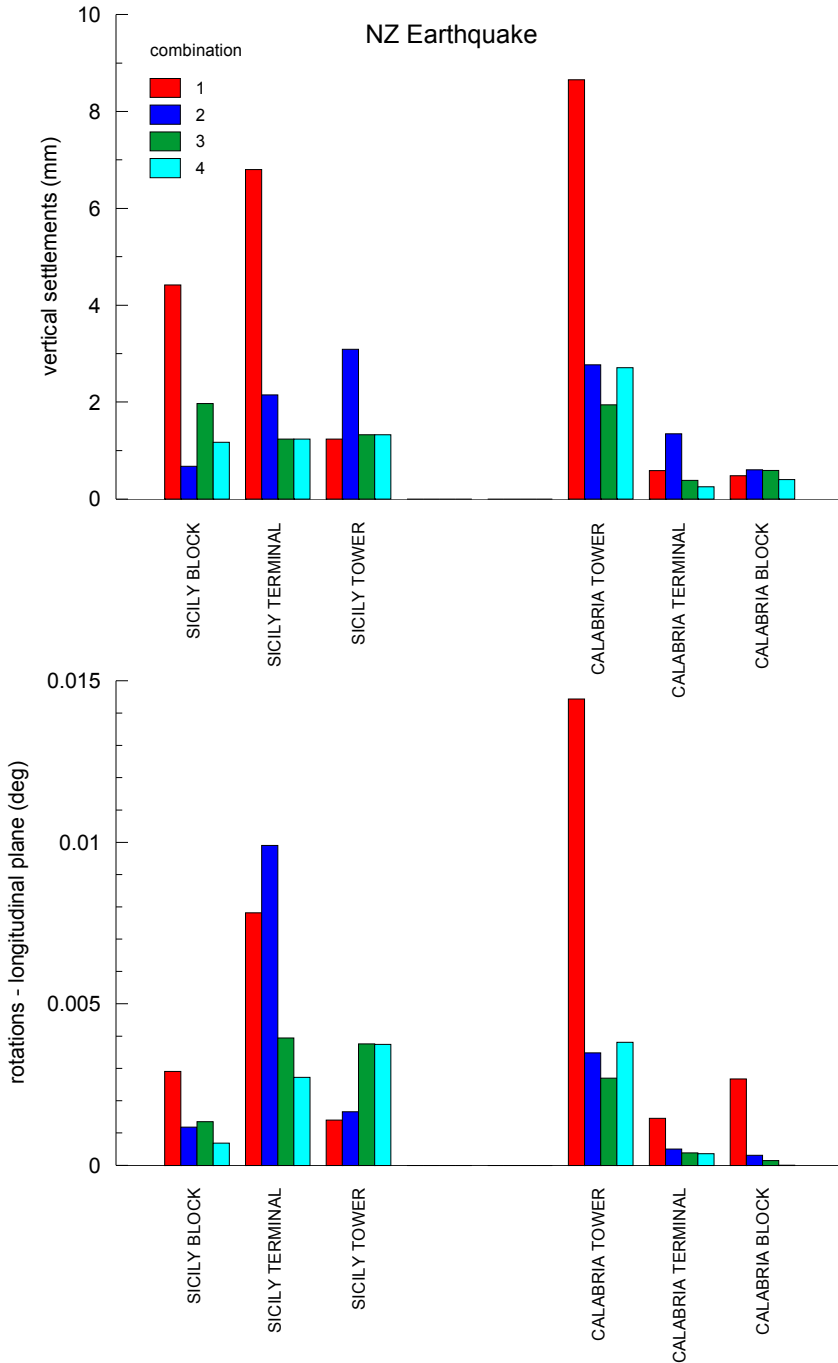


Figure 65. Permanent settlements and rotations produced by the NZ record

N14 Earthquake

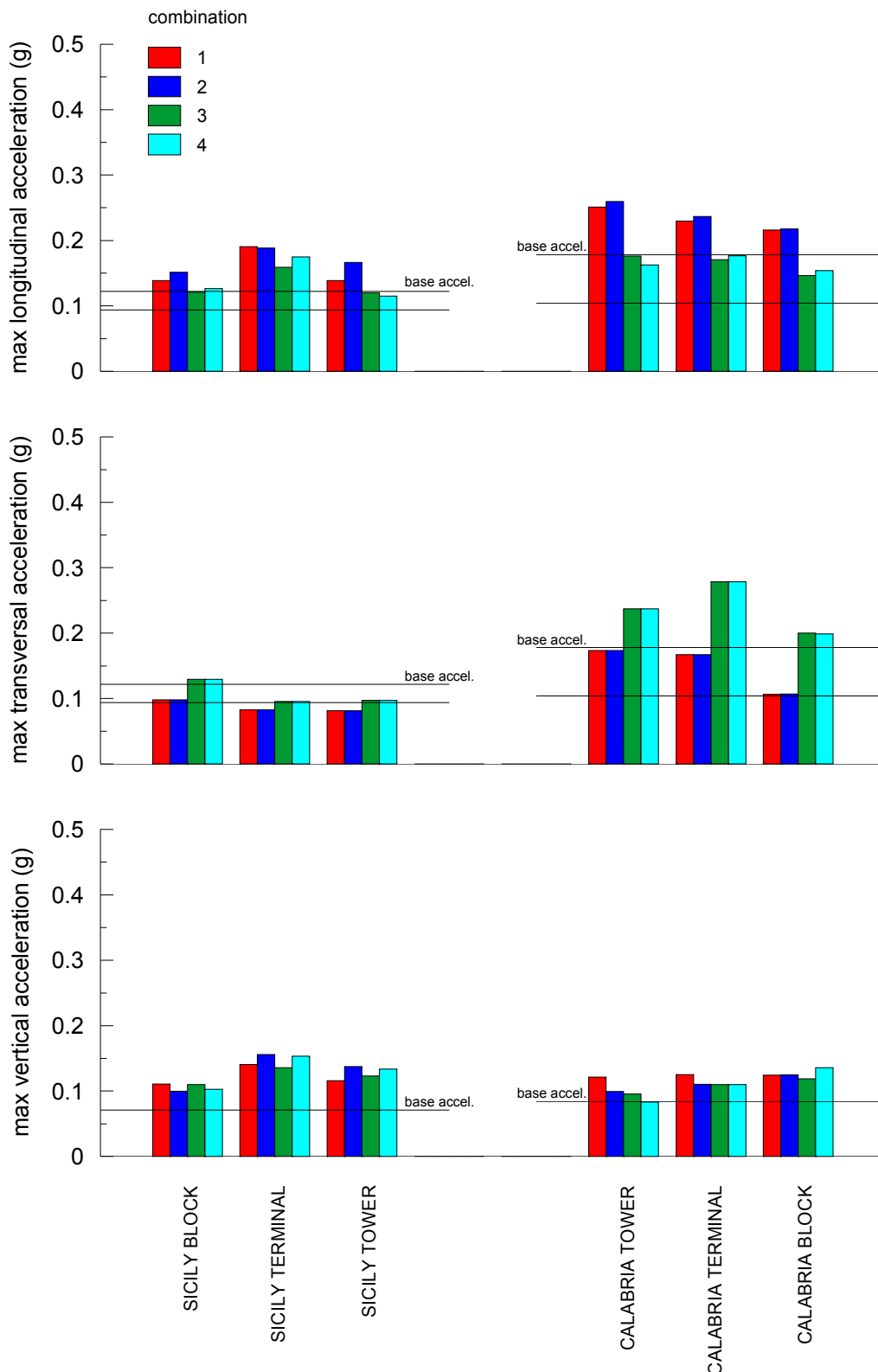


Figure 66. Maximum accelerations computed during the N14 record

NZ Earthquake

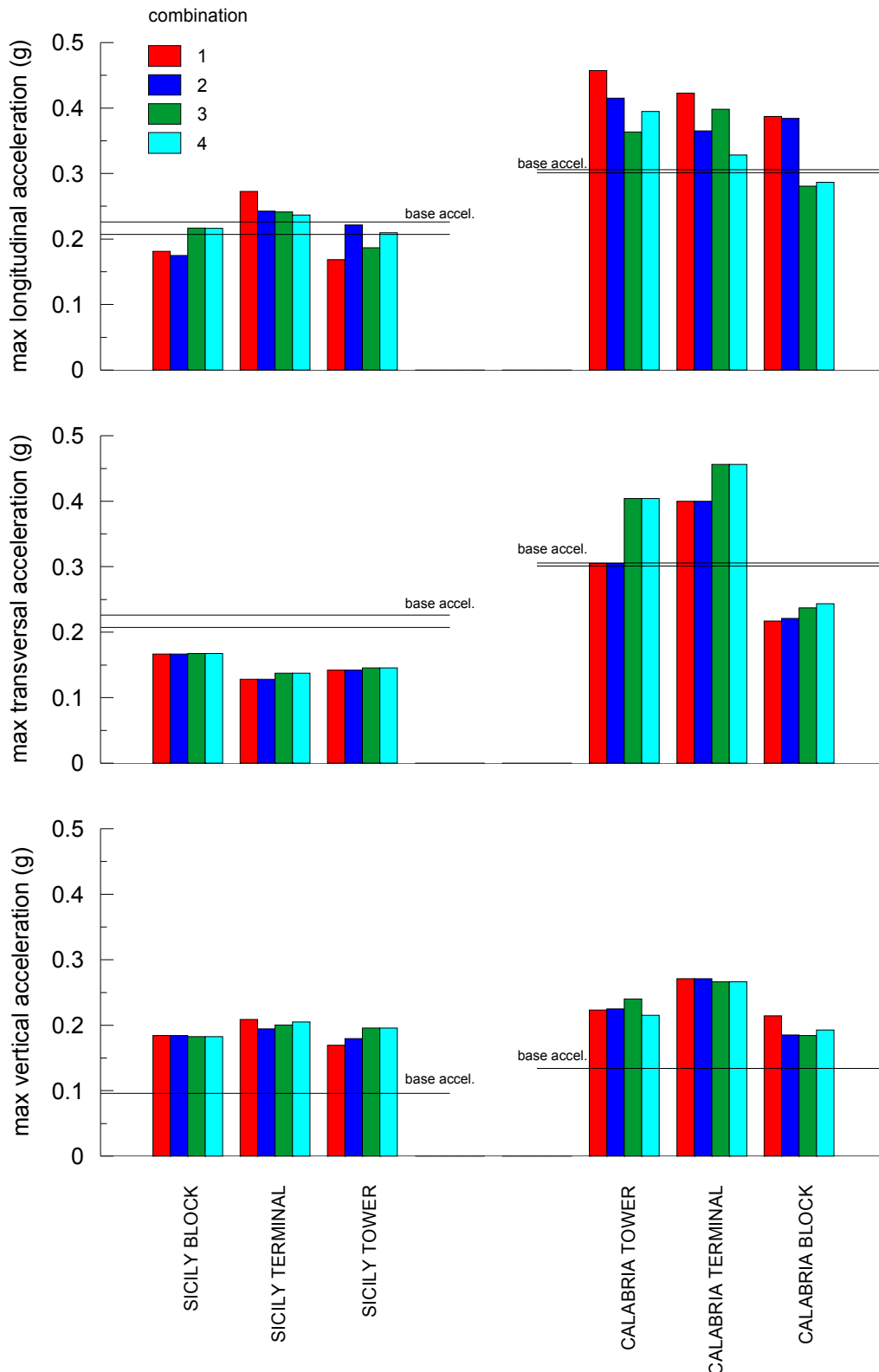


Figure 67. Maximum accelerations computed during the NZ record

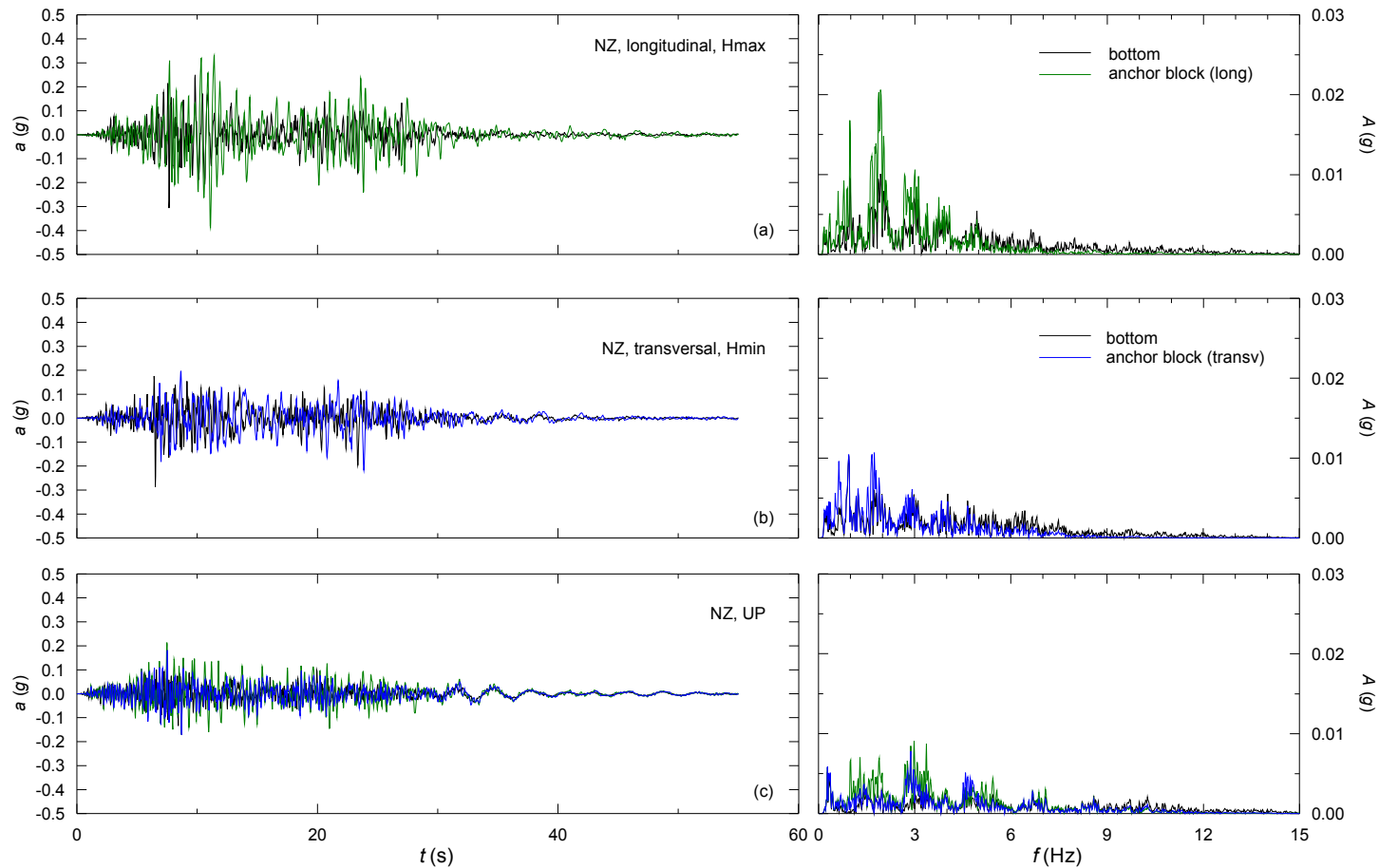


Figure 68. Earthquake NZ, comb.1, Calabria shore. Acceleration time histories and Fourier spectra at the centre of mass of the anchor block: (a) horizontal acceleration in the longitudinal direction, (b) horizontal acceleration in the transversal direction and (c) vertical acceleration

		Ponte sullo Stretto di Messina PROGETTO DEFINITIVO		
Seismic analyses for soil-foundation systems, Annex	<i>Codice documento</i> PB0032_F0_ANX	<i>Rev</i> F0	<i>Data</i> 20/06/2011	

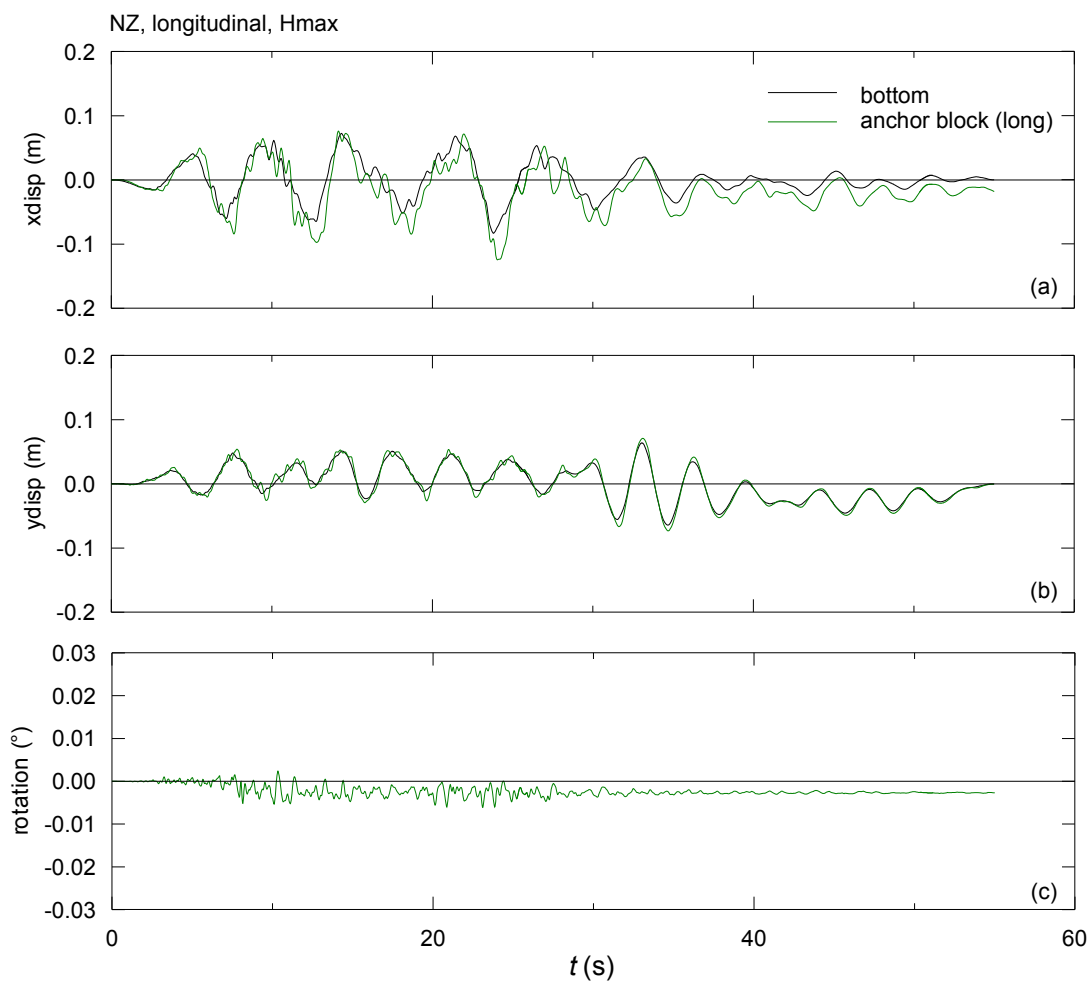


Figure 69. Earthquake NZ, comb.1. Longitudinal section of the Calabria shore: (a) horizontal and (b) vertical displacements, and (c) rotation time histories at the centre of mass of the anchor block

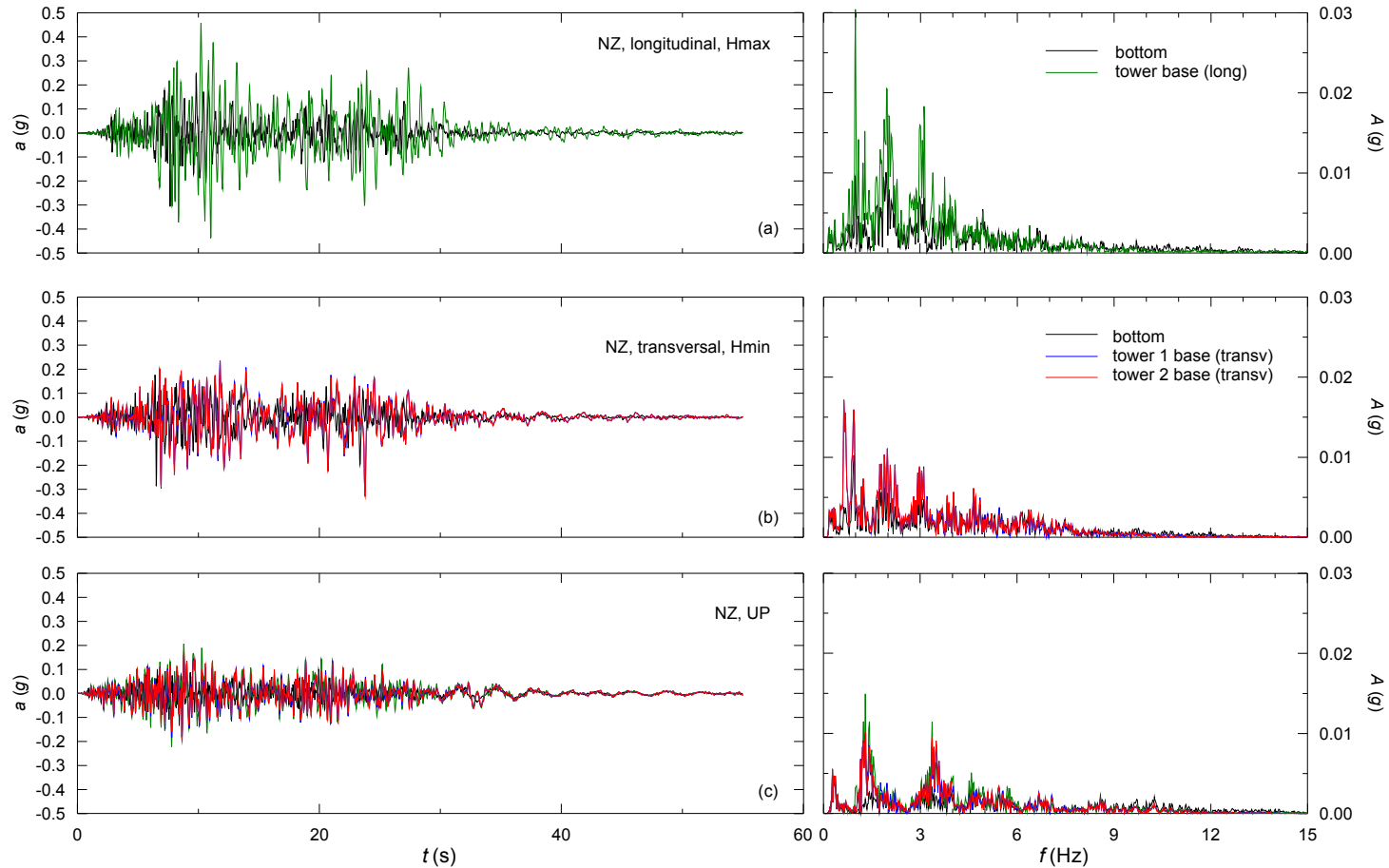


Figure 70. Earthquake NZ, comb.1, Calabria shore. Acceleration time histories and Fourier spectra at the base of the tower: (a) horizontal acceleration in the longitudinal direction, (b) horizontal acceleration in the transversal direction and (c) vertical acceleration

		Ponte sullo Stretto di Messina PROGETTO DEFINITIVO		
Seismic analyses for soil-foundation systems, Annex	<i>Codice documento</i> PB0032_F0_ANX	<i>Rev</i> F0	<i>Data</i> 20/06/2011	

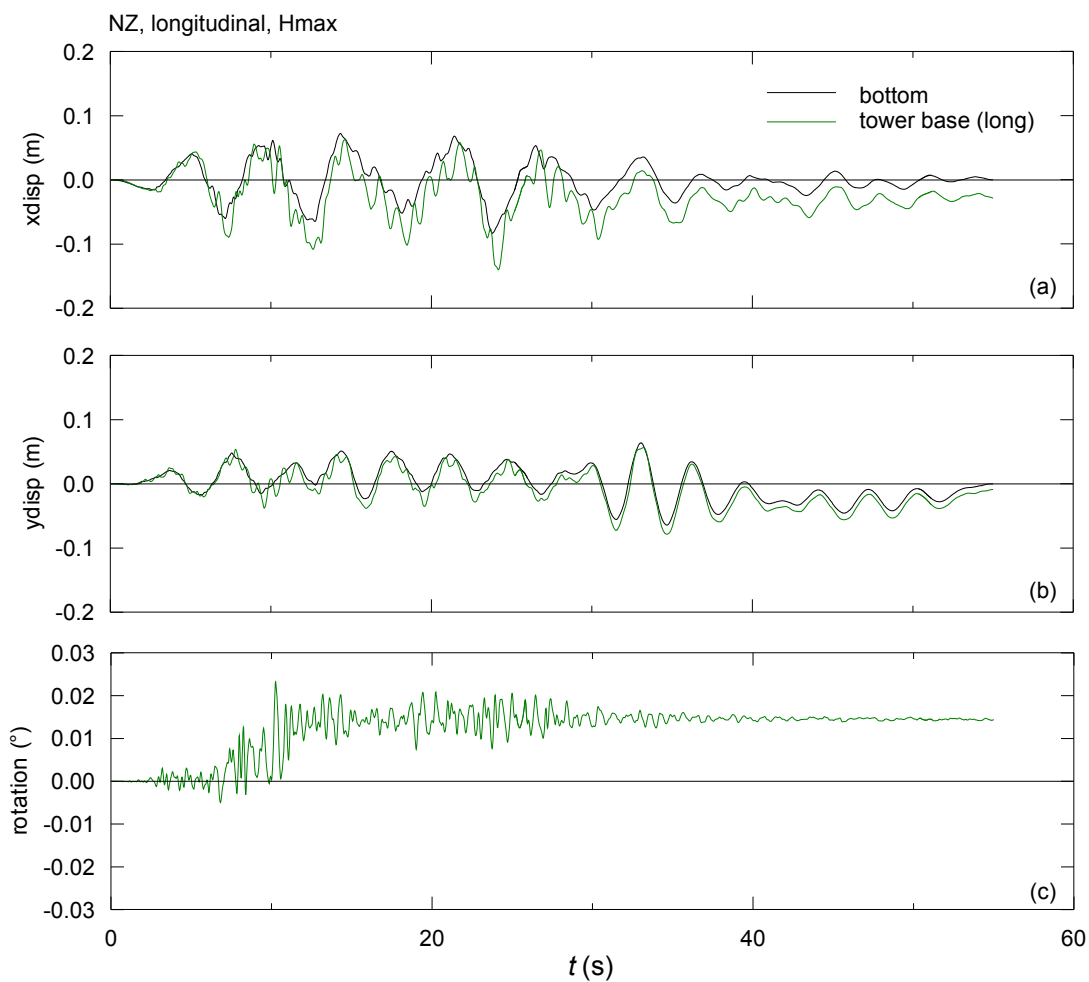


Figure 71. Earthquake NZ, comb.1. Longitudinal section of the Calabria shore: (a) horizontal and (b) vertical displacements, and (c) rotation time histories at the base of the tower

		Ponte sullo Stretto di Messina PROGETTO DEFINITIVO		
Seismic analyses for soil-foundation systems, Annex		<i>Codice documento</i> PB0032_F0_ANX	<i>Rev</i> F0	<i>Data</i> 20/06/2011

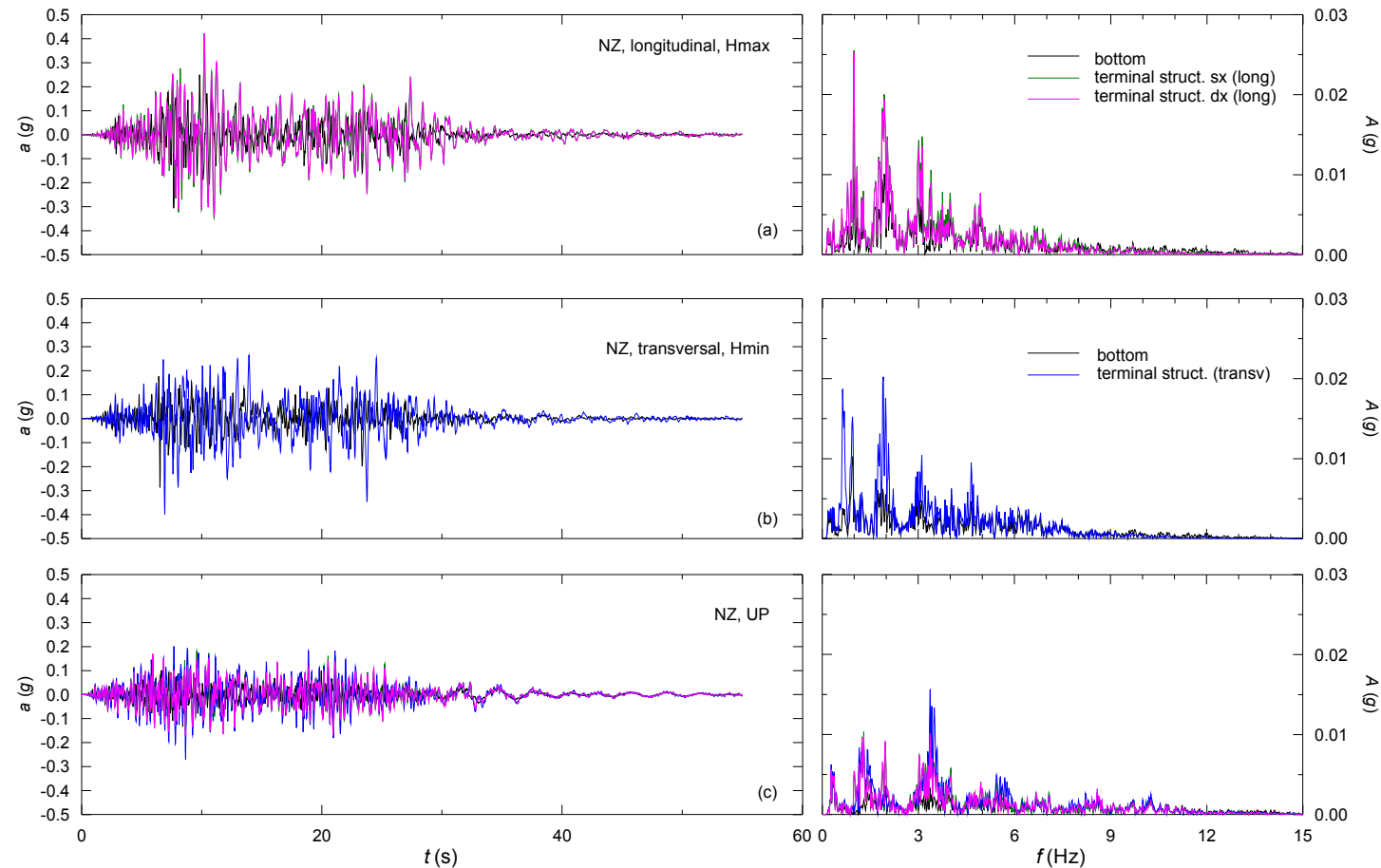


Figure 72. Earthquake NZ, comb.1, Calabria shore. Acceleration time histories and Fourier spectra at the centre of mass of the terminal structures: (a) horizontal acceleration in the longitudinal direction, (b) horizontal acceleration in the transversal direction and (c) vertical acceleration

		Ponte sullo Stretto di Messina PROGETTO DEFINITIVO		
Seismic analyses for soil-foundation systems, Annex		<i>Codice documento</i> PB0032_F0_ANX	<i>Rev</i> F0	<i>Data</i> 20/06/2011

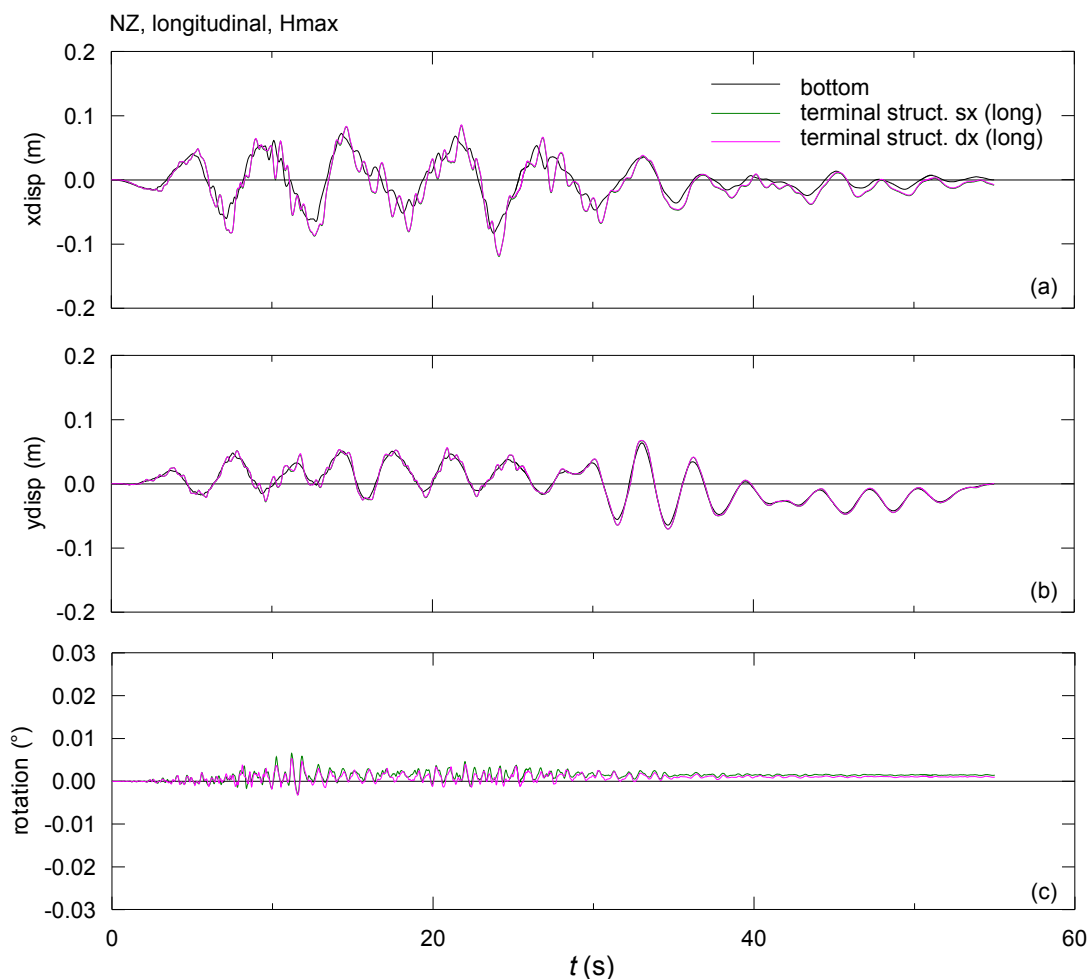


Figure 73. Earthquake NZ, comb.1. Longitudinal section of the Calabria shore: (a) horizontal and (b) vertical displacements, and (c) rotation time histories at the centre of mass of the terminal structures

		Ponte sullo Stretto di Messina PROGETTO DEFINITIVO					
Seismic analyses for soil-foundation systems, Annex		<i>Codice documento</i> PB0032_F0_ANX	<table border="1"> <thead> <tr> <th><i>Rev</i></th> <th><i>Data</i></th> </tr> </thead> <tbody> <tr> <td>F0</td> <td>20/06/2011</td> </tr> </tbody> </table>	<i>Rev</i>	<i>Data</i>	F0	20/06/2011
<i>Rev</i>	<i>Data</i>						
F0	20/06/2011						

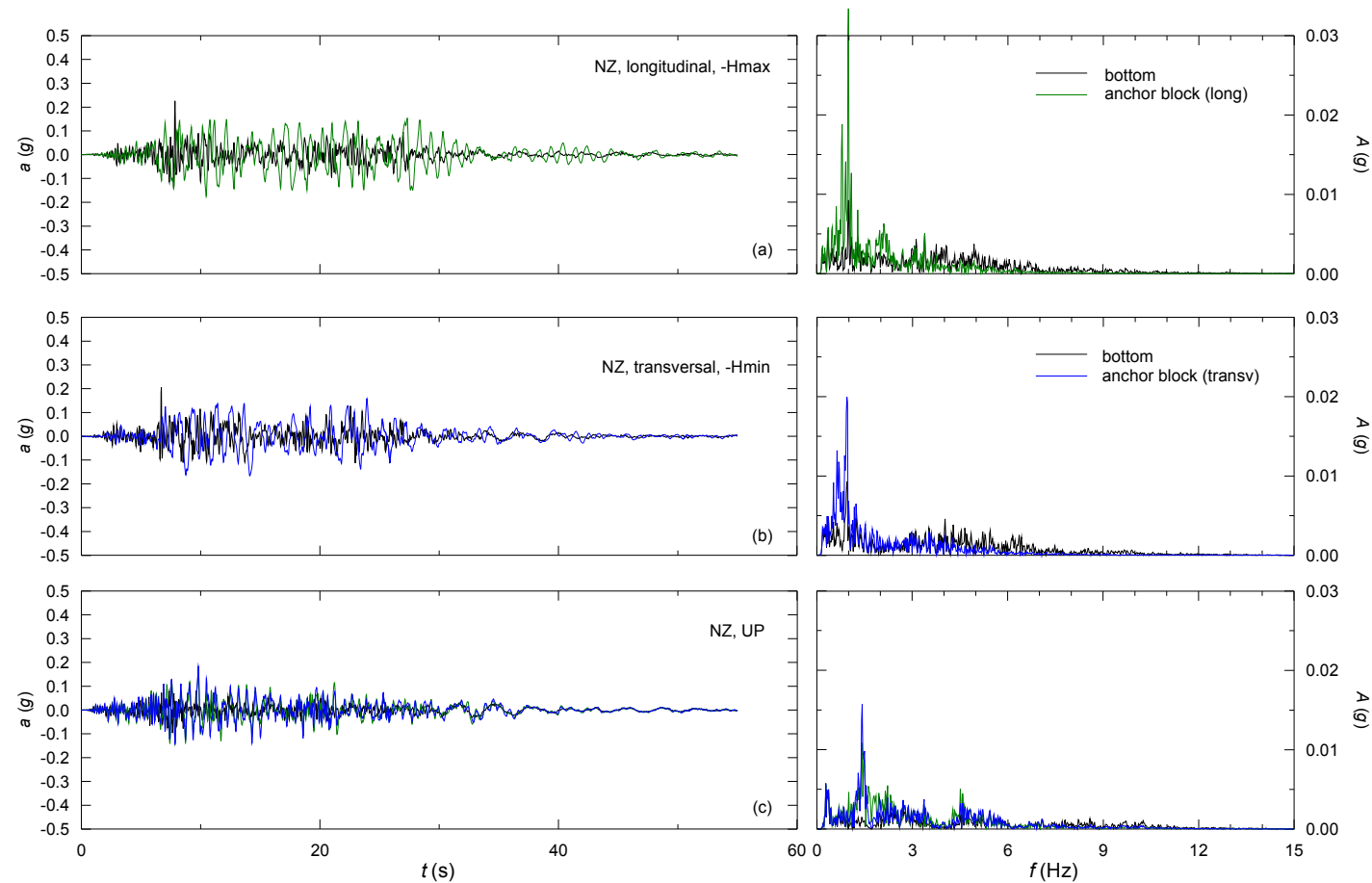


Figure 74. Earthquake NZ, comb.2, Sicilia shore. Acceleration time histories and Fourier spectra at the centre of mass of the anchor block: (a) horizontal acceleration in the longitudinal direction, (b) horizontal acceleration in the transversal direction and (c) vertical acceleration

		Ponte sullo Stretto di Messina PROGETTO DEFINITIVO		
Seismic analyses for soil-foundation systems, Annex	<i>Codice documento</i> PB0032_F0_ANX	<i>Rev</i> F0	<i>Data</i> 20/06/2011	

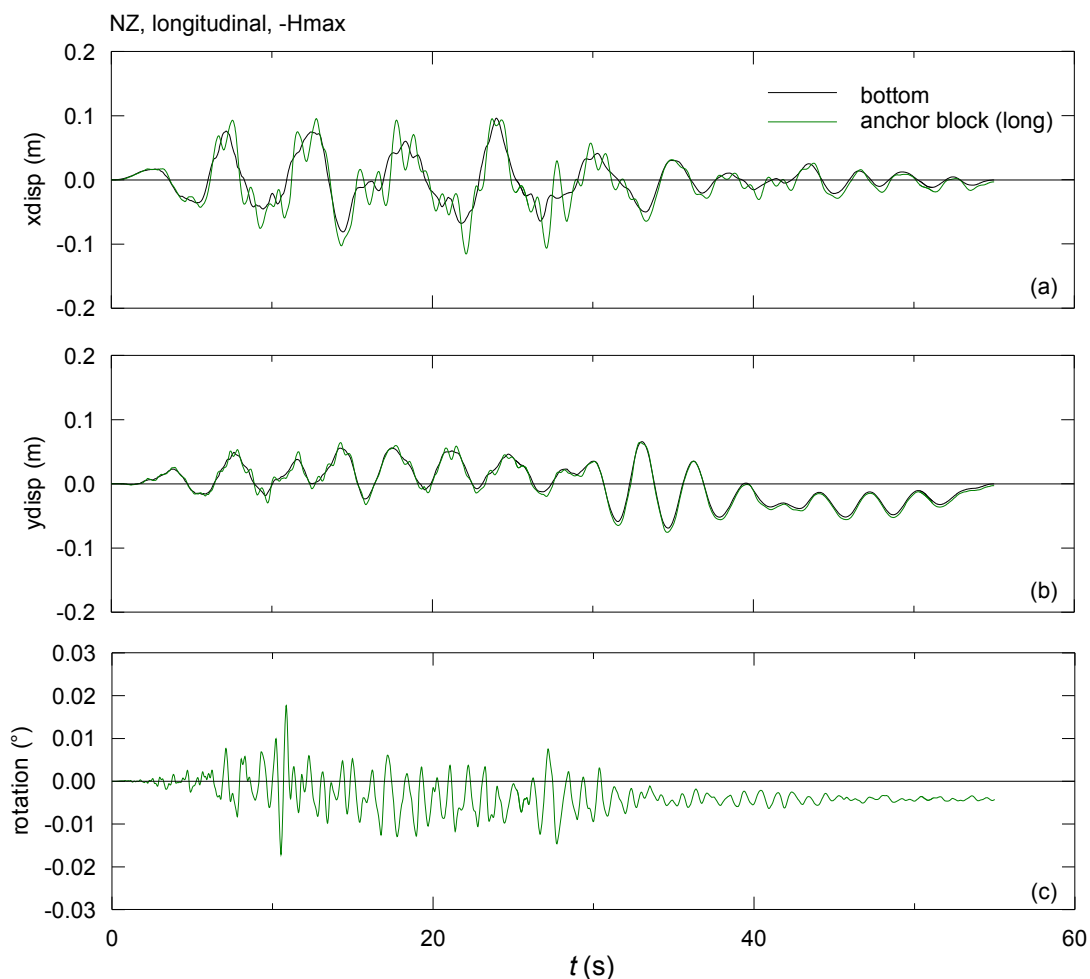


Figure 75. Earthquake NZ, comb.2. Longitudinal section of the Sicilia shore: (a) horizontal and (b) vertical displacements, and (c) rotation time histories at the centre of mass of the anchor block

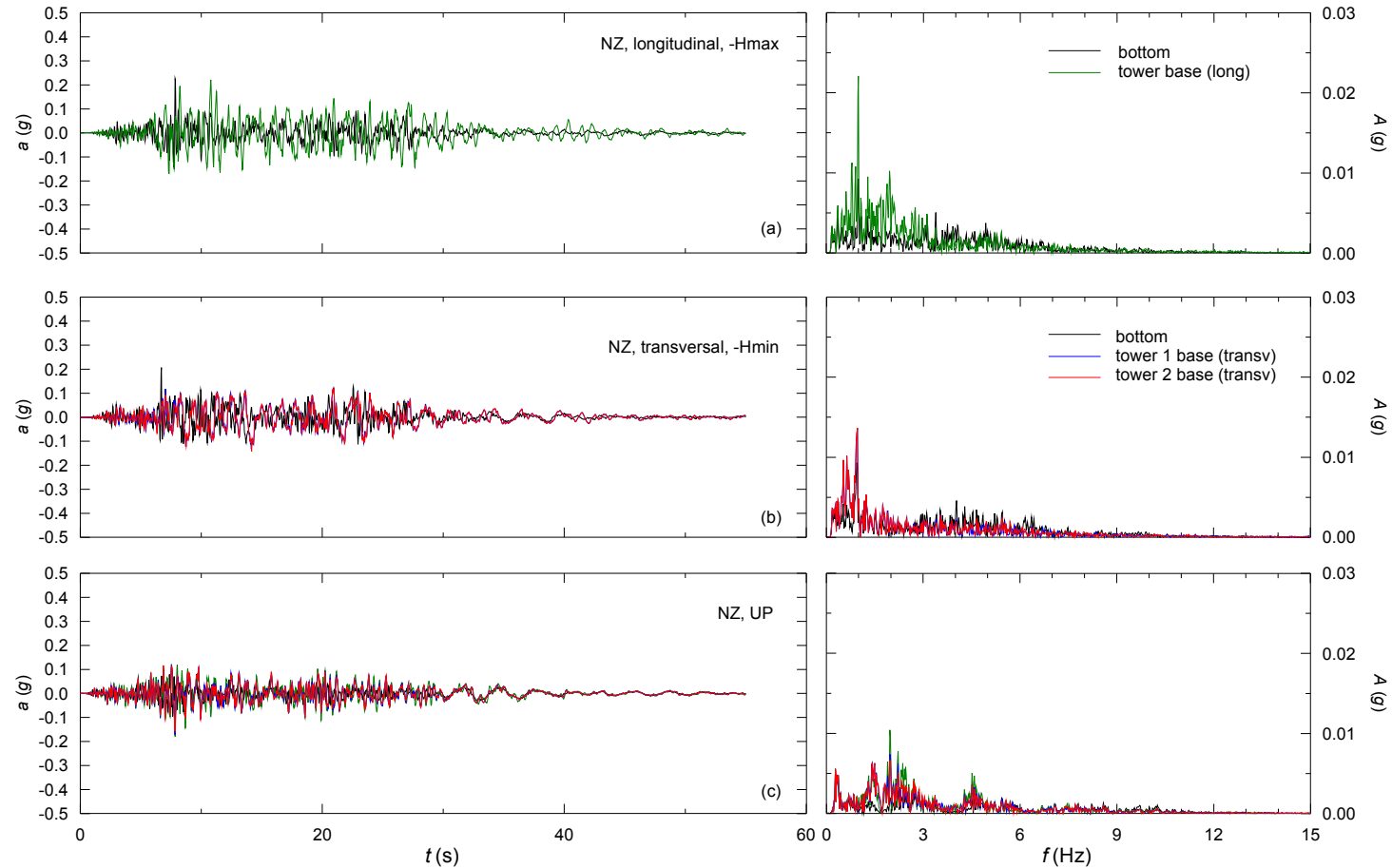


Figure 76. Earthquake NZ, comb.2, Sicilia shore. Acceleration time histories and Fourier spectra at the base of the tower: (a) horizontal acceleration in the longitudinal direction, (b) horizontal acceleration in the transversal direction and (c) vertical acceleration

		Ponte sullo Stretto di Messina PROGETTO DEFINITIVO		
Seismic analyses for soil-foundation systems, Annex	<i>Codice documento</i> PB0032_F0_ANX	<i>Rev</i> F0	<i>Data</i> 20/06/2011	

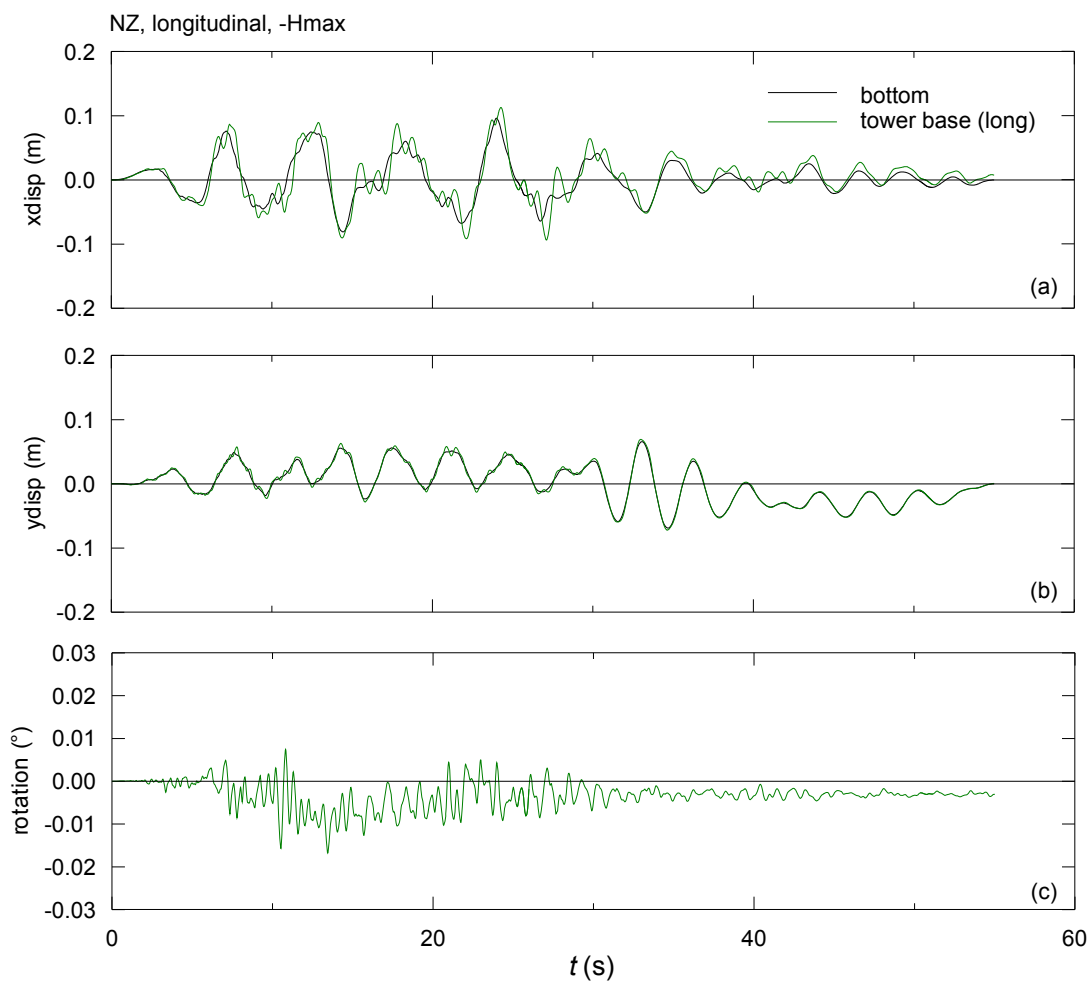


Figure 77. Earthquake NZ, comb.2. Longitudinal section of the Sicilia shore: (a) horizontal and (b) vertical displacements, and (c) rotation time histories at the base of the tower

		Ponte sullo Stretto di Messina PROGETTO DEFINITIVO		
Seismic analyses for soil-foundation systems, Annex		<i>Codice documento</i> PB0032_F0_ANX	<i>Rev</i> F0	<i>Data</i> 20/06/2011

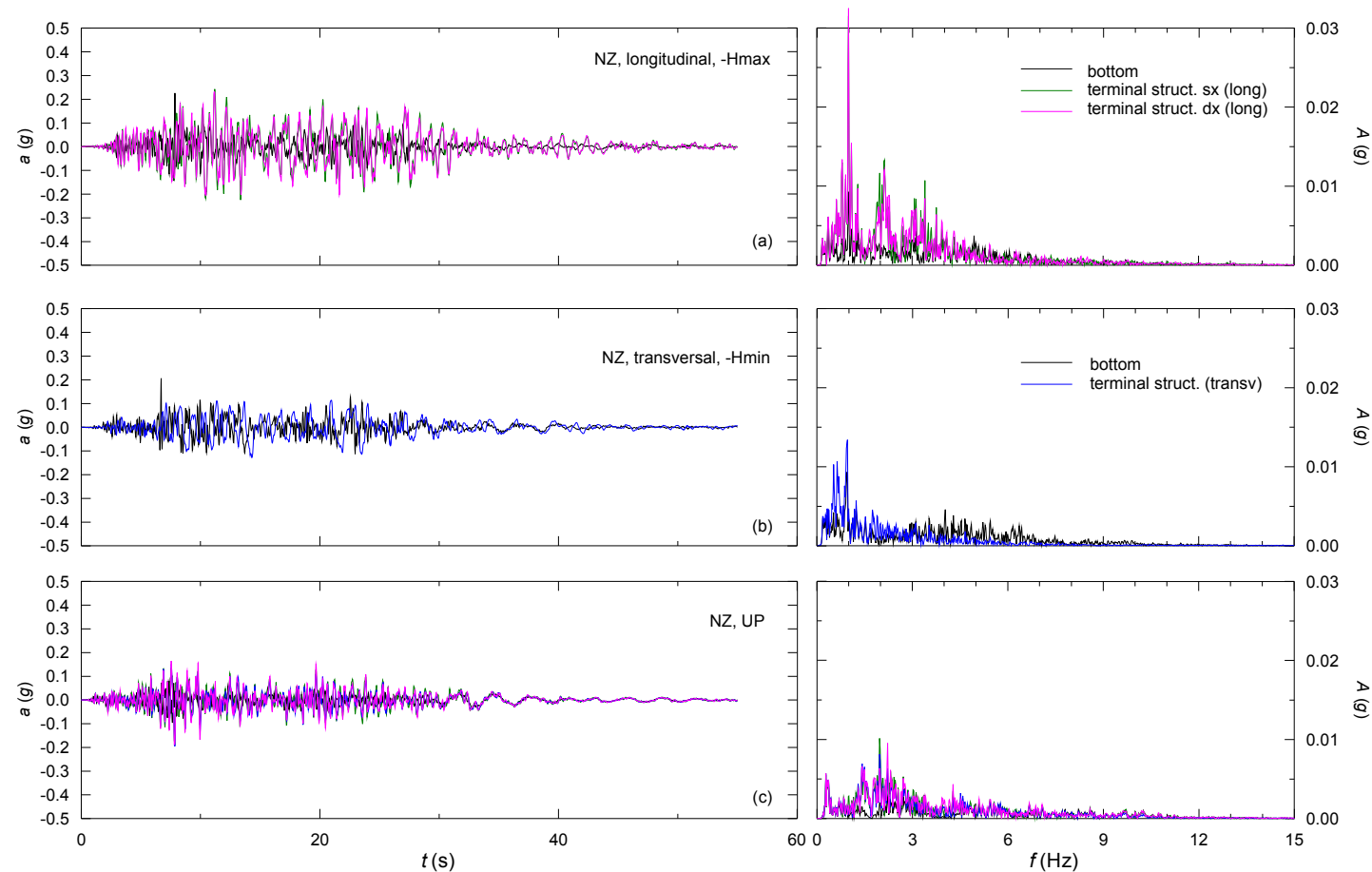


Figure 78. Earthquake NZ, comb.2, Sicilia shore. Acceleration time histories and Fourier spectra at the centre of mass of the terminal structures: (a) horizontal acceleration in the longitudinal direction, (b) horizontal acceleration in the transversal direction and (c) vertical acceleration

		Ponte sullo Stretto di Messina PROGETTO DEFINITIVO		
Seismic analyses for soil-foundation systems, Annex	<i>Codice documento</i> PB0032_F0_ANX	<i>Rev</i> F0	<i>Data</i> 20/06/2011	

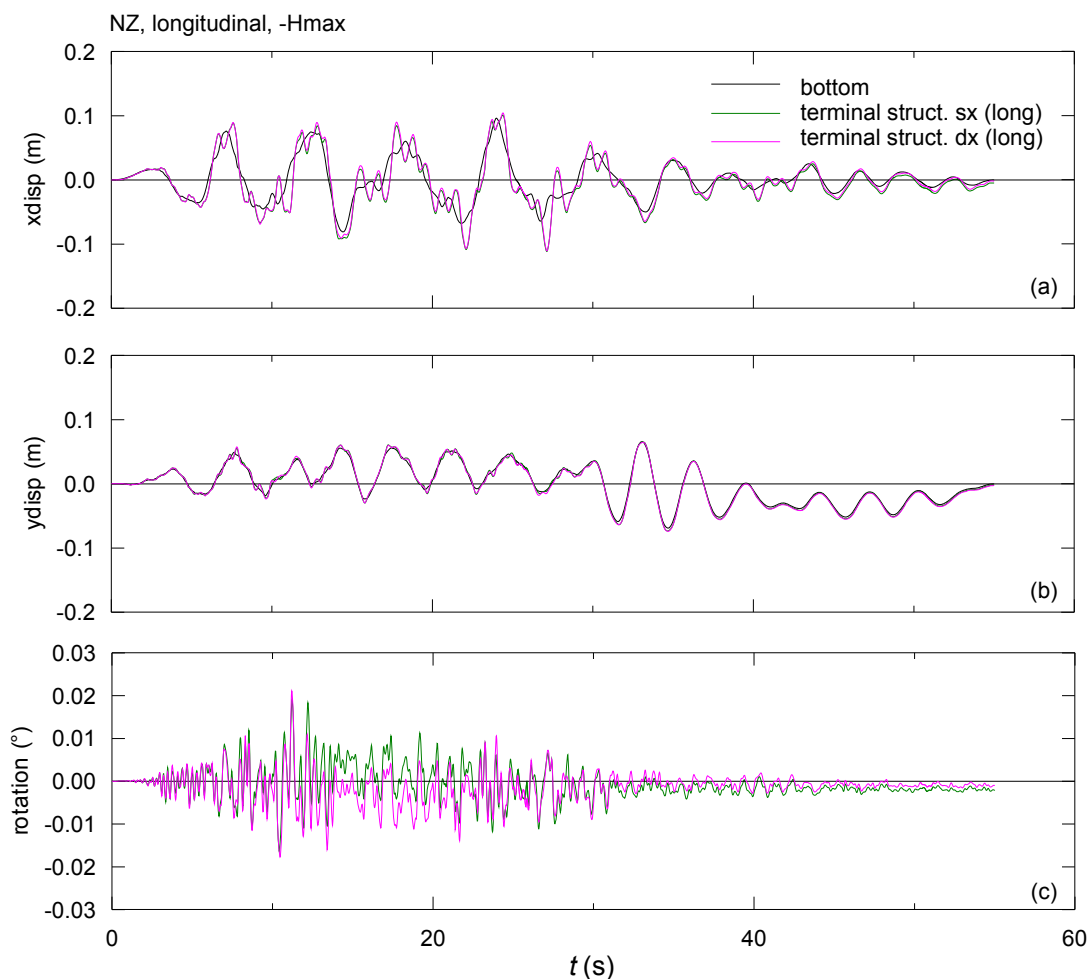


Figure 79. Earthquake NZ, comb.2. Longitudinal section of the Sicilia shore: (a) horizontal and (b) vertical displacements, and (c) rotation time histories at the centre of mass of the terminal structures

		Ponte sullo Stretto di Messina PROGETTO DEFINITIVO		
Seismic analyses for soil-foundation systems, Annex	<i>Codice documento</i> PB0032_F0_ANX	<i>Rev</i> F0	<i>Data</i> 20/06/2011	

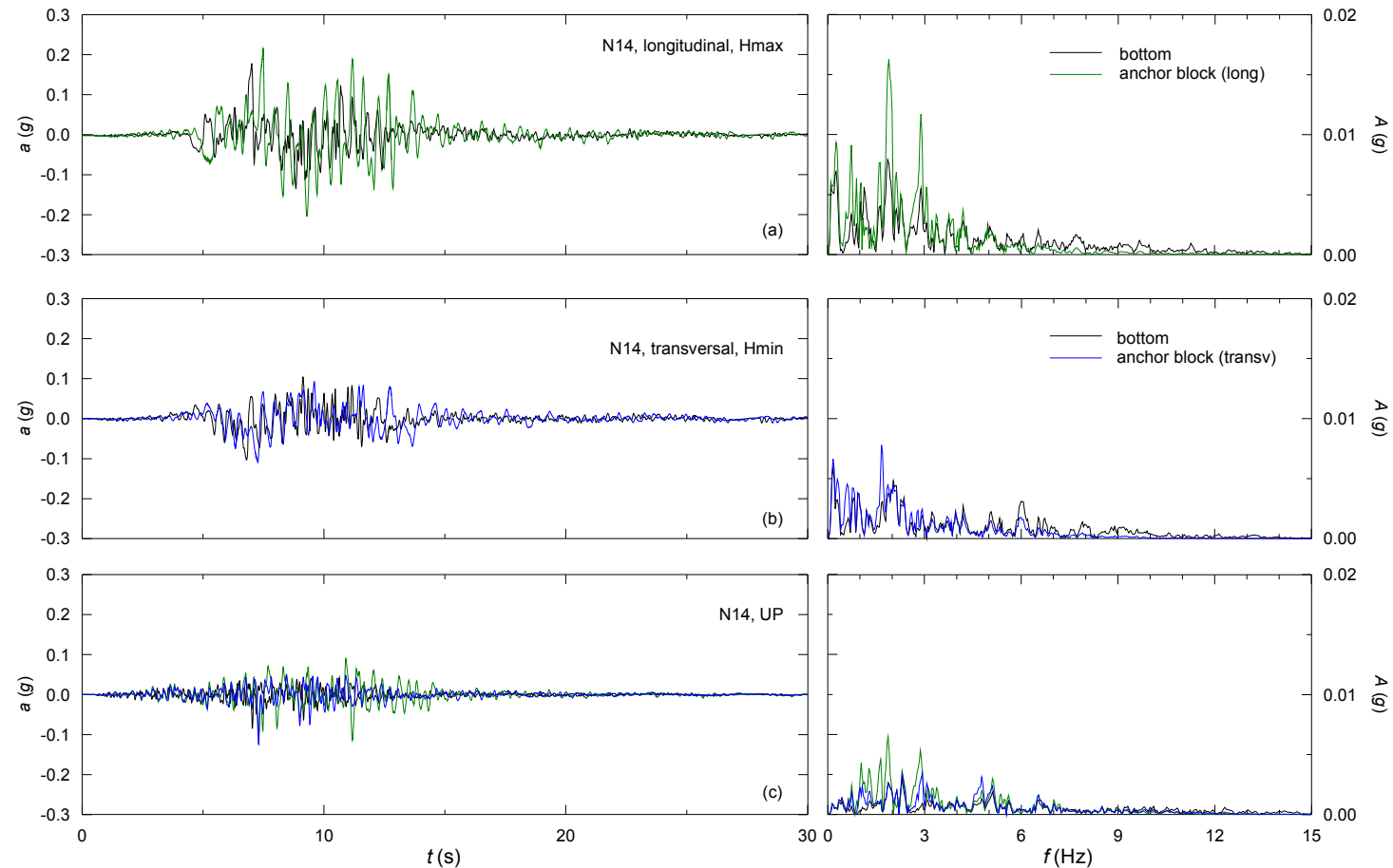


Figure 80. Earthquake N14, comb.1, Calabria shore. Acceleration time histories and Fourier spectra at the centre of mass of the anchor block: (a) horizontal acceleration in the longitudinal direction, (b) horizontal acceleration in the transversal direction and (c) vertical acceleration

		Ponte sullo Stretto di Messina PROGETTO DEFINITIVO		
Seismic analyses for soil-foundation systems, Annex	<i>Codice documento</i> PB0032_F0_ANX	<i>Rev</i> F0	<i>Data</i> 20/06/2011	

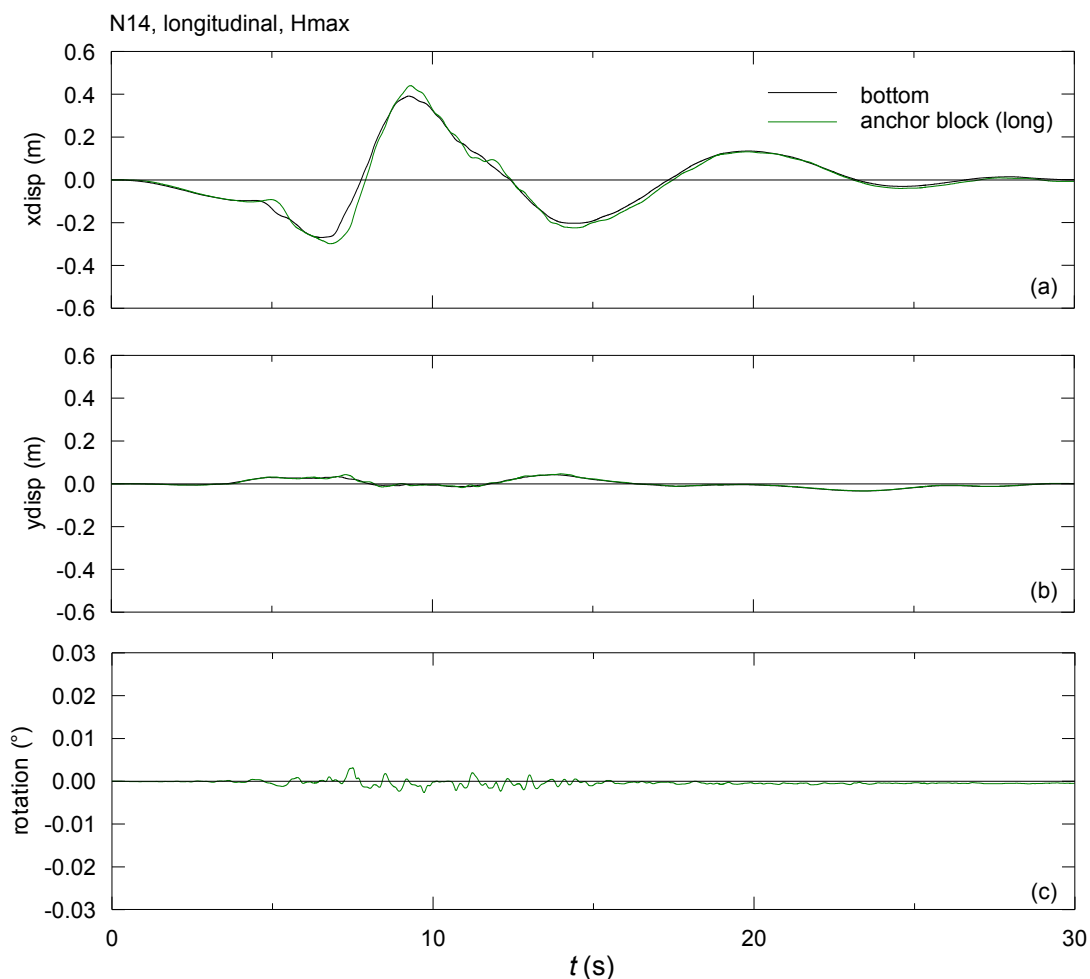


Figure 81. Earthquake N14, comb.1. Longitudinal section of the Calabria shore: (a) horizontal and (b) vertical displacements, and (c) rotation time histories at the centre of mass of the anchor block

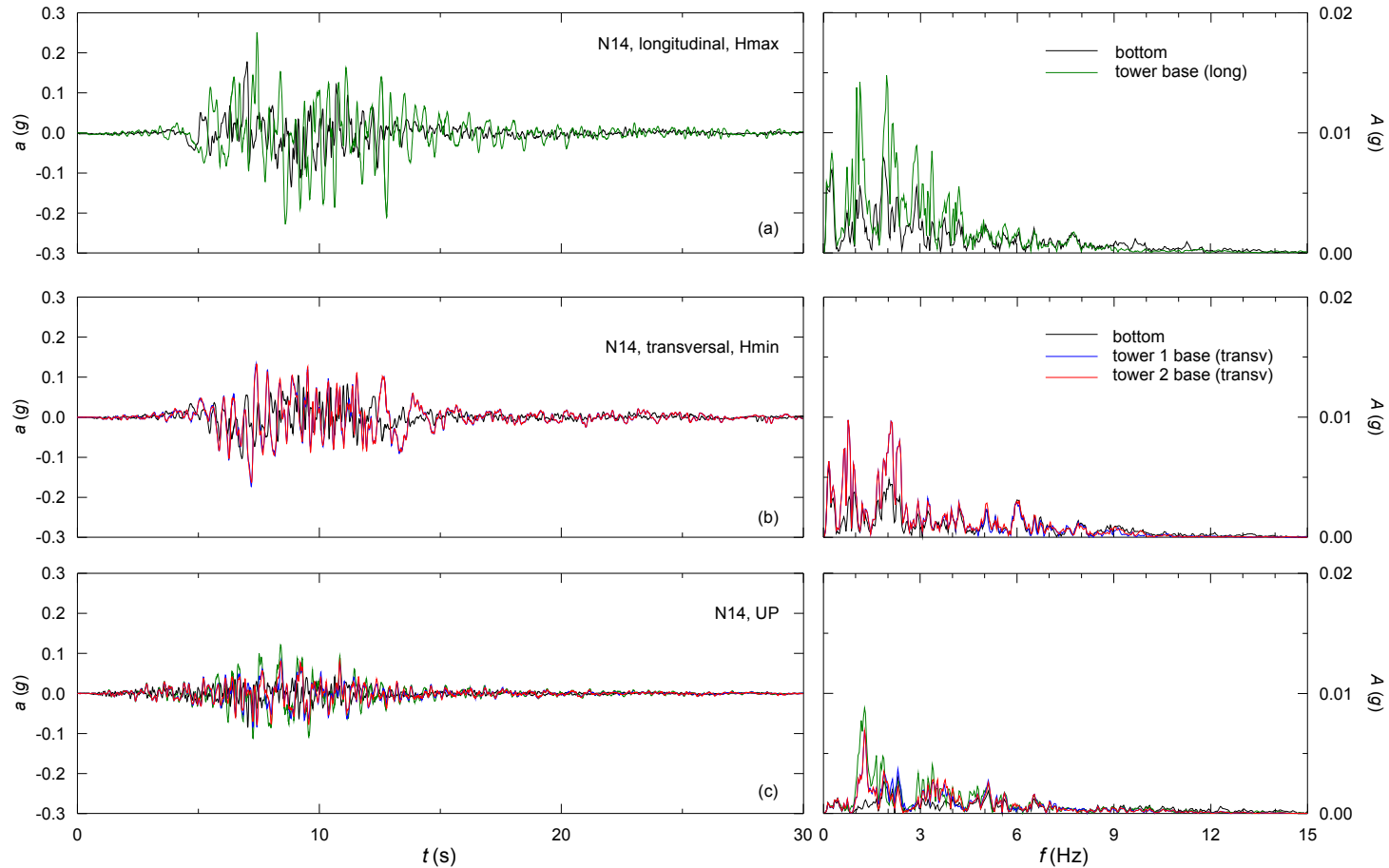


Figure 82. Earthquake N14, comb.1, Calabria shore. Acceleration time histories and Fourier spectra at the base of the tower: (a) horizontal acceleration in the longitudinal direction, (b) horizontal acceleration in the transversal direction and (c) vertical acceleration

		Ponte sullo Stretto di Messina PROGETTO DEFINITIVO	
Seismic analyses for soil-foundation systems, Annex	<i>Codice documento</i> PB0032_F0_ANX	<i>Rev</i> F0	<i>Data</i> 20/06/2011

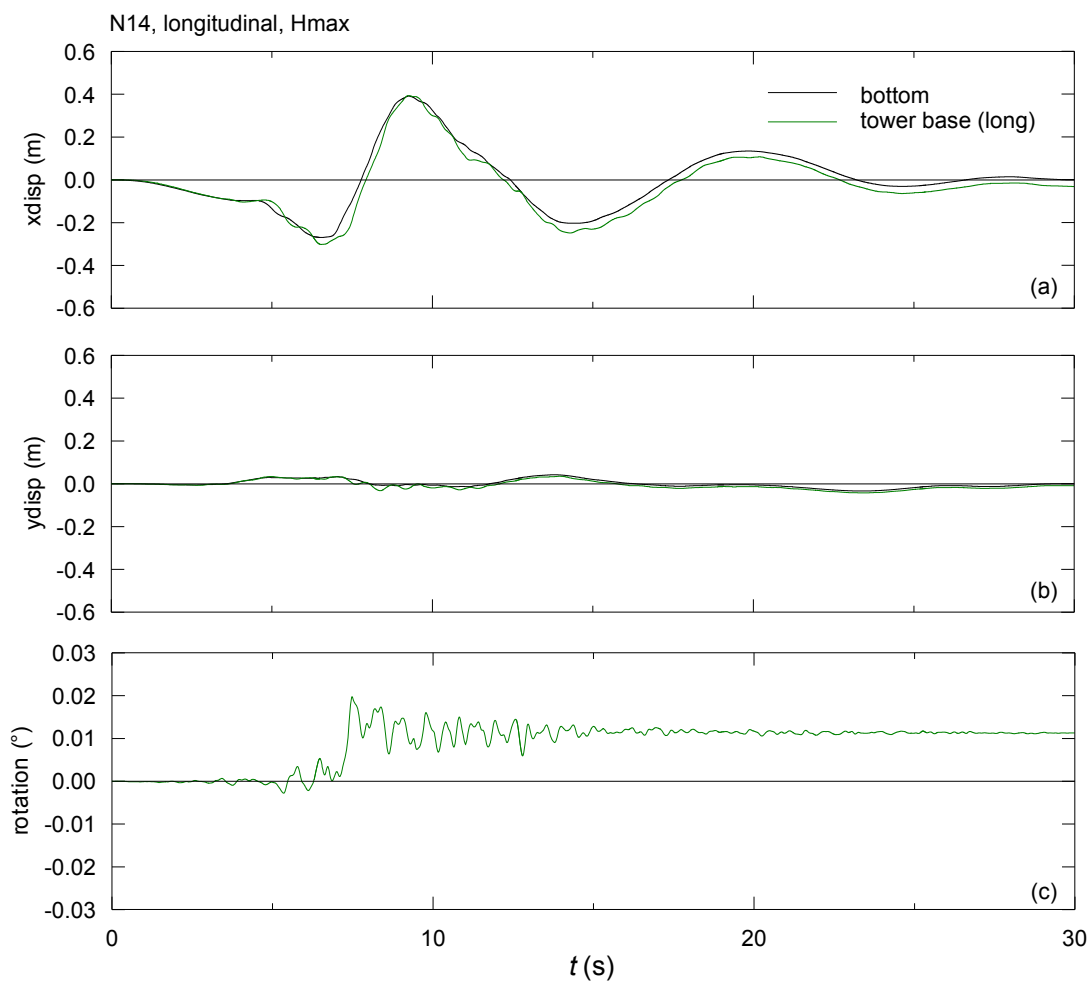


Figure 83. Earthquake N14, comb.1. Longitudinal section of the Calabria shore: (a) horizontal and (b) vertical displacements, and (c) rotation time histories at the base of the tower

		Ponte sullo Stretto di Messina PROGETTO DEFINITIVO		
Seismic analyses for soil-foundation systems, Annex		<i>Codice documento</i> PB0032_F0_ANX	<i>Rev</i> F0	<i>Data</i> 20/06/2011

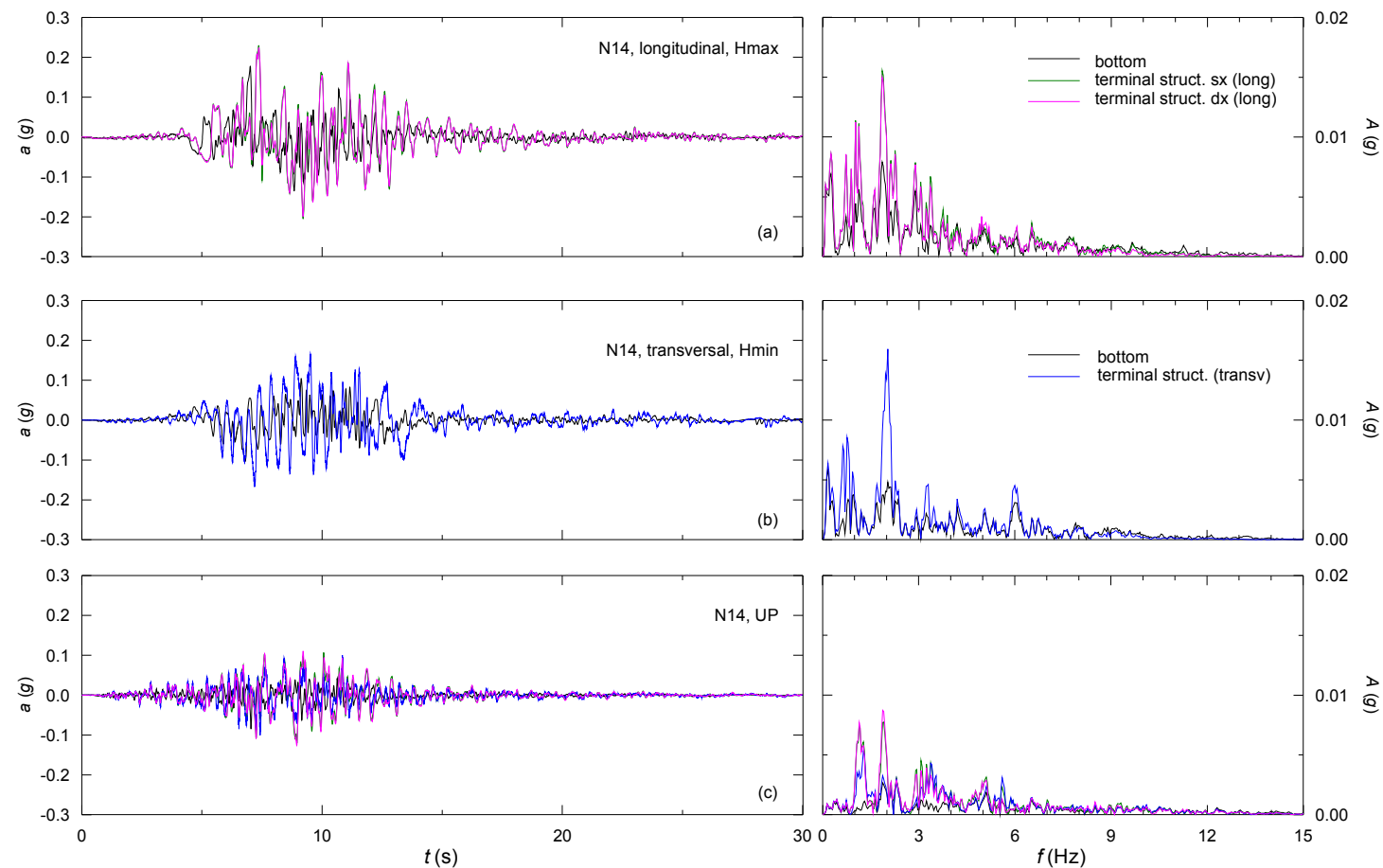


Figure 84. Earthquake N14, comb.1, Calabria shore. Acceleration and Fourier spectra at the centre of mass of the terminal structures: (a) horizontal acceleration in the longitudinal direction, (b) horizontal acceleration in the transversal direction and (c) vertical acceleration

		Ponte sullo Stretto di Messina PROGETTO DEFINITIVO	
Seismic analyses for soil-foundation systems, Annex	<i>Codice documento</i> PB0032_F0_ANX	<i>Rev</i> F0	<i>Data</i> 20/06/2011

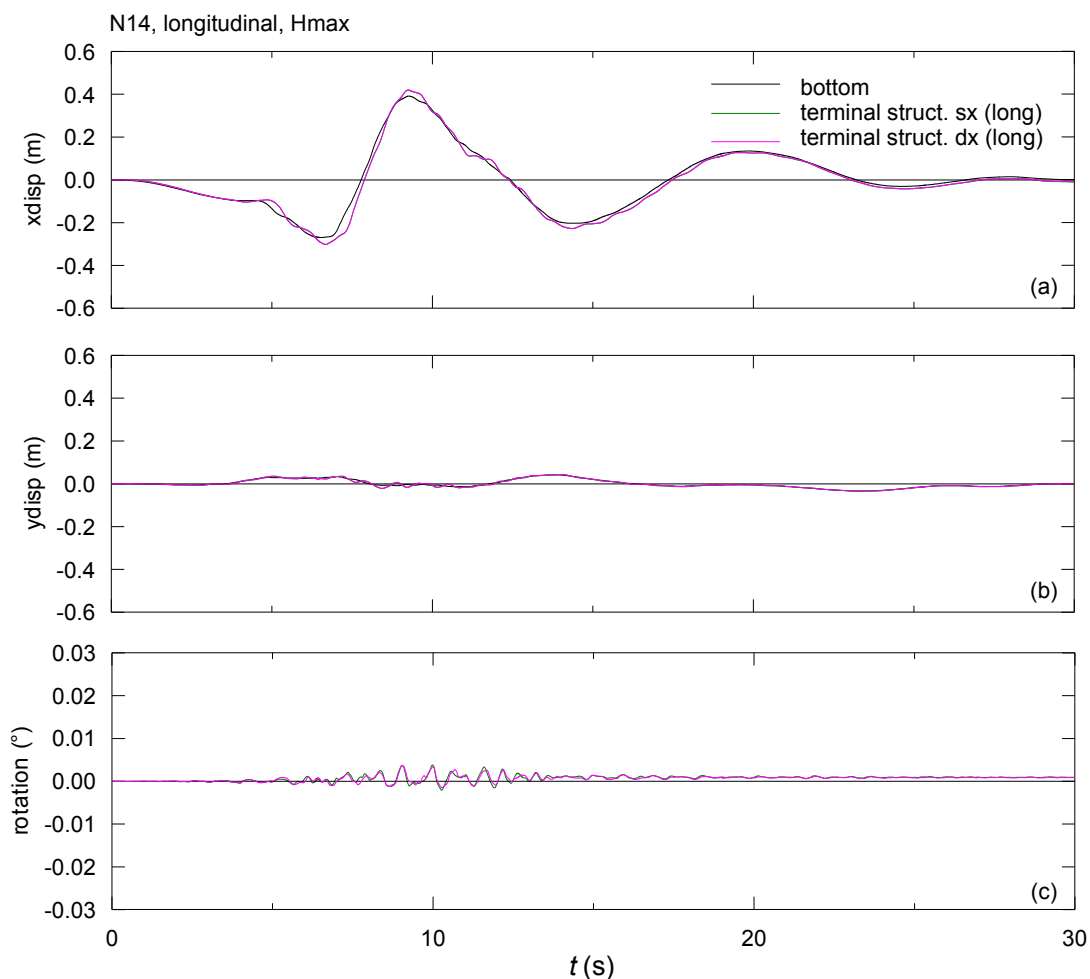


Figure 85. Earthquake N14, comb.1. Longitudinal section of the Calabria shore: (a) horizontal and (b) vertical displacements, and (c) rotation time histories at the centre of mass of the terminal structures

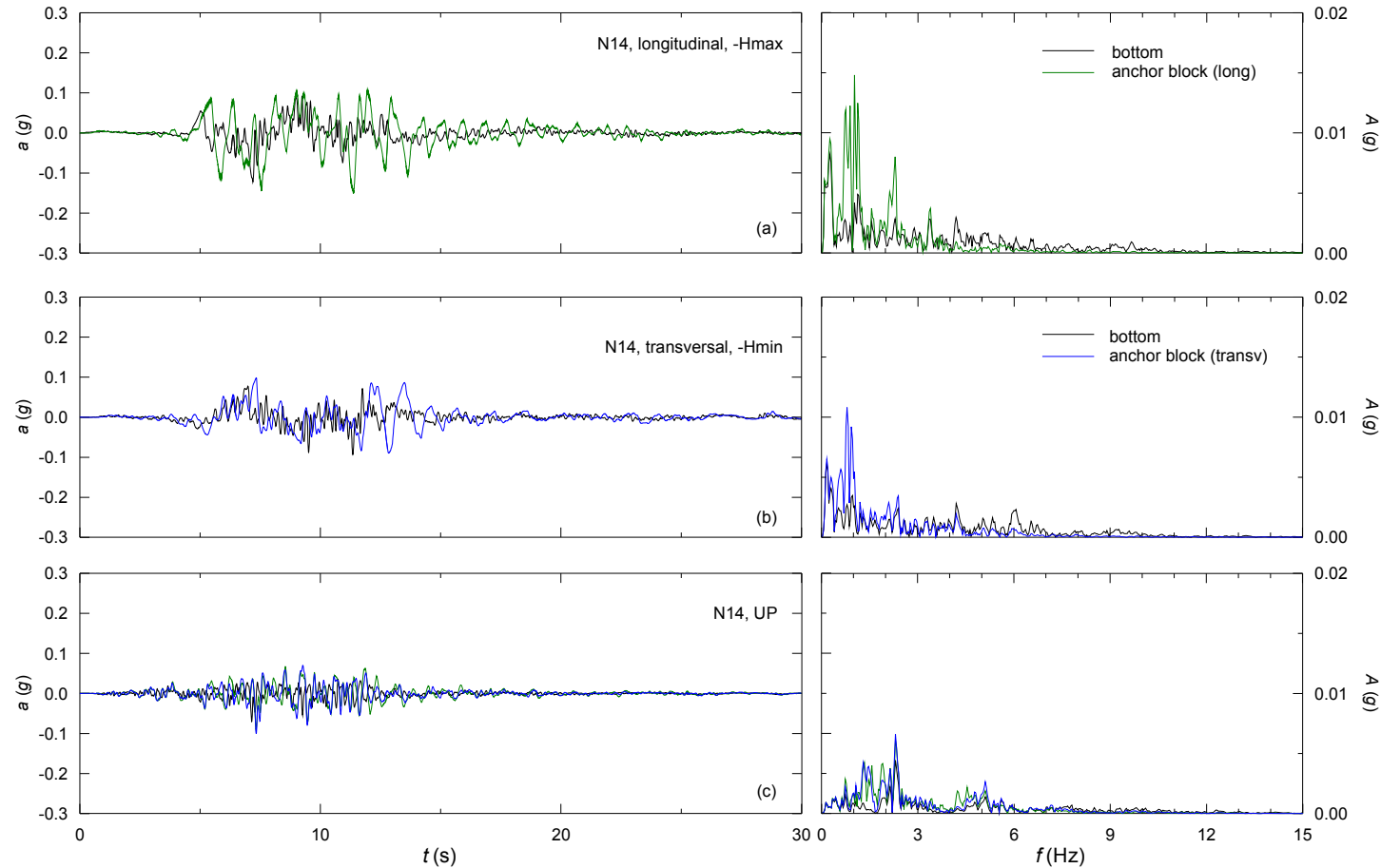


Figure 86. Earthquake N14, comb.2, Sicilia shore. Acceleration time histories and Fourier spectra at the centre of mass of the anchor block: (a) horizontal acceleration in the longitudinal direction, (b) horizontal acceleration in the transversal direction and (c) vertical acceleration

		Ponte sullo Stretto di Messina PROGETTO DEFINITIVO		
Seismic analyses for soil-foundation systems, Annex	<i>Codice documento</i> PB0032_F0_ANX	<i>Rev</i> F0	<i>Data</i> 20/06/2011	

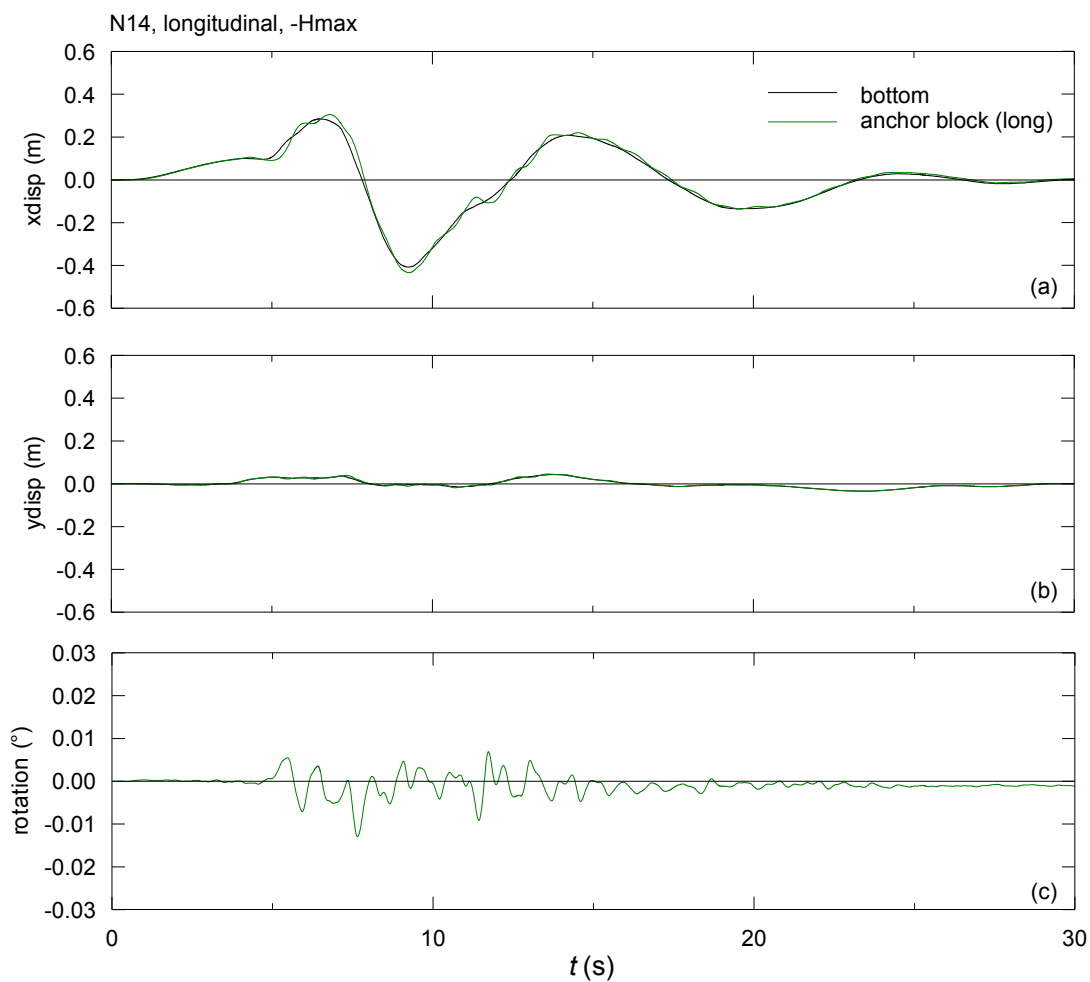


Figure 87. Earthquake N14, comb.2. Longitudinal section of the Sicilia shore: (a) horizontal and (b) vertical displacements, and (c) rotation time histories at the centre of mass of the anchor block

		Ponte sullo Stretto di Messina PROGETTO DEFINITIVO		
Seismic analyses for soil-foundation systems, Annex		<i>Codice documento</i> PB0032_F0_ANX	<i>Rev</i> F0	<i>Data</i> 20/06/2011

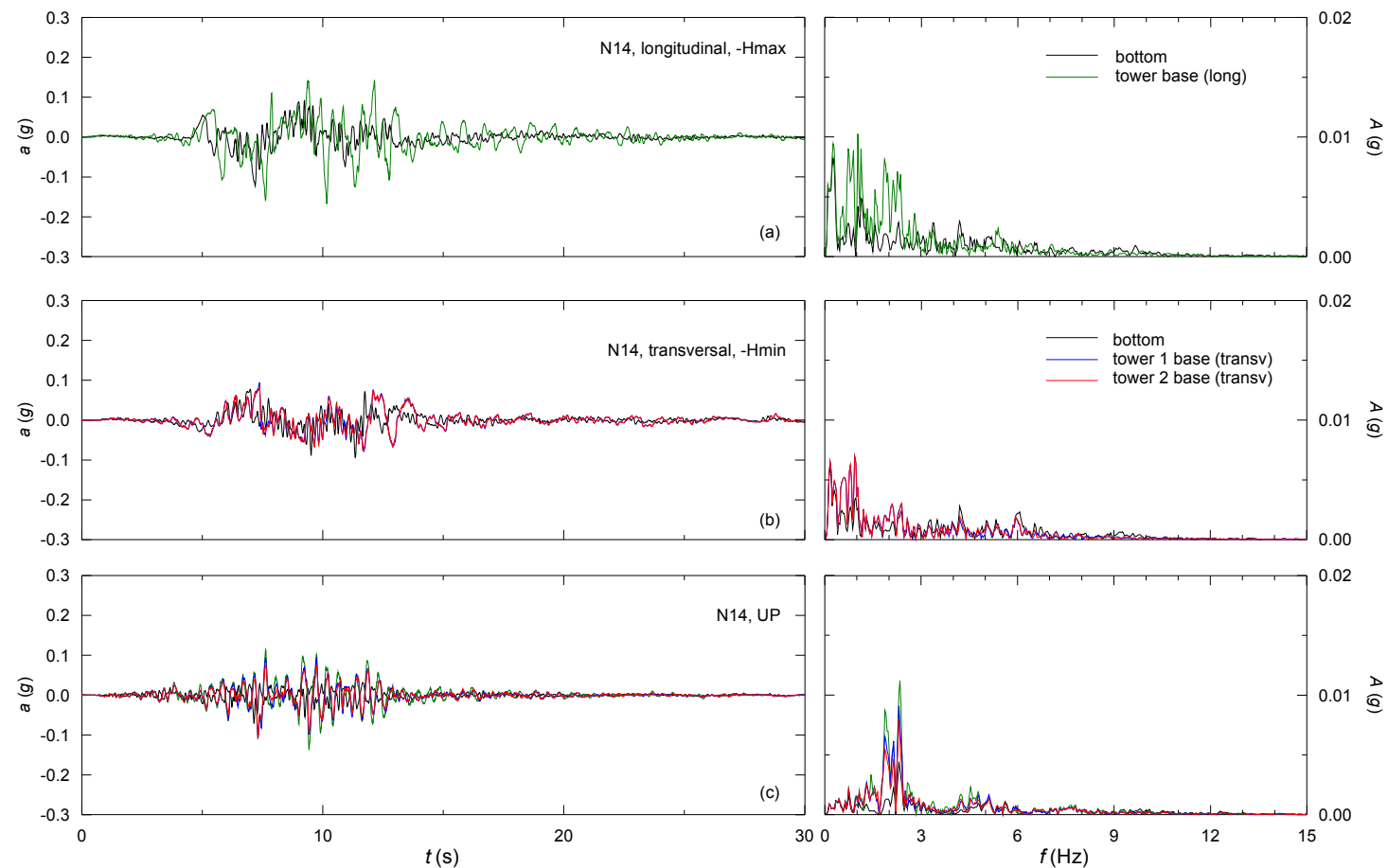


Figure 88. Earthquake N14, comb.2, Sicilia shore. Acceleration time histories and Fourier spectra at the base of the tower: (a) horizontal acceleration in the longitudinal direction, (b) horizontal acceleration in the transversal direction and (c) vertical acceleration

		Ponte sullo Stretto di Messina PROGETTO DEFINITIVO		
Seismic analyses for soil-foundation systems, Annex	<i>Codice documento</i> PB0032_F0_ANX	<i>Rev</i> F0	<i>Data</i> 20/06/2011	

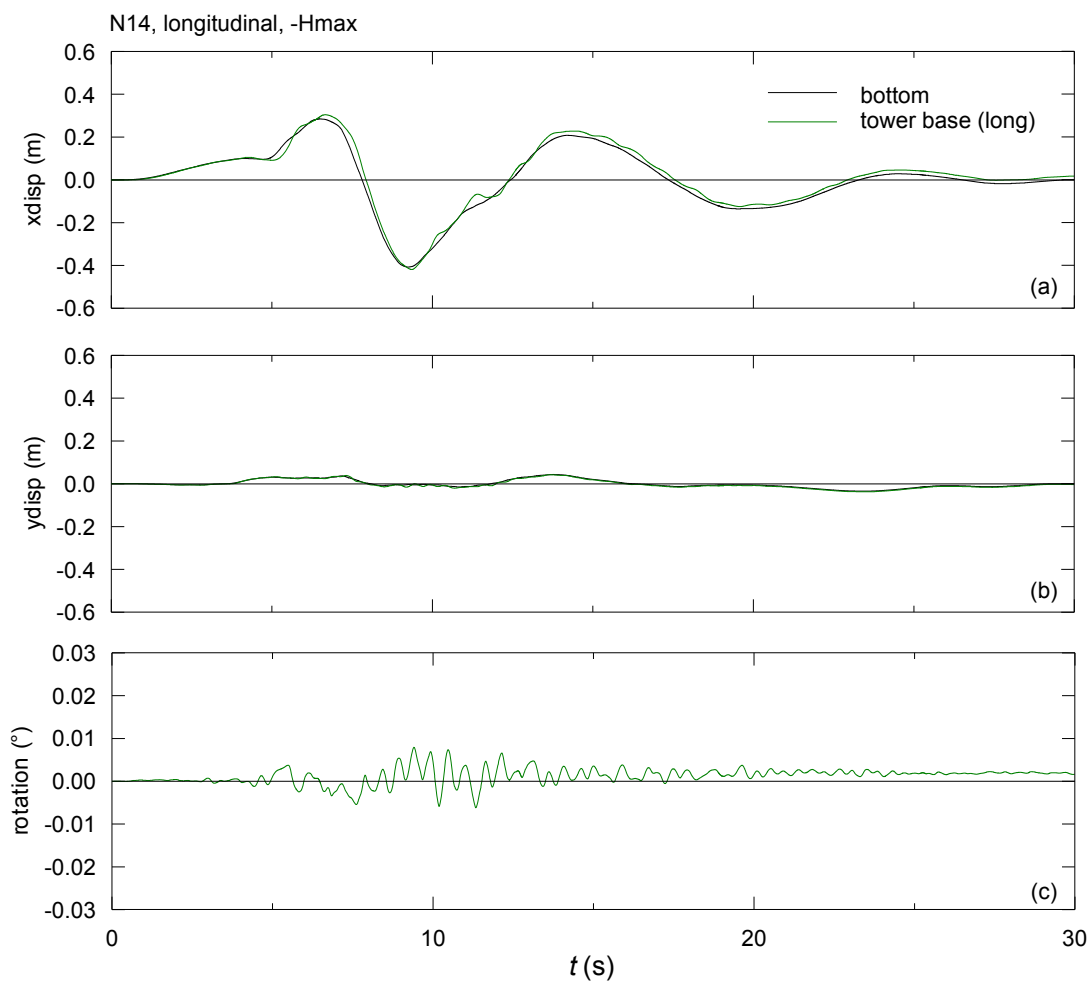


Figure 89. Earthquake N14, comb.2. Longitudinal section of the Sicilia shore: (a) horizontal and (b) vertical displacements, and (c) rotation time histories at the base of the tower

		Ponte sullo Stretto di Messina PROGETTO DEFINITIVO		
Seismic analyses for soil-foundation systems, Annex		<i>Codice documento</i> PB0032_F0_ANX	<i>Rev</i> F0	<i>Data</i> 20/06/2011

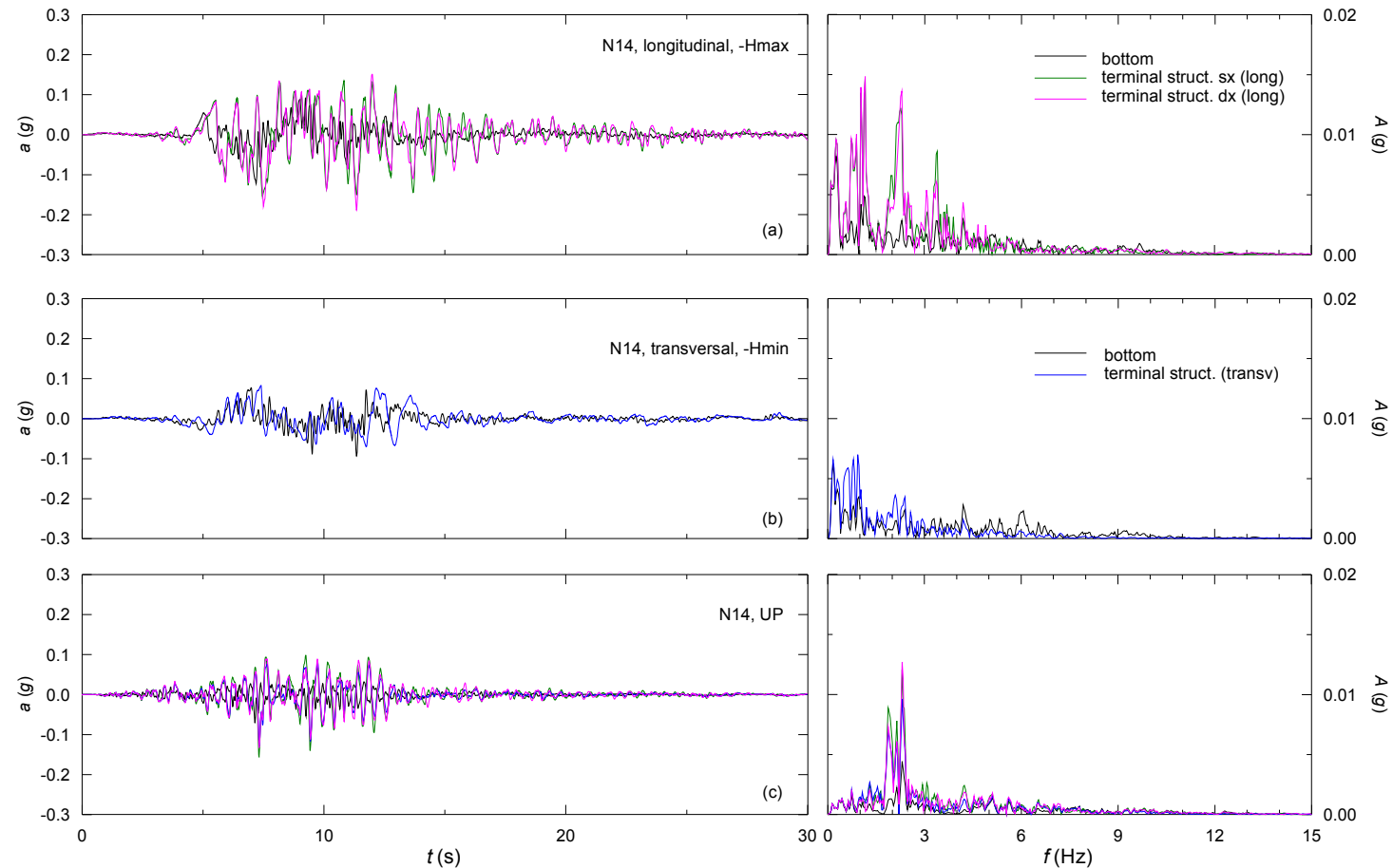


Figure 90. Earthquake N14, comb.2, Sicilia shore. Acceleration time histories and Fourier spectra at the centre of mass of the terminal structures: (a) horizontal acceleration in the longitudinal direction, (b) horizontal acceleration in the transversal direction and (c) vertical acceleration

		Ponte sullo Stretto di Messina PROGETTO DEFINITIVO		
Seismic analyses for soil-foundation systems, Annex	<i>Codice documento</i> PB0032_F0_ANX	<i>Rev</i> F0	<i>Data</i> 20/06/2011	

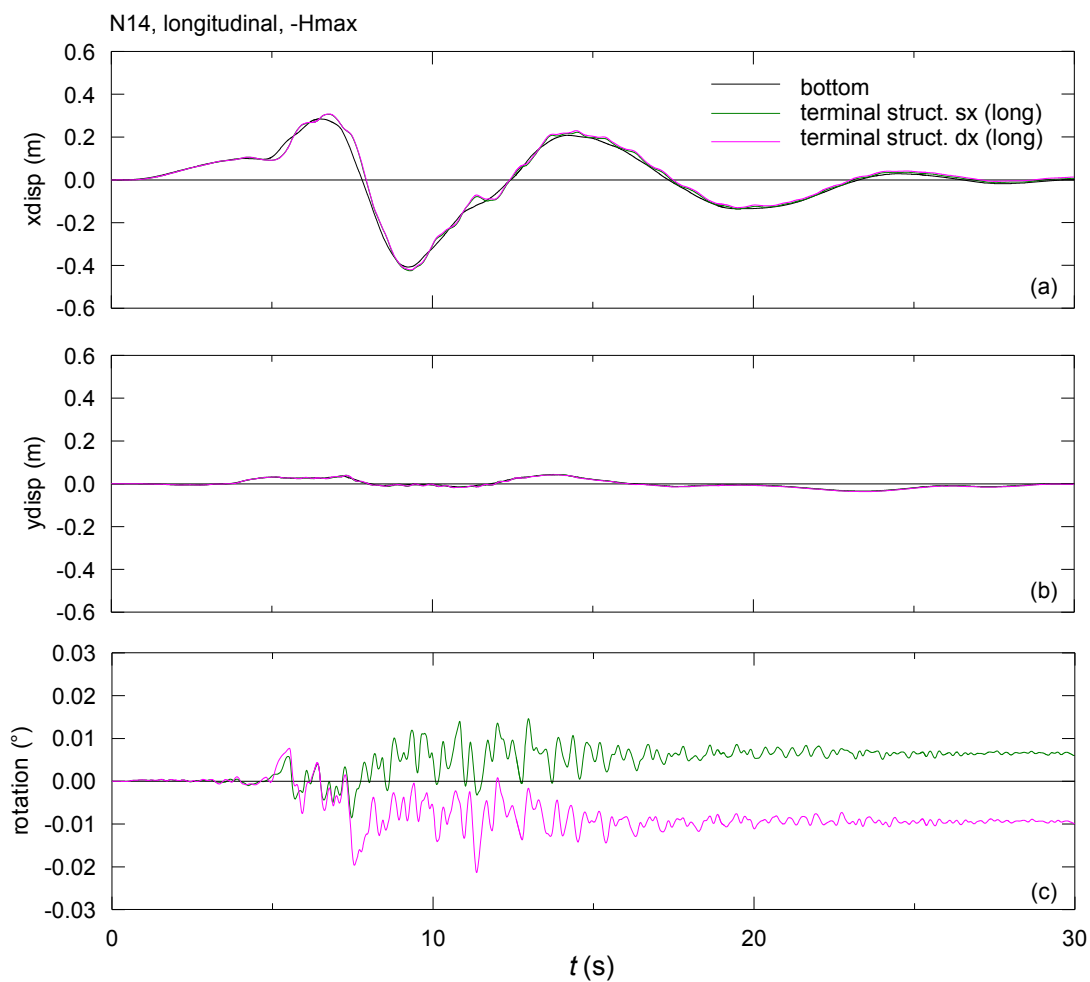


Figure 91. Earthquake N14, comb.2. Longitudinal section of the Sicilia shore: (a) horizontal and (b) vertical displacements, and (c) rotation time histories at the centre of mass of the terminal structures